AMPK promotes xenophagy through ‘priming’ of autophagic kinases upon detection of *Salmonella* outer membrane vesicles

Truc To

Thesis submitted to the Faculty of Graduate and Postdoctoral Studies in partial fulfillment of the requirements for the degree of Master of Science, Cellular and Molecular Medicine

Department of Cellular and Molecular Medicine

Faculty of Medicine

University of Ottawa

Abstract

The autophagy pathway is an essential component of the innate immune response, capable of rapidly targeting intracellular bacteria, which are subsequently degraded by lysosomal enzymes. Recent work has begun to elucidate the regulatory signalling for autophagy induction in response to pathogenic bacteria. However, the initial signalling regulating autophagy induction in response to the detection of pathogens remains largely unclear. Here we report that AMPK, an important upstream activator of the autophagy pathway, is rapidly stimulated upon detection of pathogenic bacteria, prior to bacterial invasion. Bacterial recognition is initially achieved through detection of outer membrane vesicles (OMVs). Additionally, we show that AMPK signalling relieves mTORC1-mediated repression of the autophagy pathway in response to *Salmonella* infection, positioning the cell for a rapid induction of autophagy. Surprisingly, we found that the activation of AMPK and inhibition of mTORC1 in response to extracellular *Salmonella* are not accompanied by an induction of bulk autophagy. However, upon *Salmonella* invasion AMPK signalling is required for efficient and selective targeting of bacteria-containing vesicles by the autophagy pathway through activation of pro-autophagic kinase complexes. Collectively, these results demonstrate a key role for AMPK signalling in coordinating the rapid autophagic response prior to invasion of pathogenic bacteria.

Table of contents

List of tables

List of figures

List of abbreviations

4EBP1	eIF4E binding protein
ADP	Adenosine diphosphate
Akt	Protein kinase B
AMP	Adenosine monophosphate
AMPK	AMP-activated protein kinase
AR	Autoradiography
ATG	Autophagy-related
ATP	Adenosine Triphosphate
Bcl-2	B-cell lymphoma 2
CAMKKβ	Calcium/calmodulin-dependent protein kinase
CBM	Carbohydrate-binding module
CBS	Cystathione β-synthase
CFU	Colony Forming Unit
DEPTOR	DEP domain containing mTOR interacting protein
DMEM	Dulbecco's Modified Eagle'smedium
ER	Endoplasmic reticulum
FIP200	Focal adhesion kinase family interacting protein of 200kD
GAP	GTPase activating protein
GDP	Guanosine 5’-diphosphate
GTP	Guanosine 5’-triphosphate

GWAS	Genome-wide association studies
HCT116	Human COLORECTAL CARCINOMA Cell Line.
HEAT	Huntington, EF3, PR65/A, TOR
HEK293A	Human embryonic kidney cells 293
HOPS	Homotypic fusion and vacuole protein sorting
HORMA	Hop1, Rev7, Mad2 domain
iE-DAP	γ-D-glutamyl-*meso*-diaminopimelic acid
IF	Immunofluorescence
IFN	Interferon
IKKα	IκB kinase subunit
IRGM	Immunity related GTPase M
KO	Knockout
LAP	LC3-associated phagocytosis
LC3	Microtubule-associated protein 1 light chain 3
LIR	LC3-interacting region
LPS	Lipopolysaccharide
MAP	Mitogen-activated protein
MCF7	Michigan Cancer Foundation-7
MDP	Muramyl dipeptide
MEF	Mouse embryonic fibroblasts
mLST8	Mammalian homolog of lethal with sec-13 gene 8
MNV	Murine noroviruses

MOI	The multiplicity of infection
mTORC1	The mechanistic target of rapamycin complex 1
NDP52	Nuclear domain 10 protein 52
NF-κB	Nuclear factor-κB
NOD2	Nucleotide-binding oligomerization domain-containing protein 2
OMV	Outer membrane vesicle
OPTN	Optineurin
p62/SQSTM1	Sequestosome 1
PAMP	Pathogen-associated molecular pattern molecule
PFA	Paraformaldehyde
PGN	Peptidoglycan
PIKK	Phosphatidylinositol-kinase-related kinase
PRAS40	Proline-rich Akt substrate of 40 kDa
PROPPIN	β-propellers that bind phosphoinositides
PRR	Pattern recognition receptor
PtdEth	Phosphatidylethanolamine
PtdIns 3-kinase	Phosphatidylinositide 3-kinases
PtdIns(3)P	Phosphatidylinositol(3)phosphate
PTM	Post-translational modification
R848	Resiquimod
Raptor	Regulatory associated protein of mTOR

RB1CC1	RB1-inducible coiled-coil protein 1
Rheb	Ras homolog enriched in brain
RIP2	Receptor-interacting protein kinase 2
ROS	Reactive oxygen species
Rubicon	RUN domain Beclin 1-interacting and cysteine-rich containing protein
S6K	P70S6 kinase
SCV	*Salmonella*-containing vacuole
Sif	*Salmonella*-induced filament
STK11 /LKB1	Liver kinase B1
T3SS	Type III secretion system
TBC1D7	Tre2-Bub2-CDC16 (TBC) 1 domain family member 7
TLR4	Toll-like receptor 4
TOS	TOR signalling
TP53INP2	Tumor protein 53-induced nuclear protein 2
TPR	Tetratricopeptide
TSC2	Tuberous sclerosis 2
Ub	Ubiquitin
UC	ulcerative colitis
ULK	unc-51-like kinase
UPR	Unfolded protein response
UVRAG	UV irradiation resistance-associated gene

VMP1	Vacuole membrane protein 1
VPS34	Vacuolar protein sorting 34
WB	Western blot
WIPI	WD-repeat protein interacting with phosphoinositides

Acknowledgements

I would like to thank the University of Ottawa for giving me an opportunity to study here despite all struggles and challenges. I acknowledge with gratitude to Dr. Ryan Russell, my considerate supervisor. He constantly gives me useful advice, support, and encouragement, which not only helps me build better research skills, but also motivates me to improve soft skills necessary to be successful in life. Next, I would like to thank my Thesis Advisory Committee members, Dr. Gibbings and Dr. Stintzi, and my co-supervisor, Dr. Copeland, for constructive comments and suggestions, which promotes me to consider potential challenges in my project and eventually helps me well-prepared to complete master's degree successfully.

I would like to thank the Russell lab members: Zhihao, Reham, Wensheng, Yujin, Karyn, and Mercy for their huge support. Last but not least, I would like to give deep thank to my family and my husband, Jared Losier, for his continuous love and encouragement, without whom I could not pursue my academic dream.

Sources of Funding

This work was supported by Canadian Institutes of Health Research (CIHR) Project Grants awarded to Ryan Russell (#PJT153034).

Introduction

Macroautophagy (hereafter referred to as autophagy) is a heavily regulated degradative process activated by a range of cellular stressors including nutrient starvation, proteotoxic aggregates, and pathogen infection[1]. Autophagy is driven by a set of highly conserved 'AuTophaGy-related' (abbreviated ATG) proteins, which stimulate the *de novo* formation of a double-membraned vesicle called an autophagosome[2]. The fully formed autophagosome achieves its degradative potential after fusion with the lysosome, which provides the acid hydrolases responsible for the breakdown of sequestered macromolecules[2].

I.1 History of autophagy

In 1949, Christian de Duve, a scientist at the University of Louvain in Belgium and father of Cell Biology, was working with his colleagues to study carbohydrate metabolism and the mechanism of insulin[3]. Specifically, they were curious to characterize the distribution of an enzyme called glucose-6-phosphatase or hexose phosphatase, which regulates blood sugar[3]. De Duve group adapted a protocol, which used acid phosphatase as a control and utilized centrifugation to fractionate subcellular organelles without disrupting their integrity[3]. However, they found the activity of the acid phosphatase in all off the fractions was too low compared to their experimentally expected value[3]. Frustrated, the researchers stored the samples in the refrigerator for later analysis[4]. Five days later, the group decided to re-examine the samples and to their surprise, they found that the enzymatic activities of the acid phosphatase increased proportionally in all of the fractions[4]. In order to confirm there was no mistake they repeated the experiments several times[4]. Every time, the scientists observed that the fresh samples gave them very low enzymatic activities while old samples (five days in the fridge) showed expectedly proportionally increased levels, which led them hypothesize that the enzyme (acid phosphatase) was contained in membrane-like sacs, which prevented it to access to substrates and freeze-thaw cycles disrupted the membrane and allowed the enzyme to diffuse[4].

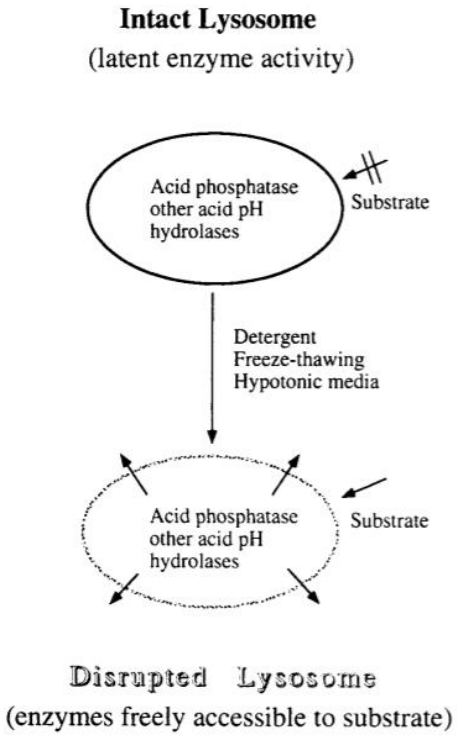

Fig 1. Scheme of lysosome hypothesis: Detergent, freeze-thawing, or hypotonic media permeabilizes the lysosomal membrane, which releases enzymes and substrate[5].

Later, four additional acid hydrolases – β-glucuronidase, cathepsin D, ribonuclease, and DNase – were found in these membrane-bound organelles, which led de Duve to name them “lysosome” to demonstrate their lytic nature[4]. In 1955, du Duve collaborated with Alex Novikoff, an expert microscopist from the University of Vermont, to capture the first electron microscopic image of lysosomes[6]. Additionally, du Duve and Novikoff confirmed the presence of acid phosphatases in the lysosome through light and electron microscope[6]. In 1974, du Duve was deservingly awarded the Nobel Prize in Physiology or Medicine for his discovery of lysosomes[7]. The finding of the lysosomes opened the gate to more interesting questions and great discoveries.

Next, the most critical question was what the biological function of the lysosomes was. Originally, du Duve suggested that the lysosomes may be involved in intracellular digestion of macromolecules in his first paper on activity of acid phosphatase[8]. Interestingly, the first convincing evidence for the digestive functions of lysosomes

emerged from the work of Werner Straus, who was a scientist at the University of North Carolina and was close to co-discovering lysosomes[8]. In the mid-1950s, Straus, who was interested in renal endocytosis, observed that the droplets of the proximal tubule of the kidney responsible for storage and degradation of reabsorbed proteins were lysosomes which were rich in acid hydrolases shown in liver lysosomes[9]. In addition, in the 1960s, when Zanvil Cohn and James Hirsch infected macrophages with radiolabeled bacteria, they discovered that bacterial components such as lipids or proteins accumulated in the lysosomes[10]. Together, these were the first data linking lysosomal digestion to endocytotic uptake of materials such as pathogens or cellular debris. During the same time, Marilyn Farquhar and her colleagues, scientists at the University of California, observed vesicles containing engulfed cytoplasmic material and were the first to hypothesize that theses vesicles were pre-lysosomes[8]. In the cytoplasm, purported pre-lysosomes emerge from a cup-shaped membrane called a phagophore, which expands and fuses its edges to form a double-membraned structure called autophagosomes[11]. Autophagosomes engulf damaged molecules or organelles and recruit these to the lysosomes[11]. When de Duve recognized that the cells were capable of breaking down their own components through autophagosomes, he coined the term “autophagy” to describe this process for the first time[12].

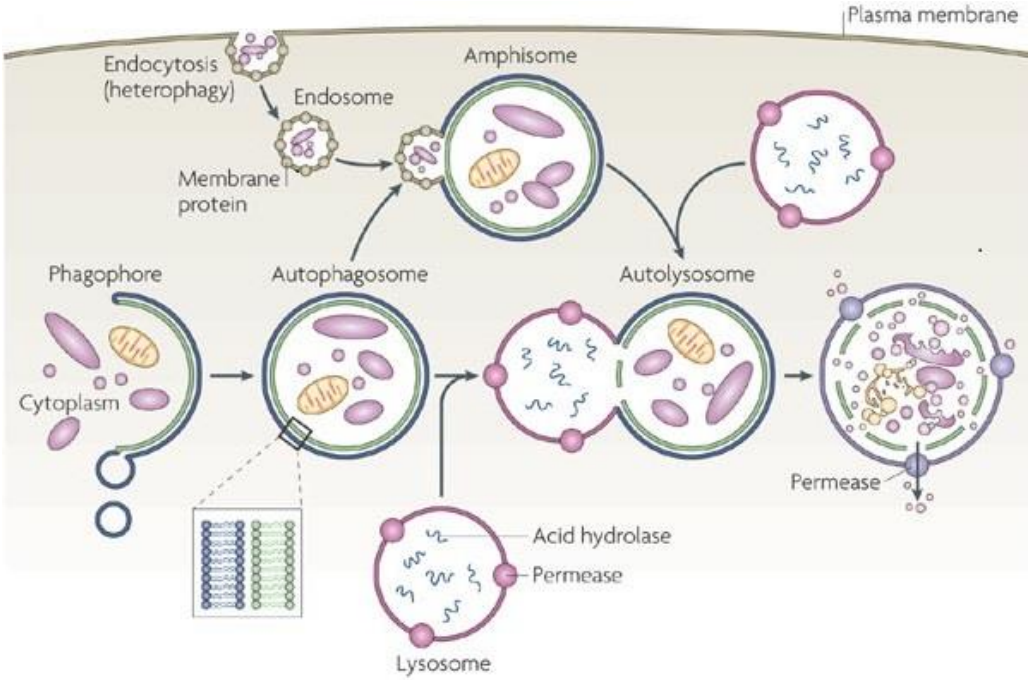

Fig 2. The formation of phagolysosomes[8].

I.2 Autophagy biogenesis

I.2.1 Autophagy initiators

Autophagy is an evolutionarily conserved degradative process from yeast to mammals and plays important roles in maintaining normal cellular homeostasis[1]. Nevertheless, the pathway leading to autophagosome formation remained enigmatic until 1993 when Yoshinori Oshumi, a scientist at University of Tokyo, discovered at least 15 now-called ATG genes associated with the pathway through a high content genetic screen in yeast treated with nitrogen withdrawal[13]. This fascinating discovery not only opened up the gate for further understanding autophagy mechanisms, but it also won Oshumi the Nobel Prize in Physiology or Medicine 2016[13]. Currently, over 41 ATG genes have been discovered[14].

I.2.1.1 ULK kinases

ATG1 is the most upstream autophagy protein identified in yeast and has two homologues in mammals, ULK1 and 2 (Unc-51-like kinase). ULK kinases are the only protein kinases in the autophagy pathway and are critical for autophagy initiation[15]. ULK1 and ULK2 are functionally redundant for autophagy induction and are collectively

referred to as ULK1 hereafter. Autophagic ULK1 complex consists of ULK1 itself, ATG13, FIP200 (focal adhesion kinase family interacting protein of 200 kDa and homologue of yeast Atg17), and ATG101[16]. Binding of ULK1 with ATG13 or FIP200 has been shown to increase stability and subsequent kinase activity of ULK1, which is essential for autophagy initiation[16].

The structure of the entire ULK1 complex remains unclear, although we have partial crystallographic data on specific subunits. ULK1 has been described to contain a relatively standard kinase fold with multiple unique features including a large and positively charged loop between the N- and C-terminal lobes[17]. In addition, ULK1 also possesses an autophosphorylation site on T180 in the activation loop, which is required for its catalytic activity[18].

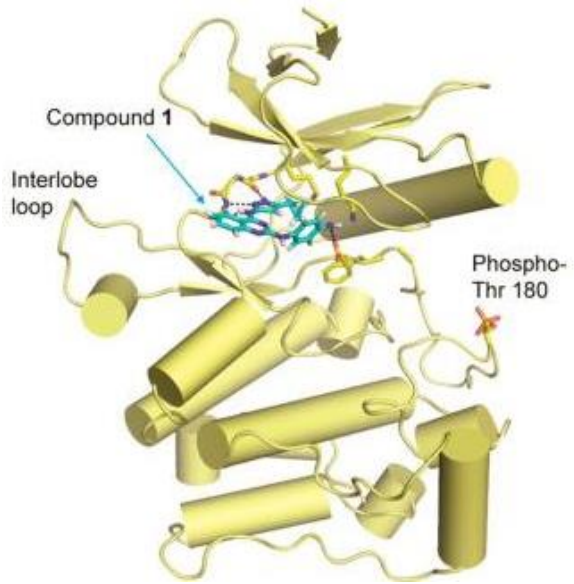

Fig 3. Overall structure of ULK1[17].

Crystal structures of the ATG13-ATG101 heterodimer have recently been characterized. ATG13 possesses a HORMA (Hop1, Rev7, Mad2) domain in its N terminus while ATG101 is encoded by a HORMA domain entirely[19]. ATG101 has been shown to recruit downstream components to the site of autophagy initiation[20]. Interaction with ATG101 promotes stabilization of mammalian ATG13 HORMA[19]. Moreover, ATG13-ATG101 heterodimer functions to bridge the interaction of ULK1 to

FIP200, which enhances enzymatic activity of ULK1 complex[21]. Disruption of any of these binding sites result in autophagy impairment[21].

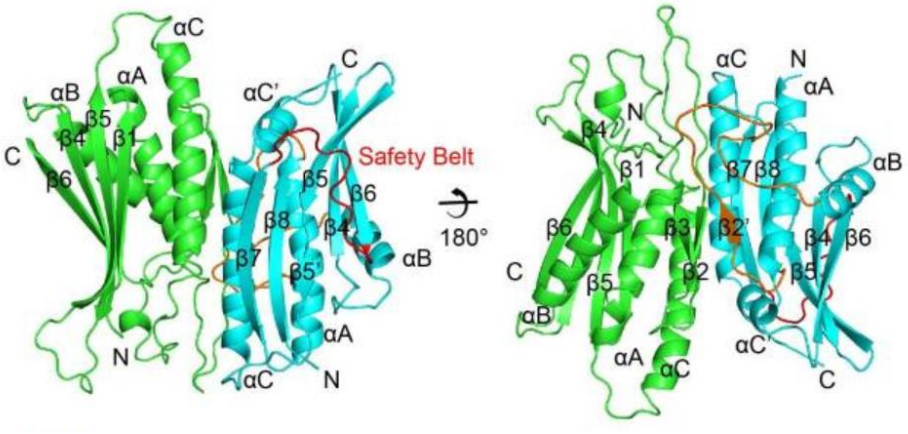

Fig 4. The overall structure of the Atg101 and Atg13 HORMA dimer shown in a ribbon representation colored as above. From left to right: Atg101-Atg13 (green and cyan)[19].

AMPK (AMP activated kinase) and mTORC1 (mTOR complex 1) are stress-sensitive kinases that are upstream regulators of autophagy and ULK1[22]. ULK1 activity is tightly regulated through inhibitory phosphorylation by the mTORC1 kinase and activating phosphorylation by AMPK[22]. Different cellular stressors including; nutrient starvation, ROS (reactive oxygen species) accumulation, and reduced cytokine signalling are capable of activating autophagy by shifting the balance of activating and inhibitory phosphorylation of ULK1 by mTORC1 (on S757) and AMPK (on S317, S467, S555, S574, S637, S659 and/or S777)[23].

I.2.1.2 mTORC1

mTOR (mechanistic target of Rapamycin) is a master regulator of eukaryotic cell growth and metabolism that responds to a variety of intracellular and environmental stresses such as nutrient starvation, hypoxia, or DNA damage[24]. mTORC1 consists of three core components: mTOR, Raptor (regulatory associated protein of mTOR), and mLST8 (mammalian lethal with Sec13 protein 8, also known as GBL)[25]. mTOR is a member of the PIKK (phosphatidylinositol-kinase-related kinase) family of serine and threonine kinases[25]. The kinase domain is located at the C-terminus following HEAT (Huntington, EF3A, ATM, TOR) and TPR (tetratricopeptide) repeats[25]. Raptor functions

as a scaffold to recruit substrates including S6K1 (p70S6 kinase) and 4EBP1 (eIF4E binding protein) to the complex through interacting with the TOS (TOR signaling) motif on canonical mTORC1 substrates and is essential for the correct localization of mTORC1[26]. mLST8 has been described to promote catalytic function although recent studies suggest it is dispensable for the critical role of mTORC1[27]. Besides three core factors, mTORC1 also possesses two inhibitory subunits including PRAS40 (proline-rich Akt substrate of 40 kDa) and DEPTOR (DEP domain containing mTOR interacting protein)[25].

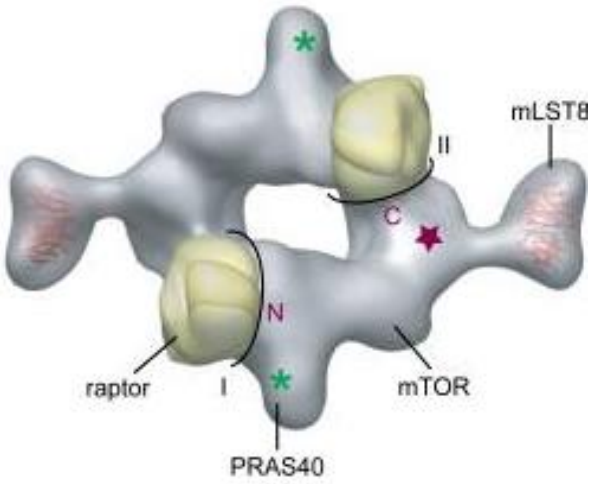

Fig 5. Overall structure of mTORC1. The proposed locations of the N- and C-terminal domains (marked “N” and “C”) and the kinase domain of mTOR (*purple star*). The black lines labeled “I” and “II” delineate the two interaction interfaces formed by each mTOR molecule with the two raptor subunits[28].

It has been discovered that under nutrient rich conditions mTORC1 is recruited to the lysosomal membrane and this is required for its activation[29]. Perturbation of mTORC1 localization to the lysosomes mostly abrogates its amino acid-mediated activation[30]. Interestingly, synthetically tethering mTORC1 to lysosomes promotes constitutive mTORC1 activation independently of nutrient availability[30]. In addition, mTORC1 activation also depends on Rheb (Ras homolog enriched in brain)[31]. As a small GTPase protein, Rheb is sensitive to the change in GTP (guanosine 5'-triphosphate) and GDP (guanosine 5'-diphosphate) levels[31]. When GTP is available, Rheb works as a potent activator of mTORC1 kinase activity[31]. Previous studies have

demonstrated that Rheb localizes on several cellular compartments through farnesylation on its “CAAX” motif[32]. The mutation of cysteine in this motif interferes with the membrane localization of Rheb and subsequently inhibits Rheb function to activate mTORC1[32]. However, the exact mechanism how Rheb stimulates mTORC1 kinase activity remains unclear[33].

The well-known negative regulator of mTORC1 signaling is the Tuberous Sclerosis Complex (TSC), which is a heterotrimeric complex consisting of TSC1, TSC2, and TBC1D7 (Tre2-Bub2-CDC16 (TBC) 1 domain family member 7)[34]. Among the listed subunits, TSC2 possesses a GTPase activating protein (GAP) domain, which converts Rheb from the GTP-bound active form to GDP-bound inactive form[34]. Under basal conditions, several growth factor and mitogen-dependent pathways promotes Akt (Protein kinase B)-mediated phosphorylation of TSC2 on at least four serine and threonine residues[35]. This phosphorylation enhances TSC dissociation from the lysosomes and eventually its inactivation, which protects mTORC1 activity[35].

In addition to regulating synthesis of macromolecules, mTORC1 is also known to inhibit catabolic pathways such as autophagy, establishing the balance between anabolism and catabolism in response to several environmental conditions[24]. An early key event in autophagy initiation is the activation of ULK complex[16]. Under basal conditions, mTORC1 phosphorylates ULK directly and inhibits AMPK-mediated activation of ULK[22]. Therefore, the level of autophagy induction depends on the relative activity of mTORC1 and AMPK in a variety of cellular contexts.

I.2.1.3 AMPK

AMPK exists as a heterotrimer including a catalytic α subunit and two regulatory β and γ subunits[36]. In humans, each of these subunits exist in several isoforms encoded by distinct genes[36].

Subunit	Gene	Yeast ortholog	Function
α1	*PRKAA1*	Snf1	catalytic subunit
α2	*PRKAA2*	Snf1	catalytic subunit
β1	*PRKAB1*	Sip1/Sip2/Gal83	glycogen binding, α/γ binding
β2	*PRKAB2*	Sip1/Sip2/Gal83	glycogen binding, α/γ binding
γ1	*PRKAG1*	Snf4	Binding of AMP/ADP/ATP
γ2	*PRKAG2*	Snf4	Binding of AMP/ADP/ATP
γ3	*PRKAG3*	Snf4	Binding of AMP/ADP/ATP

Table 1: Characteristics of AMPK subunits[36].

The AMPK α subunit contains a typical serine or threonine kinase domain at the N-terminus consisting a small N-lobe and a larger C-lobe and a critical T172 residue in the activation loop, whose phosphorylation increases activity of AMPK by more than 100-fold[37]. The β subunit possesses two conserved regions including the carbohydrate-binding module (CBM) and the C-terminus[38]. The CBM functions to recruit AMPK to the surface of glycogen particles, although the physiological significance of this binding remains unclear[38]. The γ subunit has regulatory binding sites consisting of four tandem cystathione β-synthase (CBS) repeats, which allows AMPK to respond to changes in the ATP (adenosine triphosphate)-to-AMP (adenosine monophosphate) ratio[38].

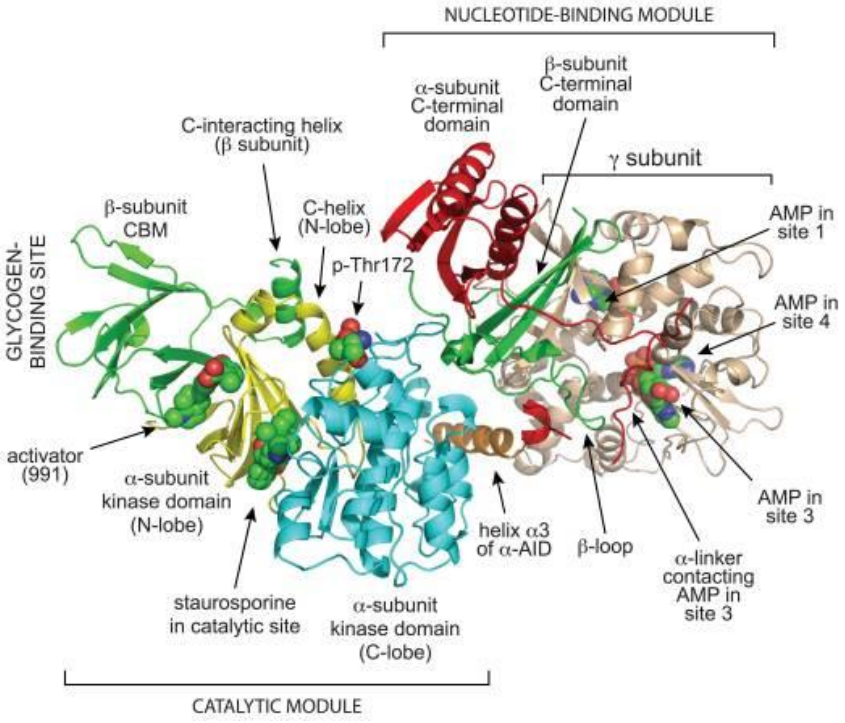

Fig 6. Proposed structure of complete α2β1γ1 heterotrimer of AMPK. The α, β and γ subunits are shown with different domains color coded, while the activator 991, the kinase inhibitor staurosporine, the three bound molecules of AMP, and phospho-Thr172 are shown in "sphere view" with C atoms green, O red, N blue and P orange[39].

There are three proposed mechanisms for AMPK activation. First, LKB1 (liver kinase B1) or CAMKKβ (Calcium/calmodulin-dependent protein kinase) can directly activate AMPK through phosphorylation of T172[40]. In addition, AMPK is sensitive to changes in intracellular adenosine nucleotide levels due to stresses[41]. Upon low intracellular ATP levels, AMP or ADP (adenosine diphosphate) can induce a conformational change in AMPK through direct binding to the γ subunits, thereby protecting the activating phosphorylation T172 from protein phosphatases and enhancing kinase activity of AMPK[41]. Finally, interacting with AMP, but not ATP, can lead to allosteric activation of the kinase and the level of this activation can significantly increase[42]. Together, AMP and ADP interaction with the nucleotide binding pockets in the γ subunits of AMPK provides the mechanistic link between AMPK activation and a variety of cellular stresses[41].

Under conditions where nutrients are limited, AMPK functions as a metabolic checkpoint preventing cellular growth and promotes catabolic pathways such as autophagy to produce more ATP[41]. AMPK regulates cell growth and initiates autophagy primarily through repression of mTORC1-signalling[22]. In response to nutrient withdrawal, AMPK suppresses mTORC1 activity through AMPK-mediated phosphorylation of the human tumor suppressor TSC2 on S1387 resulting in the inhibition of the small GTPase Rheb, mTORC1 activator[43]. Interestingly, cells lacking TSC2 can still respond to nutrient starvation (mTORC1 inhibition following AMPK activation), which led to the recognition of another mode of AMPK-mediated mTORC1 inhibition[44]. AMPK can directly inhibit mTORC1 activity though phosphorylation of the Raptor subunit on conserved serines[44]. Besides mTORC1, active AMPK can initiate autophagy through direct regulation of ULK1[41]. Therefore, AMPK activation can induce autophagy through a two-fold mechanism, which consists of not only suppression of mTORC1 but also direct stimulation of ULK1 activity.

I.2.2 Critical autophagy-associated complexes

In addition to ULK, there are four critical sets of proteins required for autophagosome formation including: 1) the class III phosphoinositide 3-kinase/VPS34 complex I, 2) two ubiquitin-like protein conjugation systems (ATG12–ATG5-ATG16L1 and MAP1LC3 (LC3), the mammalian ortholog of yeast Atg8), 3) WIPI proteins, and 4) transmembrane proteins including ATG9[45].

	Yeast	Mammal	Characteristics
Atg1/ULK kinase complex	Atg1	ULK1/2	Serine/threonine protein kinase
	Atg13	ATG13	Regulator of the Atg1 complex through phosphorylation
	Atg17	RB1CC1/FIP200 (functional homolog)	Component of the Atg1 complex
	Atg29		Component of the Atg1 complex
	Atg31		Component of the Atg1 complex
		C12orf44/ATG101	Component of the ULK complex in mammals
Atg9 and its cycling system	Atg2	ATG2	Peripheral membrane protein
	Atg9	ATG9	Transmembrane protein
	Atg18	WIPI1/2	Peripheral membrane protein
Class III PtdIns3K complex	Vps15	PIK3R4/VPS15/p150	Serine/threonine protein kinase
	Vps34	PIK3C3/VPS34	PtdIns3K
	Vps30/Atg6	BECN1	Component of PtdIns3K (complex I and II in yeast)
	Atg14	ATG14	Component of PtdIns3K (complex I in yeast)
Ubiquitin-like conjugation systems	Atg3	ATG3	E2-like enzyme for Atg8 conjugation
	Atg4	ATG4A to ATG4D	Cysteine proteinase
	Atg5	ATG5	Conjugated with Atg12
	Atg7	ATG7	E1-like enzyme
	Atg8	LC3A,B,B2,C, GABARAP,L1,L2	Ubl, conjugated to PE
	Atg10	ATG10	E2-like enzyme for Atg12 conjugation
	Atg12	ATG12	Ubl
	Atg16	ATG16L1,L2	Forms Atg12—Atg5–Atg16 complex

This table was modified from table 1 of Mizushima et al. (2011)

Table 2: The core molecular complexes of autophagosome formation[46].

I.2.2.1 The class III phosphoinositide (PtdIns) 3-kinase/VPS34 complex I

The Class III PtdIns 3-kinase plays a variety of essential functions in autophagy, endocytic trafficking, cytokinesis, phagocytosis, and nutrient sensing[47]. VPS34 (vacuolar

protein sorting 34) is a member of the PtdIns 3-kinase family of lipid kinases and exists in several different complexes to regulate a wide range of cellular processes[47]. The VPS34 complexes associated with the autophagy pathway consist of the catalytic subunit VPS34 itself, the VPS15 scaffold, and the regulatory beclin-1 (homologue of the yeast Atg6), and either ATG14 or UVRAG (UV resistance-associated gene) subunits[48]. Activity of pro-autophagic VPS34 complexes have been described to be regulated by three upstream initiators mTORC1, ULK, and AMPK[15]. Under nutrient rich conditions, while ULK and AMPK signaling is inhibited, active mTORC1 directly represses pro-autophagic VPS34 complexes through phosphorylation of subunit ATG14[49]. Interestingly, incubation of mTORC1 with VPS34-VPS15-beclin-1 complexes *in vitro* has no effect on the activity of the lipid kinase[50]. However, supplementation of recombinant ATG14 to the VPS34 complex results in inhibition of lipid kinase activity through mTORC1-mediated phosphorylation[51]. This suggests the critical role of ATG14 in linking the VPS34 complex substrate to the kinase[51]. In amino acid-withdrawn cells, ULK has been shown to phosphorylate pro-autophagic VPS34 complex subunit beclin-1 on S14, which results in phosphorylation of phosphatidylinositol (PtdIns) at the 3′ position on the inositol ring to produce pool of phosphatidylinositol(3)phosphate (PtdIns(3)P)[52]. PtdIns(3)P production is responsible for the recruitment of downstream components of the autophagy pathway and is indispensable for autophagosome formation[53]. In addition, upon starvation, AMPK phosphorylates beclin-1 on S91/94, which is sufficient to induce lipid kinase activity of VPS34 complexes[54].

Bcl-2 (B-cell lymphoma 2) and Rubicon (RUN domain Beclin 1-interacting and cysteine-rich containing protein) are two known negative regulators of VPS34 complexes[55]. Under nutrient-enriched conditions, the hydrophobic groove in Bcl-2 interacts with the BH3 domain of beclin-1, which disrupts the beclin-1/VPS34 binding, reduces lipid kinase activity, and subsequently inhibits autophagy induction[56]. In contrast, upon stresses, Bcl-2 dissociates from beclin-1[56]. In addition, UVRAG induces the autophagy pathway by enhancing interaction of released beclin-1 with VPS34 and upregulates activity of VPS34 complexes[57]. Besides early stages of autophagy, UVRAG has been described to mediate autophagosome maturation via binding to the HOPS (homotypic fusion and vacuole protein sorting) complex[58]. This interaction promotes

lysosomal fusion with autophagosome[58]. Under basal conditions, Rubicon binds to the UVRAG subunit of VPS34 complexes, which results in disruption of the UVRAG-HOPS interaction and decreases VPS34 lipid kinase activity[58]. In addition, nutrient-activated mTORC1 has been shown to enhance Rubicon-UVRAG-containing VPS34 complexes through direct phosphorylation of UVRAG[50]. Taken together, mTORC1, ULK, and AMPK have been described to directly regulate the activity of the pro-autophagic VPS34 kinases, thus ensuring a tightly controlled burst of autophagy initiation in response to cellular stresses and underscoring the importance of VPS34 regulation.

I.2.2.2 Two ubiquitin-like protein conjugation systems (ATG12–ATG5-ATG16L1 and MAP1LC3 (LC3)

ATG12 and microtubule-associated protein 1 light chain 3 LC3 (the best characterized homologue of the yeast ATG8), involved in the autophagy pathway, are structurally related to ubiquitin[59]. Each of these proteins forms a distinct ubiquitin-like conjugation system, which is critical for autophagosome biogenesis[59].

First, ATG12 is activated by the E1-like enzyme ATG7 through the formation of a thioester bond[60]. Active ATG12 is recruited to the E2-like enzyme ATG10, which results in ATG12 conjugation to its target protein ATG5[61]. This interaction is irreversible, so ATG12 and ATG5 primarily exist in conjugated forms[61]. ATG5 recruits the complex to the coiled-coil protein ATG16L1 to form a trimeric ATG16L1-ATG5-ATG12 complex, which is essential for the formation and elongation of the autophagosomes through its function in LC3 lipidation[62].

The second ubiquitin-like conjugation system involves the conjugation of LC3 to the lipid PtdEth (phosphatidylethanolamine), which is commonly referred to as LC3-lipidation[63]. The C-terminus of ubiquitin-like protein LC3 is cleaved by ATG4 to form LC3-I, which allows it to be transferred to and activated by E1-like enzyme ATG7[63]. The active LC3-I is then transferred to E2-like enzyme ATG3[63]. ATG16L1-ATG5-ATG12 complex acts as an E3-like enzyme and recruits LC3-I to the membrane lipid PtdEth to form LC3-II, lipidated form of LC3[64]. Each subunit of the trimeric ATG16L1-ATG5-ATG12 has a distinct function in the processing of LC3[64]. ATG12 binds to ATG3 of the LC3-I complex, ATG5 functions as a catalytic subunit, and ATG16L1 is responsible for

the localization of the complex to the phagophore site[59]. LC3 lipidation catalyzed by ATG16L1 complex is critical to the autophagy pathway and is used as the measurement for autophagy induction[59].

I.2.2.3 WIPI proteins

WIPI (WD-repeat protein interacting with phosphoinositides) proteins belong to the human PROPPIN (β-propellers that bind phosphoinositides) family and consist of four members (WIPI1 to WIPI4) along with their splice variants[65]. WIPI1 and WIPI2 have been shown to localize at the inner and outer membrane of autophagosomes, which can be the result of their specific interaction with PtdIns(3)P through evolutionarily conserved residues[65]. In addition to PtdIns(3)P binding, WIPI proteins also function as essential PtdIns(3)P effectors at the nascent autophagosome[66]. More specifically, WIPI2 has been demonstrated to recruit the downstream ATG16L1 complex to the phagophore site for LC3 lipidation[66].

I.2.2.4 Transmembrane proteins

The two transmembrane proteins required for the autophagy pathway are ATG9 and VMP1 (vacuole membrane protein 1)[67]. Upon starvation conditions, ATG9 translocates from the Golgi network and late endosomes to peripheral sites overlapped with LC3-positive autophagosomes[68]. Starvation-mediated cycling of ATG9 requires ULK as well as VPS34 complexes[69,70]. ATG9 cycling has been shown to contribute to the delivery of membrane source to the autophagosome formation[71].

The induction of autophagy in response to stresses such as starvation or rapamycin treatment is VMP1-dependent and overexpression of VMP1 drives autophagy even under nutrient-enriched conditions[72]. In addition, VMP1 has been described to bind to the VPS34 complex subunit beclin-1[72]. Interestingly, a study has recently shown that TP53INP2 (tumor protein 53-induced nuclear protein 2), a novel VMP1-binding protein, translocates from the nucleus to autophagosomes and is responsible for recruiting beclin-1 and LC3 to autophagosomal sites, potentially via its interaction with VMP1[73]. Moreover, TP53INP2 only binds to LC3 and VMP1, but not

beclin-1[73]. Taken together, VMP1 might act as a transmembrane protein that targets downstream components to the phagophore during the process of autophagy.

I.3 Bulk versus selective autophagy

Autophagy has long been thought of as an essential but non-selective bulk degradation pathway triggered by nutrient deprivation[74]. However, research over the past decade has shown that autophagy also plays roles in maintaining intracellular homeostasis in non-starved cells by selectively breaking down cargo such as dysfunctional organelles, aberrant protein aggregates, lipid droplets, excess peroxisomes and invading pathogens[2]. Specific autophagy adapters are required for selective autophagy to recruit cargo to the site of autophagosome[75]. Moreover, it has been described that post-translational modifications add additional selectivity to substrate recognition and clearance[75].

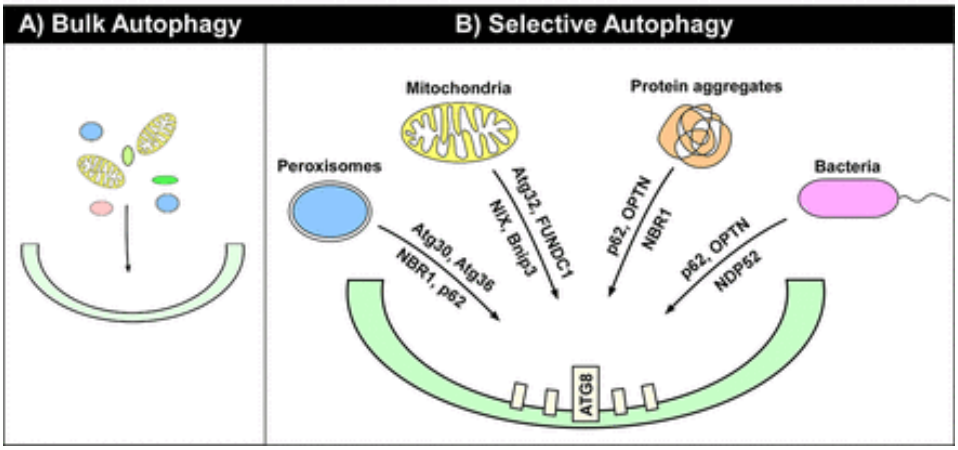

Fig 7. Bulk autophagy and selective autophagy[76].

I.4 Pathogens versus the host cells

I.4.1 Model pathogen

The genus *Salmonella*, a Gram-negative facultative intracellular anaerobic pathogen, consists of 2 species, *S. bongori* and *S. enterica* (*Salmonella bongori and Salmonella enterica,* respectively)[77]. Most of the *Salmonella* causing diseases in humans and animals are members of *S. enterica*[78]. *S. enterica* has been classified into 6 subspecies, which are further subdivided into over 2500 serovars differentiated by their flagellar, carbohydrate, and LPS (lipopolysaccharides) components[77]. Among the

studied bacterial strains, *Salmonella enterica* serovar Typhimurium (hereafter referred to as *Salmonella*) is perhaps the best characterized example of bacterial interaction with the host autophagic machinery and was therefore selected as a model pathogen for this study[79]. *Salmonella* can infect several phagocytic and non-phagocytic cells, including macrophages, dendritic cells, neutrophils, M cells, enterocytes, and epithelial cells[78]. Critical virulence genes in *Salmonella* have been mapped to SPIs (*Salmonella* pathogenicity islands)[80]. Of the 22 discovered SPIs in the genus *Salmonella,* SPI-1 and SPI-2 are the best-characterized[80]. SPI-1, which contains 40 kb of DNA, is responsible for injecting bacterial proteins into the cytosol of host cell and promoting cytoskeletal perturbation, thereby allowing bacterial invasion of host[81]. SPI-2 also consists of about 40 kb of DNA and is required for intracellular replication and survival of the bacteria[82]. SPI-1 and SPI-2 encode 2 distinct T3SS-1 and T3SS-2 (type III secretion system 1 and 2), which are syringe-like protein complexes capable of delivering virulence bacterial effectors into host cells and interfering with normal host cell signalling pathways[83]. Following insertion of effectors in the host, *Salmonella* are internalized and reside in a unique membrane-bound compartment, termed SCVs (*Salmonella*-containing vacuoles), a protected niche where they can replicate[84].

In addition, *Salmonella* can translocate virulence factors into host cells via production of OMVs (outer membrane vesicles) independently of SPI-1 T3SS and SPI-2 T3SS[85]. OMVs are produced from the surface of Gram-negative bacteria and consist of several outer membrane and periplasmic components, including proteins, LPS, phospholipids, and DNA. The vesicle sizes range from 10 to 300 nm[85]. OMVs not only disseminate toxins and protease-protected virulence factors distantly into the hosts to promote bacterial survival, but also function as bacterium-like decoys to uptake antimicrobial peptides to neutralize host immune responses[86].

I.4.2 Intracellular *Salmonella* fate

Following invasion into the host cell the majority of *Salmonella* reside in the SCV, an intracellular replicative niche adapted and modified by actions of both T3SS-1 and T3SS-2, to avoid the host defense systems[87]. The SCVs form a tubular network of long

and membranous structures termed *Salmonella*-induced filaments (Sifs), which promotes bacterial growth[88].

Intracellular *Salmonella* cause membrane damage to the SCV due to the pore-forming activity of T3SS-1 shortly after internalization to enter the host cytosol[89]. However, *Salmonella* can maintain the integrity of the SCV membrane through the function of a SPI-2 effector, SifA[88]. If damage to the SCV by T3SS-1 is not repaired, it may be cleared by the host cell innate immune response. *Salmonella* that escape the SCV are also capable of replicating in the cytosol; however, cytosolic growth is cell-dependent[90]. Cytosolic *Salmonella* in epithelial cells have been shown to hyper-proliferate, while replication is severely limited in the hostile cytosolic environment of macrophages[90]. While escape from the SCVs and cytosolic growth is a critical step for *Salmonella* infectious cycle[91], *Salmonella* with ruptured SCVs are targeted for ubiquitination and subsequently degradation in the autophagosomes[92]. *Salmonella* can also be recruited to the lysosomal compartment through a process called LC3-associated phagocytosis (LAP)[93]. LAP is a biologically and mechanistically distinct pathway from autophagy and is independent of core autophagy proteins including ULK1 and autophagy adaptors[93].

I.4.3 *Salmonella*-mediated induction of inflammation

The immune system induces a diverse array of inflammatory and antimicrobial responses to defend against invading pathogens[94]. The first line of defense is regulated by host-derived pattern recognition receptors (PRRs), which are capable of detecting pathogen-associated molecular pattern molecules (PAMPs)[95].

Among discovered PRRs, Toll-like receptors (TLRs) are the best-characterized[96]. Human TLR family consists of 10 isoforms (TLR1 to TLR10) located on the outer membrane of the cell (TLR1, 2, 4, 5, 6, and 10) or in intracellular compartments (TLR3, 7, 8, or 9)[96]. TLRs are the first PRRs to sense the presence of *Salmonella* and can detect several extracellular and endosomal *Salmonella*-derived PAMPs, including LPS (sensed by TLR4), peptidoglycan (sensed by TLR1/2), lipoproteins (sensed by TLR1/2/6), flagellin (sensed by TLR5), and DNA (sensed by TLR9)[97]. Upon recognition of PAMPs, TLRs recruit the downstream adaptors MyD88 and TRIF, which initiate

signal transduction pathways leading to the activation of the transcription factor NF-κB (nuclear factor-κB) or MAP (mitogen-activated protein) kinases to trigger the production of inflammatory cytokines, chemokines, and type I IFNs (interferon)[98].

In addition to TLRs which can detect the extracellular and intracellular PAMPs, NOD-like receptors (NLRs) are PRRs that sense infection and stress exclusively in the intracellular compartments[97]. Of the 22 human NLR genes, NOD1 and NOD2 are key sensors of distinct cytosolic bacterial peptidoglycan (PGN) fragments and are critical for host protection against pathogens[99]. NOD1 is activated in response to intracellular γ-D-glutamyl-*meso*-diaminopimelic acid (iE-DAP) present on Gram-negative bacteria and some Gram-positive bacteria[100]. NOD2 detects cytosolic muramyl dipeptide (MDP) found in all bacterial cell walls[101]. Upon binding to PAMPs, NOD1 and NOD2 self-oligomerize and recruit the CARD-containing adaptor RIP2 (receptor-interacting protein kinase 2) through homotypic CARD-CARD interactions, which initiates signalling cascades resulting in downstream NF-κB and MAPK-mediated inflammatory and antimicrobial responses[102].

I.4.4 Anti-bacterial autophagy (xenophagy)

Ubiquitination of *Salmonella* signals to the host cell defense triggering activation of inflammation and anti-bacterial responses[92]. Ubiquitination is a reversible enzymatic cascade reaction resulting in covalent binding of ubiquitin (Ub) to protein substrates, catalyzed by E1 (Ub-activating enzyme), E2 (Ub-conjugating enzyme), and E3 (Ub ligase enzyme)[103]. Ub can oligomerize through isopeptide bonds to create 8 unique chain patterns, including 7 lysine-branched chains (K6, 11, 27, 29, 33, 48, and 63) or a linear methionine chain M1[104]. Different Ub chains recruit different autophagy receptors[105]. *Salmonella* with damaged SCVs are marked with M1- and K63-linked Ub chains, which are detected by Ub-binding autophagy receptors, subsequently resulting in autophagic degradation of the bacteria[92].

Anti-bacterial autophagy (hereafter referred to as xenophagy) requires the core autophagy machinery as well as specialized mechanisms for targeting the pathogens[2]. The autophagy receptors p62 (sequesterosome 1), NDP52 (nuclear domain 10 protein52), and OPTN (Optineurin) consist of a LC3-interacting region (LIR) and a Ub-

binding motif, which can bind to ubiquitinated *Salmonella*[106]. LC3 is found on the autophagosomal membrane[66]. As such, upon infection, the autophagy adaptors serve as a platform to recruit the bacteria to the autophagosome site for degradation[107]. p62 was the first discovered mammalian autophagy cargo and plays a critical role in several autophagy pathways, including the selective degradation of protein aggregates and the removal of intracellular pathogens[108]. In addition to the ubiquitination pathway, ruptured SCVs can also be recognized by galectin-8, a cytosolic lectin[109]. NDP52 selectively binds and recruits galectin-8 to LC3 through LIR motif, thereby bridging the bacteria to phagophores to induce autophagy[109]. NDP52 has also been shown to work with OPTN to regulate *Salmonella* degradation[110].

Emerging evidence suggests a significant overlap between signalling in starvation- and pathogen-induced autophagy. For example, membrane damage from *Salmonella* has been described to induce a transient reduction in intracellular amino acid levels, which alleviates mTORC1-mediated repression of the autophagy pathway[111]. Additionally, xenophagy-specific protein IRGM (immunity-related GTPase M) has been shown to bind and/or regulate several factors involved in autophagy initiation including the VPS34 kinase complex, ULK1, and AMPK[112]. Importantly, loss of IRGM does not abrogate starvation-induced autophagy, but is required for efficient clearance of bacteria and is the most commonly targeted component of the autophagy pathway by RNA viruses[113]. Together these studies highlight that the induction of xenophagy involves several of the same upstream signalling regulators used in starvation-induced autophagy that are coupled with bacterial stress-specific factors including IRGM and galectins to coordinate the cellular response to pathogen. However, the precise signalling upstream of the autophagy pathway in response to bacterial infection and the specificity of these signals remain to be elucidated.

Materials and Methods

Antibodies and Reagents

Anti-PtdIns(3)P antibody was a generous gift from Millennium Pharmaceuticals. Anti-Beclin-1 (Cat#3495 for WB), phospho-Beclin-1 S15 (Cat#84966), phospho-Beclin-1 S93 (Cat#14717), phospho-ULK1 S757 (Cat#6888), phospho-ULK1 S317 (Cat#12753), ACC (Cat#3676), phospho-ACC S79 (Cat#11818), Raptor (Cat#2280), phospho-Raptor S792 (Cat#2083), mTOR (Cat#2983 for immunostaining), S6 (Cat#2317), phospho-S6 S235/236 (Cat#4858), phospho-S6K T389 (Cat#9234), phospho-p38 T180/182 (Cat#4511), and phospho-NF-κB S536 (Cat#3033) antibodies were purchased from Cell Signaling Technology. Anti-LC3B (Cat#PM036 for immunofluorescence) antibody was purchased from MBL. Anti-Vinculin (Cat#V9131), beta-Actin (Cat#A5441 clone AC-15) antibodies, lipopolysaccharides from Escherichia coli 0111:B4 (Cat#L4391-1MG), Resiquimod (Cat#SML0196-10MG), and Filipin III from Streptomyces filipinensis (Cat# F4767-1MG) were obtained from Sigma. Anti-LC3B (Cat#NB100-2220 for WB) and DYKDDDDK Epitope Tag (Cat#NBP1-06712 for WB) antibodies were purchased from Novus Biologicals. Anti-LPS FITC (Cat#SC-52223), VPS34 (Cat#SC-365404), and GST (Cat#SC-138) antibodies were purchased from Santa Cruz Biotechnology. Anti-p62 (Cat#ab207305 for immunofluorescence), S6K (Cat#ab32529), ATG14 (Cat#ab139727 for immunoprecipitation and WB), ULK1 555 (Cat#ab206612 for immunofluorescence), LAMP1 (Cat#ab25245 for immunofluorescence) antibodies, and dynasore (Cat# ab120192) were obtained from Abcam. Anti-p62 (Cat#GP62-C for WB) antibody was purchased from Progen Biotechnik. Anti-Sirtuin-1 (Cat#07-131) was obtained from Upstate/Millipore. Proteinase K (Cat# P8107S) was obtained from New England BioLabs. Digitonin (Cat#10188-874) was obtained from VWR. Neuron-derived exosomes were a kind gift from Dr. Gibbings, University of Ottawa.

Cell Culture

MEFs, HEK293A, and HCT116 were cultured in DMEM supplemented with 10% Bovine Calf Serum (VWR Life Science Seradigm). A549 cells were cultured in F-12K medium supplemented with 10% Fetal Bovine Serum (Hyclone). MCF-7 were cultured in EMEM

supplemented with 10% Fetal Bovine Serum (Hyclone). Amino acid free medium was made according to Gibco standard recipe omitting all amino acids and supplemented as above without addition of non-essential amino acids and substitution with dialyzed FBS (Invitrogen). Media was changed 1 hour before experiments. Bone marrow deprived macrophages (BMDMs) were a kind gift from Dr. Fullerton, University of Ottawa. LKB1 wild-type and knock-out MEF cell were a generous gift from Russell Jones. NOD1 knock-out and NOD1/2 knock-out HCT116 cells were a kind gift from Dr. Girardin, University of Toronto.

Generation of Stable Cell Line

Flag ULK1 with puromycin resistance was used to create a stable polyclonal population of cells expressing near endogenous level of ULK1. The cells expressing tagged ULK1 were maintained by 1 µg/mL.

Generation of knock-out cell lines using CRISPR/Cas9

HCT116 IRAK, TRAF6, STING, and NOD2 knockouts were generated using CRISPR/Cas9 targeting exon 1. IRAK guide RNA sequences: CACCGTCTTGTACGAGGTGCCGCCC and CACCGCCGACTGGTGCCAGTTCGGT. TRAF6 guide RNA sequence: CACCGTGTTACAGCGCTACAGGAGC. STING guide RNA sequences: CACCGAGAGCACACTCTCCGGTACC and CACCGCTGGGACTGCTGTTAAACG.

Bacterial and Viral Strains

Wild-type (SL1344), Inva mutant, and SsaR mutant *Salmonella* were kind gifts from Dr. Sad, University of Ottawa. Wild-type *Shigella* was obtained from Dr. Campbell-Valois, University of Ottawa. AIEC was a generous gift from Dr. Coombes, McMaster University. Bacteria were grown in Luria-Bertani broth (Fisher). Murine norovirus (MNV) were generous gifts from Dr. Thomas Smith, University of Texas.

Bacterial Infection

Overnight bacterial cultures of *Salmonella* were diluted 30-fold and grown to log phase (OD_{600} = 1.5), collected by centrifugation 10,000 g for 2 min, and resuspended in 1 mL

of PBS. Bacterial stock was then diluted 10-fold (MOI = 450) in DMEM supplemented with heat-inactivated BCS for infection. Cells cultured in antibiotic-free medium were infected with *Salmonella* and incubated at 37 degrees Celsius in 5% CO_2 for the indicated time. Cells were washed in PBS once before lysis. For gentamycin assays, the cells were infected, preceded or followed by incubation with gentamicin (50 µg/mL) for 0.5 hour. Gentamicin was added before and after bacterial infection to control for potential off-target effects of the drug (for example: the possibility that mTORC1 signalling may be altered by gentamycin addition). Bacteria were killed by incubation with 4% PFA for 15 min.

Preparation of bacterial supernatant

Overnight bacterial cultures of *Salmonella* were diluted 30-fold and grown to log phase (OD_{600} = 1.5), 1ml was collected by centrifugation at 10,000 g for 2 min, and resuspended in 5 mL of heat-inactivated DMEM. *Salmonella*-containing media was then shaken at 250 rpm for the indicate time points. Following the incubation, the bacteria were removed by centrifugation (10000 g for 2 min) and supernatant was filtered through a 0.45 uM filter.

OMV Purification

Wild-type *Salmonella* was grown in 4 mL of LB broth supplemented with carbenicillin at 37 degrees Celsius at 250 rpm. After 16-18 hours of incubation, all of bacteria were transferred to 1.5 L of LB and were shaken for extra 18 hours. The bacteria were then removed by centrifugation (15000 rpm, 30 min, 4 degrees Celsius). The collected supernatant was vacuum filtered and incubated overnight with OMV precipitation solution (300g of PEG, 43.9g NaCl in water up to 1L, 3x stock) at 4 degrees Celsius. OMVs were harvested by two centrifugations (4200 rpm, 30 min, 4 degrees Celsius) and one ultracentrifugation (28500 rpm, 3 hours, 4 degrees Celsius). The pellets were suspended in clear DMEM and stored at 4 degrees Celsius for future use. The size of OMV was determined by Nanoparticle Tracking Analysis using a Particle Metrix Zetasizer (Particle Metrix GmbH, Meerbusch, Germany). OMV samples diluted 1:100000 in PBS were captured with 11 positions. Data were analysed with the ZetaView 8.02.31 software. The concentration of OMV stock is $3.6*10^{11}$ particles/mL.

OMV modifications

Heat shock

Heat-inactivated OMVs were warmed at 55ºC for 5 minutes and diluted in complete media prior to treatment.

Paraformaldehyde Fixation

OMVs were fixed with 4% PFA for 20 min followed by inactivation with 1M Tris pH-8 for 30 min. Fixed OMVs were ultracentrifuged at 100 000g for 30 min, washed 2x with 1M Tris pH=8, and re-suspended in complete media prior to treatment.

Proteinase Treatment

OMVs were incubated in the presence or absence of proteinase K (1.6 units), or buffer alone for 30 mins prior to nucleofection (Lonza, used X-001 setting). The nucleofected OMVs were resuspended, washed 3x with PBS, and harvested by ultracentrifugation (100 000g for 30 min).

Western blot and Immunoprecipitation

Whole cell lysates were generated by direct lysis with 1X denaturing SDS sample buffer. Samples were boiled for 10 min at 95 degrees Celsius and resolved by SDS-PAGE. Immune complexes were obtained from cells lysed in mild lysis buffer [10mM Tris pH 7.5, 10 mM EDTA, 100 mM NaCl, 50 mM NaF, 1% NP-40, supplemented at time of lysis with protease and phosphatase inhibitor cocktails –EDTA (APExBIO)]. Protein A beads (Repligen) were washed 1X with MLB and mixed with antibodies and cleared cell lysates for 1.5-3 hours followed by one wash with MLB and inhibitors and 4 washes with MLB alone. Beads were boiled in 1X denaturing sample buffer for 10 min before resolving by SDS-PAGE.

Immunofluorescence

Cells were plated on IBDI-treated coverslips the night before treatments. Cells were fixed by 4% paraformaldehyde in PBS for 15 min, followed by permeabilization with 50 µg/mL digitonin in PBS for 10 min. Cells were blocked in blocking buffer (1% BSA and

2% serum in PBS) for 30 min then incubated with primary antibodies in the same buffer for one hour at room temperature. Slides were washed 2X in PBS and 1X in blocking buffer followed by incubation of secondary antibodies in blocking buffer for one hour at room temperature. Slides were washed 3X in PBS, stained with DAPI, and mounted. Images were captured with inverted epifluorescent Zeiss AxioObserver.Z1. In the case of outside/inside bacterial staining, before permeabilization, the cells were incubated with primary and following secondary antibodies in blocking buffer, accompanied by 3X PBS washes in between.

Quantification of immunofluorescence

Epifluorescent microscopy images were used to determine colocalization using an automated protocol built in the Volocity PerkinElmer imaging software to reduce bias. The same protocol was applied to each field of view and across samples. Quantification was performed on representative experiments with an average of 27 unique fields of view.

In vitro ULK1 Kinase Assay

ULK1 proteins were immunoprecipitated and extensively washed with MLB (once) and RIPA buffer (50 mM Tris at pH 7.5, 150 mM NaCl, 50 mM NaF, 1 mM EDTA, 1 mM EGTA, 1% SDS, 1% Triton X-100 and 0.5% deoxycholate) once, followed by washing with MLB buffer once followed by equilibration with ULK1 assay buffer (kinase base buffer supplemented with 0.05 mM DTT and 10 µM cold ATP per reaction). Reactions were rocked at 250 rpm at 37 degrees Celsius for 30 min and quenched by direct addition of 4X sample buffer followed by 10 min boiling and resolution by SDS-PAGE. The analysis of kinase reactions necessitated the separation of the kinase and substrate. *In vitro* kinase reactions were analyzed by western blot with the phospho-Beclin-1 antibody.

In vitro VPS34 Lipid Kinase Assay

Immunoprecipitated proteins were incubated with 40 µL of 1X kinase base buffer (200 mM HEPES pH 7.4, 50 mM $MgCl_2$, 10 mM EGTA, and 4 mM EDTA) supplemented with 0.5 mg/mL phosphatidylinositol, 0.25 mM cold ATP, 25 mM $MnCl_2$, and 0.25 mM DTT at

37 degrees Celsius for 30 min with vigorous shaking. After the reaction, the supernatant was separated from the beads and analyzed by dot blot. Beads were boiled in 1X denaturing sample buffer for 10 min before resolving by SDS-PAGE for the inputs.

Colony Forming Unit (CFU) Assay

Cells were infected with *Salmonella* for 1 hour. The infected cells were washed 2X and incubated with media containing 100 µg/mL Gentamicin for 0.5 hour, followed by 4-hour incubation with media containing 50 µg/mL Gentamicin. The samples were rinsed 3X with PBS and lysed with CFU buffer (0.1% Triton X-100 and 0.01% SDS in PBS). The lysates were serially diluted and plated onto LB agar plates containing Streptomycin. The plates were incubated at 37 degrees Celsius for 16-18 hours and the colonies were counted to determine the number of CFU.

Statistical analysis

Statistical analysis was performed on biological repeats using Image J. Error bars represent the standard deviation in normalized fold changes in observed induction or repression. Statistical significance was determined using paired Student's one-tailed T-test for two data sets.

Results

AMPK is activated by *Salmonella* and directly inhibits mTORC1

AMPK and mTORC1 signalling are critical upstream regulators in starvation-induced autophagy[22]. Previous reports have described that *Salmonella* infection can result in either mTORC1 activation or inhibition[111,114]. In order to determine the key upstream signalling events regulating xenophagy induction we first infected colon epithelial cells (HCT116) and bone marrow-derived macrophages (BMDM) with *Salmonella* and determined the phosphorylation status of established AMPK-target acetyl-CoA carboxylase (ACC) and mTORC1-target ribosomal protein S6 kinase (S6K), which migrates as doublet in some cell lines. Consistent with previous reports we found that mTORC1 activity is inhibited in colon epithelial cells, but activated in macrophages (Fig 8)[111,114]. Interestingly, we found that AMPK is activated in both colon epithelial cells and macrophages upon *Salmonella* infection by measuring changes in the AMPK-mediated phosphorylation of ACC (Fig 8).

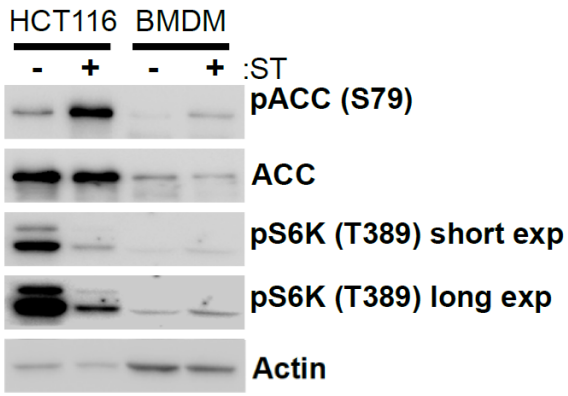

Fig 8. HCT116 cells and bone marrow-derived macrophages (BMDM) were infected with log phase *Salmonella* (ST) (unless otherwise stated a MOI of 450 was used) for 1 hour. Samples were immunoblotted for targets of mTORC1 (phospho-S6K) and AMPK (phospho-ACC).

Since both epithelial cells and macrophages are capable of inducing xenophagy, this raises the possibility that AMPK activation may be the primary signalling pathway responsible for activation of the autophagy kinases in the response to infection.

Therefore, we next sought to expand the analysis of AMPK regulation by *Salmonella* infection in multiple cell lineages including: kidney (HEK293A), lung (A549), fibroblast (MEF), and breast epithelia (MCF-7). We observed a potent activation of AMPK and repression of mTORC1 signalling as measured by downstream target phosphorylation in all cell lines tested (Fig 9). These results suggest that aside from macrophages AMPK activation and mTORC1 inhibition are the conserved response to *Salmonella* infection.

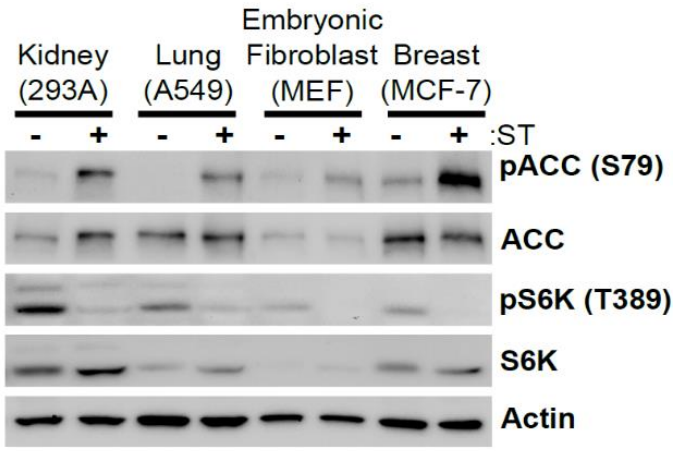

Fig 9. HEK293A, A549, MEF, and MCF-7 cells were treated with *Salmonella* for 1 hour to 1.3 hours. Whole cell lysates were immunoblotted using the antibodies indicated.

Importantly, we found that other gram negative bacteria including *Shigella flexneri and* adherent invasive *Escherichia coli* (AIEC) also elicited a potent activation of AMPK (Fig S1). As the xenophagic response is better defined in *Salmonella* than in *Shigella* or AIEC, we continued our characterization of xenophagy regulation using *Salmonella* as our model pathogen. We next confirmed that regulation of AMPK and mTORC1 signalling by *Salmonella* was consistent across various MOI used in literature. We found consistent effects on signalling from an MOI of 10 to 450, with a delay in signalling at lower MOI (Fig S2). However, the amplitude signalling changes at each MOI were consistent at peak induction (Fig S3). We moved forward with an MOI of 450, which in HCT116 cells at 1hr, gives an infection rate of 10 percent (Fig S4).

A previous report in macrophages suggested that Sirt-1 stability is an important regulator of mTORC1 activity, having maximal effect at 4-5 hours post infection, which is considerably later than the 1-hour time point we had used. In order to determine if

Sirt-1 stability is playing a role in non-macrophages at a later time point we performed a temporal analysis of AMPK and mTORC1 signalling in response to *Salmonella* infection. We found that the activation of AMPK and inhibition of mTORC1 begin at 1 hour post infection and occur in the absence of changes to Sirt-1 levels in all time points tested (Fig 10). These results indicate regulation of mTORC1 in epithelial cells does not require destabilization of Sirt-1.

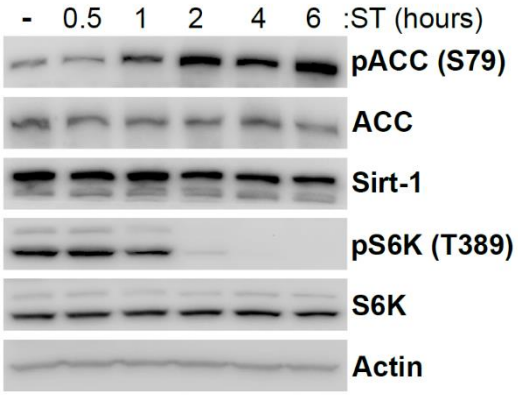

Fig 10. HCT116 cells were treated with *Salmonella* and lysed at the indicated timepoints. Samples were immunoblotted using the antibodies indicated.

Membrane damage caused by *Salmonella* infection has been shown to result in amino acid loss and mTORC1 inhibition[111]. However, AMPK is also known to inhibit mTORC1 directly and indirectly in an amino acid-independent manner[44]. This led us to ask if AMPK signalling contributes to mTORC1 inhibition upon infection. To monitor the effects of AMPK signalling on mTORC1 we infected cells in the absence or presence of AMPK inhibitor compound C, which is a potent inhibitor of AMPK most often used in conjunction with the AMPK activators such as salicylate[115,116]. Surprisingly, we found that *Salmonella*-induced inhibition of mTORC1 is blocked by AMPK inhibitors, indicating that AMPK signalling contributes to the inhibition of mTORC1 independently of regulation by amino acids (Fig 11).

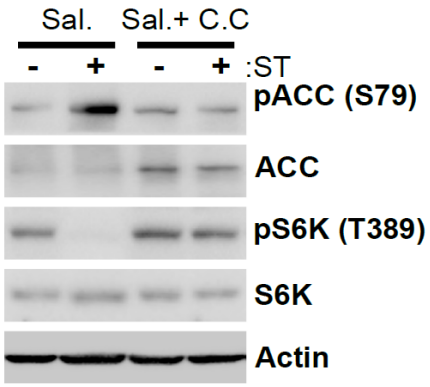

Fig 11. AMPK was activated by salicylate (Sal.) and HCT116 cells were infected with *Salmonella* in the presence or absence of AMPK inhibitor Compound C (C.C). Whole cell lysates were immunoblotted using the antibodies indicated.

In order to confirm that AMPK signalling is responsible for the reduction in mTORC1 signalling we infected the AMPK α 1 and α 2 (the catalytic subunits of AMPK) double knock-out MEF and analyzed mTORC1 activity. We found that *Salmonella*-induced inhibition of mTORC1 signalling is greatly reduced in the AMPK double knock-out MEF, indicating AMPK signalling promotes the inhibition of mTORC1 upon infection independent of amino acid loss (Fig 12).

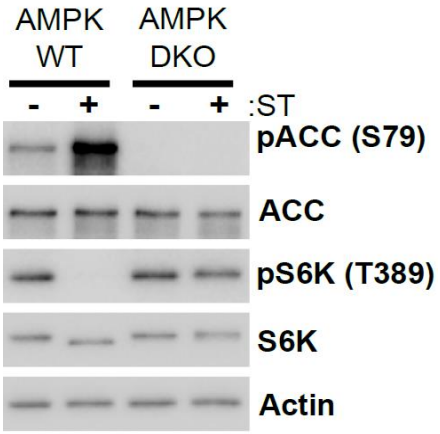

Fig 12. AMPK wild-type (WT) and deficient (AMPK alpha 1/2 knockout) MEF cells were infected with *Salmonella* for 1.3 hours. mTORC1 and AMPK activities were analyzed using the indicated antibodies.

AMPK can inhibit mTORC1 through multiple mechanisms. Arguably, the most potent and direct mechanism is AMPK-mediated inhibitory phosphorylation of the

mTORC1 subunit Raptor[44]. Therefore, we sought to determine if *Salmonella* infection results in an increase in direct inhibition of the mTORC1 kinase by AMPK. Cells were infected with *Salmonella* and inhibitory phosphorylation of the mTORC1 subunit Raptor by AMPK was analyzed in conjunction with AMPK and mTORC1 target genes. We found that *Salmonella* infection results in a potent upregulation of Raptor phosphorylation and mTORC1 inhibition (Fig 13).

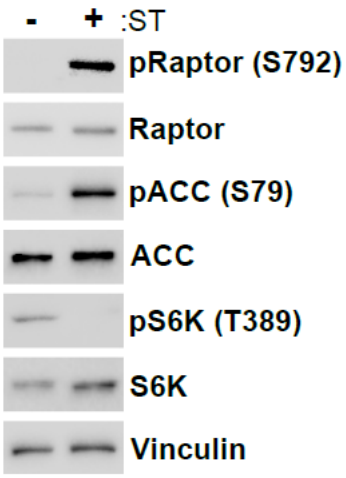

Fig 13. HEK293A cells were infected with *Salmonella* for 1.3 hours. AMPK-mediated inhibition of the mTORC1 subunit Raptor (phosphorylation of Raptor at S792) was analyzed by western blot.

Finally, we determined that LKB1, an upstream activator of AMPK, is required for activation of AMPK and inhibition of mTORC1 in response to *Salmonella* (Fig S5). Collectively, these experiments establish that in response to *Salmonella* mammalian cells activate AMPK (an upstream activator of the autophagy pathway), which in turn directly inhibits mTORC1 (a potent repressor of autophagy initiation), thereby setting the stage for autophagy initiation (Fig 14).

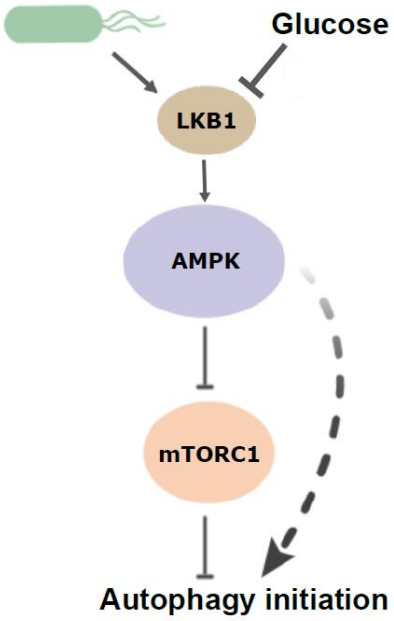

Fig 14. Diagram of signalling (A)-(F).

Salmonella-induced changes to AMPK-mTORC1 signalling do not require bacterial entry or SCV damage

Changes in mTORC1 signalling and the resulting activation of xenophagy have been described exclusively in the context of internalized bacteria[111]. Inhibition of mTORC1 upon infection has been shown to promote clearance of intracellular bacteria by xenophagy[117]. Similarly, AMPK activation has been proposed to be a result of membrane damage caused by bacterial internalization, which leads to loss in intracellular ATP levels thereby activating AMPK[114]. Intracellular expansion of *Salmonella* is promoted by 2 type three secretion systems (T3SS), encoded by two pathogenicity islands (SPI-1 and SPI-2), which promote invasion and intracellular survival respectively[80]. Membrane damage caused by *Salmonella* occurs during invasion as well as through the disruption of the SCV[118].

To determine if membrane damage is responsible for the activation of AMPK we infected cells with wild-type *Salmonella*, invasion-deficient SPI-1 mutants (InvA null)[119], or replication-compromised SPI-2 mutants (SsaR null)[120] and assayed for AMPK

activation and mTORC1 inhibition. Colony forming assays were performed from cell lysates 1 hour post infection to confirm the invasion deficiency of SPI-1 mutants (Fig 15, right panel). Surprisingly, we found that AMPK activation was still observed in *Salmonella* defective for invasion and SCV disruption (Fig 15, S6). Similarly, mTORC1 inhibition is also observed upon infection with all three *Salmonella* strains (Fig 15). This indicates that AMPK activation likely does not require membrane damage associated with bacterial entry or disruption of the SCV.

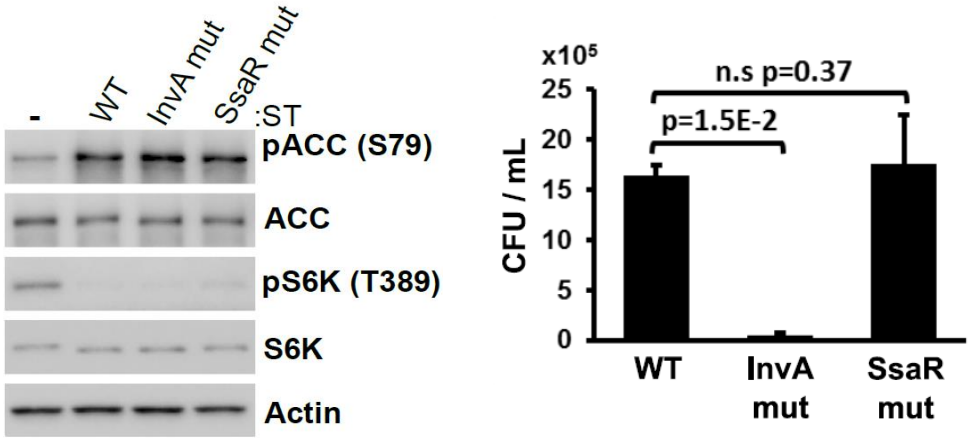

Fig 15. HCT116 cells were infected with wild-type, invasion-deficient (InvA mutant), or replication-deficient (SsaR mutant) *Salmonella* (unless otherwise stated a MOI of 450 was used) for 1 hour. Xenophagy rates were examined through Colony Forming Unit (CFU) assays. Whole cell lysates were immunoblotted for AMPK and mTORC1 activities using the antibodies indicated.

To analyze AMPK activation by *Salmonella* at a single cell level we infected cells immunostained for AMPK-mediated phosphorylation of ACC and *Salmonella*. Using identical acquisition settings we saw a clear increase in AMPK-target phosphorylation upon treatment with *Salmonella* (Fig 16). Importantly, in *Salmonella*-treated cells we observed AMPK activation homogenously throughout the sample with no difference between cells with or without internalized bacteria (Fig 16, bottom right panel). These data further support the notion that AMPK activation is due to extracellular bacteria independent of invasion or pathogenicity.

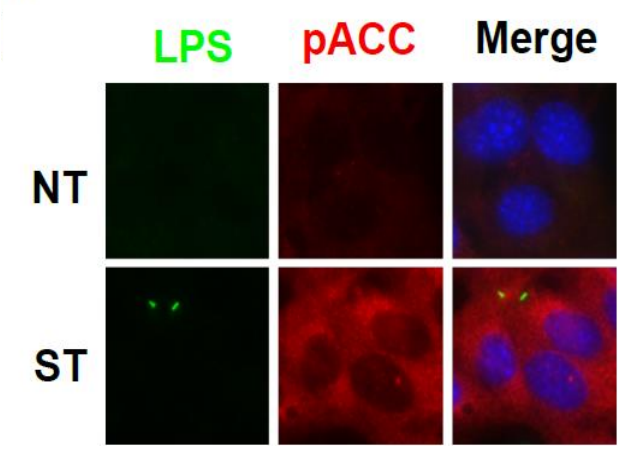

Fig 16. MEF cells were infected with *Salmonella* for 1 hour. Immunostaining was performed for AMPK-mediated phosphorylation of ACC and LPS.

Next, we sought to determine if removing extracellular *Salmonella* is sufficient to return AMPK and mTORC1 signalling to basal levels. Extracellular bacteria were removed in one set of samples or left on in another, prior to lysis. However, cells were infected and treated with gentamycin for the same duration, which controlled for potential effects of the antibiotic on signalling and produced an equivalent rate of infection (Fig S7). Consistent with previous data, we observed that removal of extracellular *Salmonella* results in a loss of AMPK activity and restoration of mTORC1 signalling (Fig S7).

Finally, we sought to show mathematically the independence of AMPK/mTORC1 signalling and bacterial entry through analysis of infection rates and mTORC1 inhibition. As in the previous sets of experiments we analyzed samples by western and IF using duplicated plates. However, in order to obtain the highest possible estimate for the percentage of infected cells we infected the cells in the presence of an inhibitor of autophagic flux Bafilomycin A1, thereby blocking autophagic clearance of bacteria, which could cause an under-representation of the actual number of infected cells. Using these stringent conditions we found that approximately 10% of cells contain internalized bacteria and that mTORC1 activity is inhibited over 90% (Fig 17). Under these conditions, we would expect that if internalized bacteria were required for

mTORC1 inhibition that the inhibition should only approach 10% (the proportion of cells infected) rather than the 90% we observed.

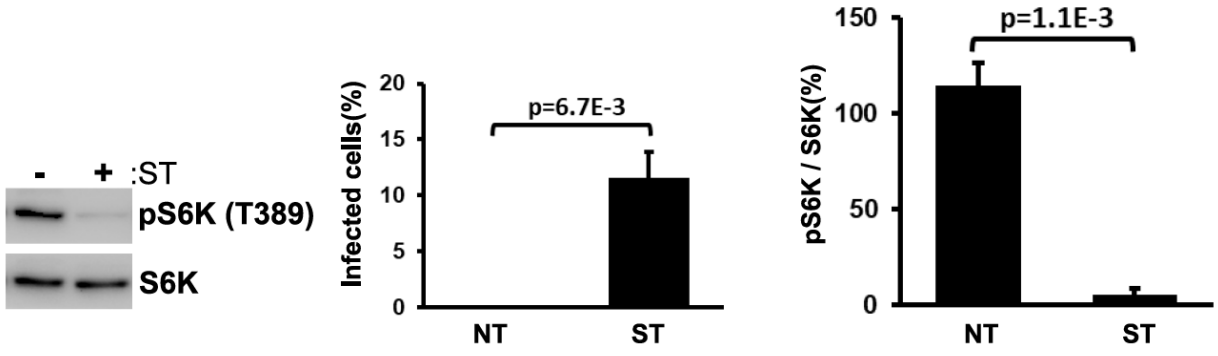

Fig 17. Inhibition of mTORC1 was quantified from western blot data derived from biological replicates and compared to overall infection rate to examine if mTORC1 inhibition could be explained by the proportion of cells with bacterial internalization.

Finally, we determined that AMPK activation could be elicited by the filtered supernatant from pelleted *Salmonella,* indicating a bacterially-released factor is sufficient for activation of AMPK in mammalian cells (Fig S8).

Collectively, our data show that regulation of AMPK and mTORC1 signalling can occur independently of *Salmonella* pathogenicity and invasion. Conceptually, this is extremely interesting as it means that the cell is poised to activate xenophagy even before the bacteria enter the cell.

Salmonella-induced signalling to AMPK and mTORC1 does not result in an induction of bulk autophagy

mTORC1 is a potent repressor of mammalian autophagy and directly inhibits the ULK1 and VPS34 kinase complexes, which are required for autophagy initiation[22,50]. Removal of amino acids is sufficient to dissociate mTORC1 from the lysosome and potently activate autophagy. We therefore sought to observe whether mTORC1 localization and autophagy induction are similarly affected by host cell detection of *Salmonella*. First, we treated cells either with *Salmonella* or amino acid withdrawal. As expected the localization of mTORC1 is primary lysosomal under basal conditions as

determined by colocalization between mTOR and lysosomal marker LAMP1 (Fig 18). Interestingly, we found that both amino acid starvation and extracellular *Salmonella* greatly reduce the localization of mTOR to the lysosome (Fig 18). The observed loss of mTORC1 localization from lysosomes under starvation or infection should both result in a de-repression of autophagy initiation.

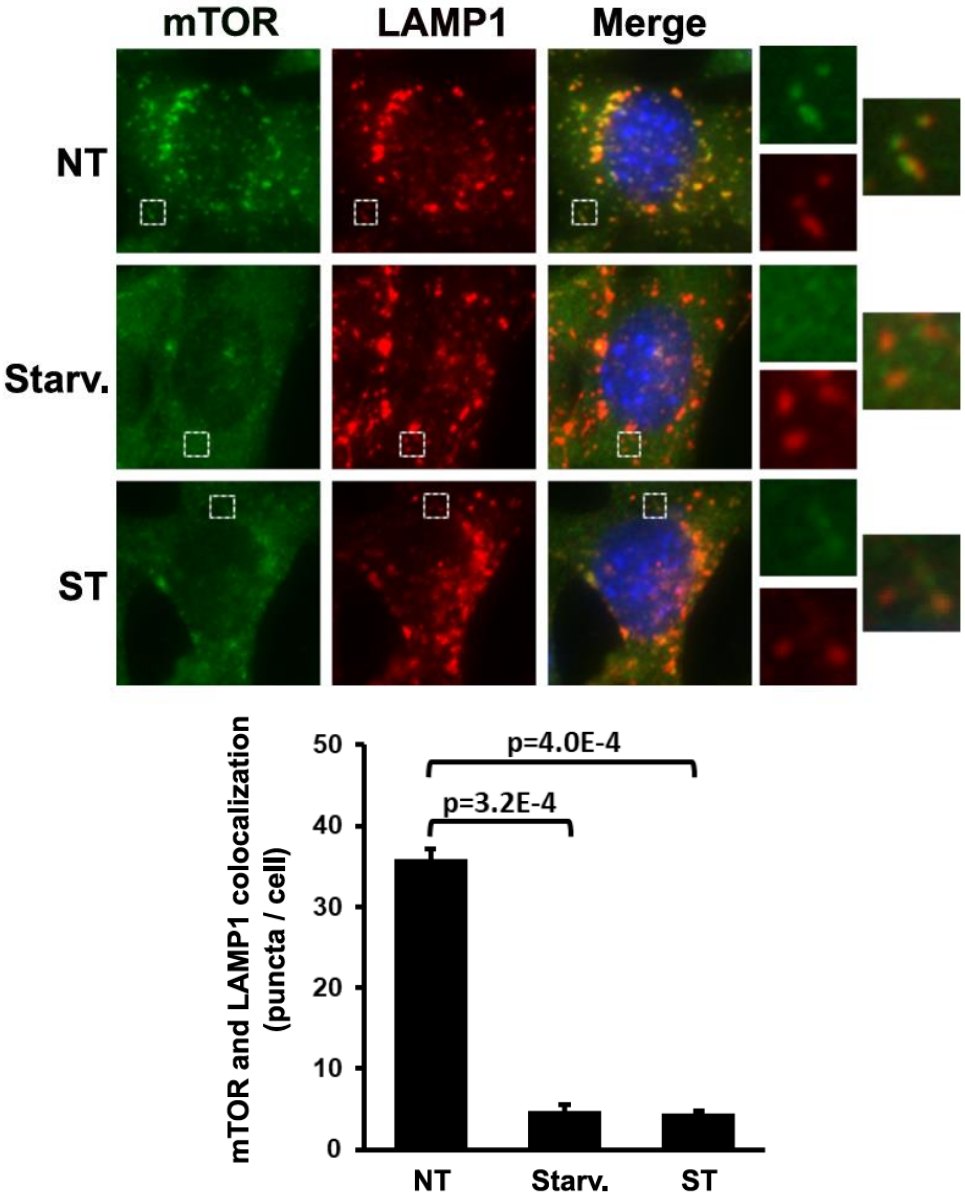

Fig 18. MEF cells were treated with either full medium, starvation medium (HBSS), or *Salmonella* for 1 hour. LAMP1 (red, lysosomal marker) and mTOR (green) co-localization was visualized and quantified by immunofluorescence.

We next sought to determine if inhibition of mTORC1 by *Salmonella* results in an increase in autophagy in uninfected cells. As expected, amino acid withdrawal results in a potent increase in autophagosome formation in the majority of cells as determined quantification of immunostaining for endogenous LC3B puncta (Fig 19). Surprisingly, we did not observe a similar induction in bulk autophagy in *Salmonella*-treated cells (Fig 19). Moreover, while we observed endogenous LC3B colocalization to internalized bacteria, infected cells similarly do not display an increase in bulk autophagy (Fig 19, S9). These data indicate mTORC1 inhibition in response to *Salmonella* is not sufficient to induce autophagy and the autophagic activity we observe is largely limited to the targeting of pathogen, sparing cytoplasmic constituents.

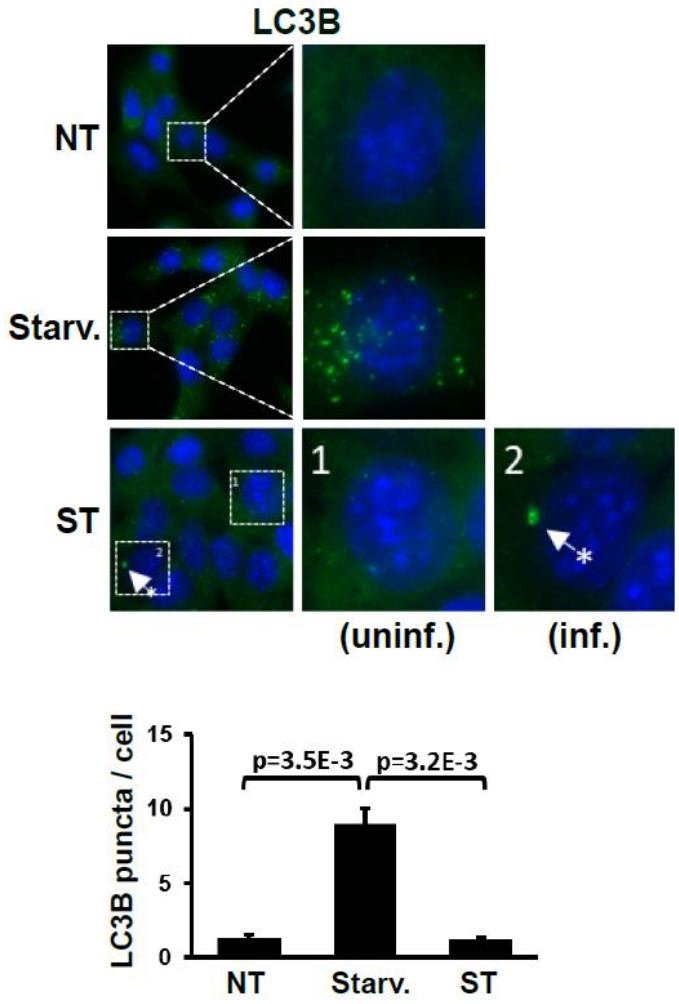

Fig 19. MEF cells were treated with either full medium, starvation medium (HBSS), or *Salmonella* for 1 hour. LC3B (green) puncta were visualized and quantified by immunofluorescence.

To further verify the regulation of autophagy in response to *Salmonella* we analyzed the autophagic adaptor p62, which will mark bacteria targeted for clearance by autophagy (as well as starvation-induced autophagosomes) but not bacteria captured by LC3-associated phagocytosis (LAP). Immunostaining for endogenous p62 shows a dramatic induction of bulk autophagy upon amino acid starvation (Fig 20). However, consistent with our LC3B staining we did not observe any increase in p62-associated bulk autophagy in *Salmonella*-treated cells even with internalized bacteria (Fig 20, S10).

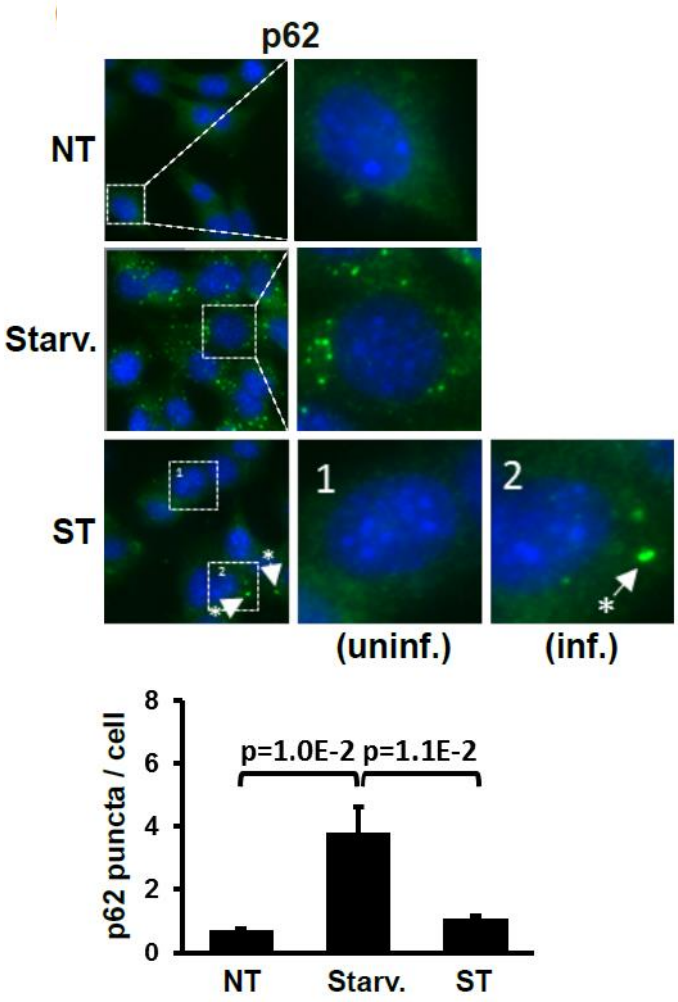

Fig 20. MEF cells were treated with either full medium, starvation medium (HBSS), or *Salmonella* for 1 hour. p62 (green) were visualized and quantified by immunofluorescence.

We next sought to confirm the effects of infection on the autophagy pathway through measurement of autophagy flux. Cells were treated with *Salmonella* or amino acid withdrawal in the presence or absence of an inhibitor for autophagosomal turnover (Chloroquine) and measured the accumulation of lipidated LC3B by western blot. We observed a robust accumulation of lipidated LC3B upon amino acid starvation, but not *Salmonella* treatment when compared to untreated samples (Fig 21).

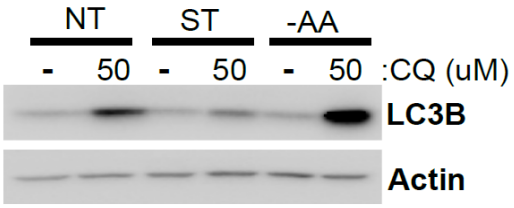

Fig 21. MEF cells were treated with either full medium, *Salmonella,* or starvation medium and with or without 50 μM chloroquine for 1 hour. LC3B signaling was then analyzed by western blot.

We next sought to compare autophagy induction to the levels of AMPK activation and mTORC1 inhibition by established methods to induce bulk autophagy to that induced by *Salmonella*. We observed that AMPK activation by glucose starvation was higher, but comparable, to that induced by infection (Fig 22). Similarly, mTORC1 signalling was undetectable after Torin-1 treatment, but still comparable to the inhibition elicited by *Salmonella* (Fig 22). However, analysis of the clearance of the autophagy adaptor p62 obviously showed the induction of bulk autophagy was absent in the cells infected with either *wild-type* or invasion-deficient *Salmonella*. This indicates that the blockage of autophagy induction occurs downstream of mTORC1 and AMPK.

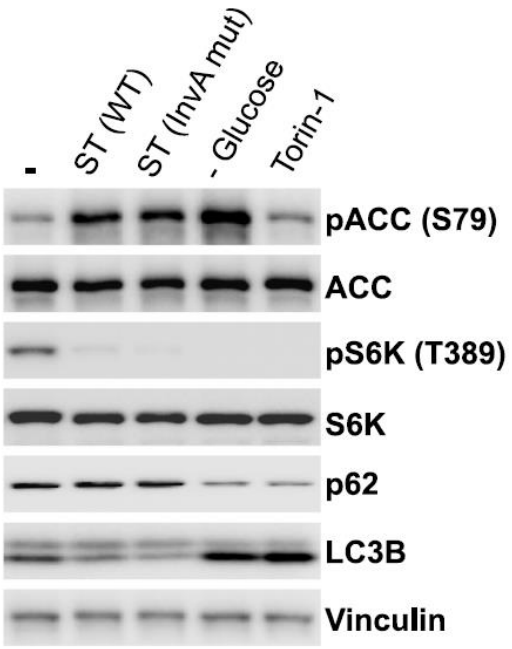

Fig 22. MEF cells were treated with either *Salmonella* (wild-type)*, Salmonella* (InvA mutant), glucose starvation medium, or 0.2 μM Torin-1 (mTORC1 inhibitor) for 1 hour. Western blot was used to examine autophagy flux (LC3B-lipidation and p62 clearance).

ULK1 kinase is a direct downstream target of both AMPK and mTORC1. Under starvation ULK1 is activated and localizes to newly forming autophagosomers to phosphorylate downstream targets required to promote autophagosome formation. Therefore, we next analyzed the localization of ULK1 to determine if autophagy initiation may be blocked under infection, downstream of mTORC1. As expected when mTORC1 was inhibited by amino acid starvation we found a robust increase in punctate ULK1 structures, which is indicative of bulk autophagy[121]. However, under infection we observed ULK1 puncta were largely limited to bacterial-containing vesicles, indicating that the *Salmonella*-induced autophagy block is at or upstream of ULK1 (Fig 23).

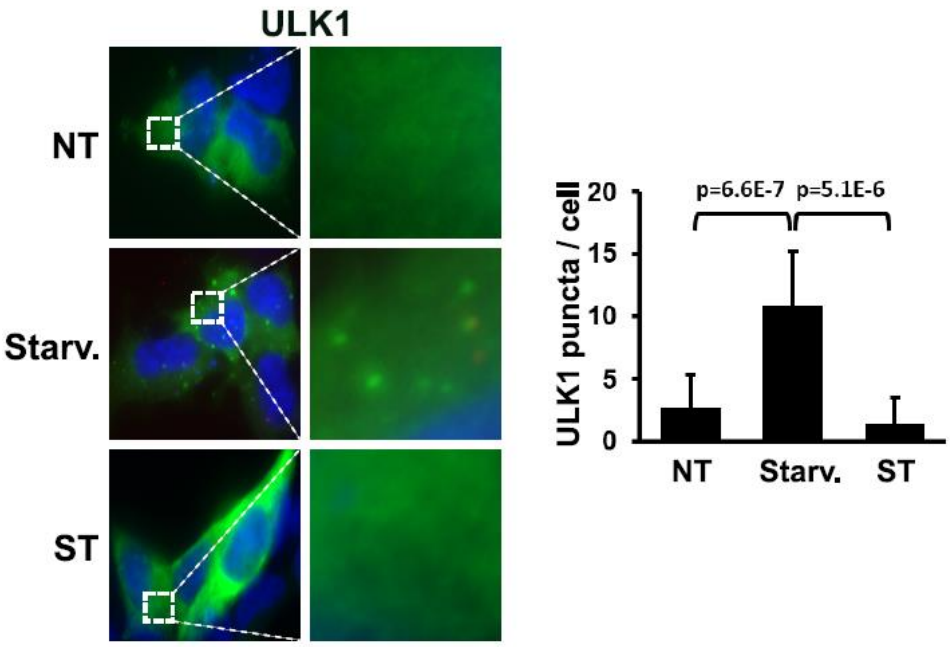

Fig 23. HEK293A transiently expressing GST HA ULK1 were treated with either full medium, amino acid starvation medium, or *Salmonella* for 1.33 hours. HA tag was immunostained to demonstrate ULK1 localization.

Next, in order to examine whether Torin-1 could rescue bulk autophagy under infection we treated cells with wild-type or InvA mutant *Salmonella* in the presence or absence of Torin-1. Surprisingly, we observed that both wild-type and InvA-null bacteria eliminate Torin-1-induced bulk autophagy independently of mTORC1 regulation and cellular invasion (Fig 24, S11).

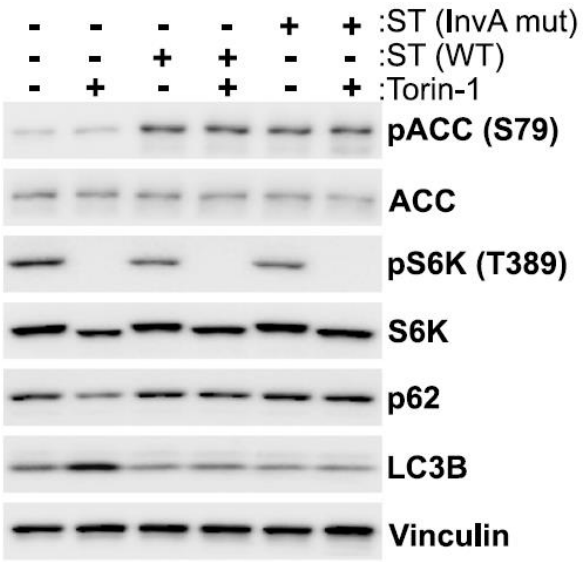

Fig 24. MEF cells were treated with either *Salmonella* (wild-type) or *Salmonella* (InvA mutant) in the presence or absence of Torin-1 for 1 hour. Autophagy markers LC3B and p62 were then analyzed by western blot.

Collectively, these data reveal a surprising level of specificity in the regulation of xenophagy induction. To our knowledge this is the first demonstration of mTORC1 inhibition, which is not accompanied by autophagy induction. This raises the exciting possibility that in response to *Salmonella* detection the cell initiates signalling events that 'prime' the cell for autophagic clearance of the bacteria without needlessly degrading components of the cytosol through induction of bulk autophagy.

AMPK activates ULK1 and VPS34 kinases in response to *Salmonella*

In order to determine if regulation of mTORC1 and AMPK signalling is capable of activating autophagy-promoting enzymes in the absence of bulk autophagy induction we first looked at phosphorylation of the ULK1 protein kinase. ULK1 activity has been described to be inhibited by mTORC1-mediated phosphorylation (Ser757) and activated by AMPK-mediated phosphorylation (Ser317) under nutrient starvation[122]. Using 293A cells stably expressing tagged ULK1 we immunoprecipitated ULK1 treated with or without *Salmonella* and immunoblotted for activating or inhibitory ULK1 phosphorylation. We observed that despite the lack of bulk autophagy induction ULK1 is phosphorylated

by AMPK and has a reduction in mTORC1-mediated phosphorylation, both of which should lead to activation of the kinase activity (Fig 25).

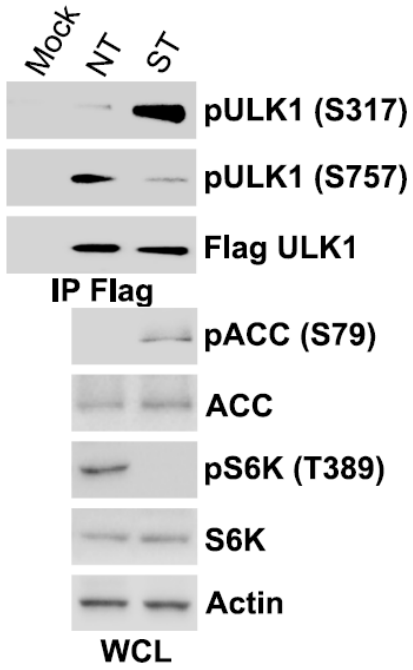

Fig 25. HEK293A cells stably expressing flag-ULK1 were infected with *Salmonella* for 1 hour, followed by flag-ULK1 pull down. AMPK-mediated activation (S317) and mTORC1-mediated inhibition (S757) of ULK1 were examined by western blot.

In order to ascertain if ULK1 activity is induced and whether this activity is dependent on AMPK signalling we transfected tagged ULK1 into AMPK wild-type and α 1/2 knockout MEF and performed an *in vitro* kinase assay using bacterially purified beclin-1, a known downstream target[52], as substrate. We observed that the kinase activity of ULK1, measured by beclin-1 (Ser15) phosphorylation, is increased upon infection in wild-type MEF but not AMPK-deficient cells (Fig 26), indicating that AMPK signalling promotes ULK1 activation in response to *Salmonella* detection.

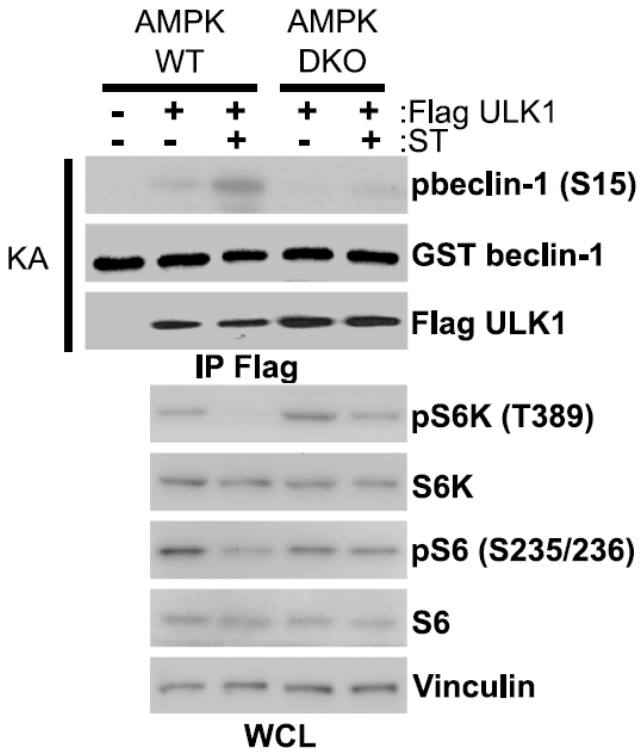

Fig 26. AMPK wild-type and AMPK alpha 1/2 knockout MEF cells transfected with flag-ULK1 were treated with or without *Salmonella* for 1 hour, followed by flag-ULK1 pulldown. An *in vitro* kinase assay was then performed using bacterially purified beclin-1, a known downstream target of ULK1, as substrate. ULK1 activity was then determined by measurement of phosphorylation of beclin-1 at S15.

In addition to regulating ULK1 activity AMPK has been shown to promote the activity of proautophagic VPS34 lipid kinase complexes through direct phosphorylation[54]. Therefore, we next sought to determine if autophagy promoting signalling from AMPK extends to VPS34, which is downstream of ULK1 in autophagy initiation. In response to glucose deprivation AMPK was previously shown to phosphorylate VPS34 component beclin-1 (on Ser93), which is sufficient to increase the activity of VPS34 containing enzymes[13]. We found that *Salmonella* treatment results in a robust increase in endogenous beclin-1 phosphorylation by AMPK (Fig 27).

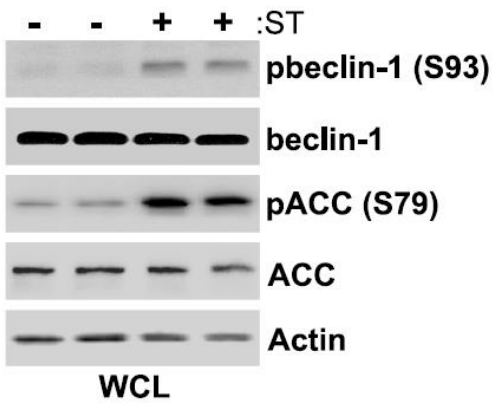

Fig 27. HCT116 cells were infected with *Salmonella* for 1 hour in duplicate. AMPK-mediated phosphorylation of the VPS34 subunit beclin-1 at S93 was determined by western blot.

Next, we wished to examine the activation of ULK1 and VPS34 kinases in comparison with amino acid and energy starvation. We observed that ULK1 activation as measured by increase in AMPK-mediated phosphorylation (S317) and loss of mTORC1-mediated inhibitory phosphorylation (S757) was similar to that induced by glucose starvation (Fig 28). Consistently, we observed a roughly equivalent AMPK-mediated activation of VPS34, indicating that AMPK-driven autophagy by energy starvation and *Salmonella* infection were comparable in promoting activation of autophagy kinases (Fig 28).

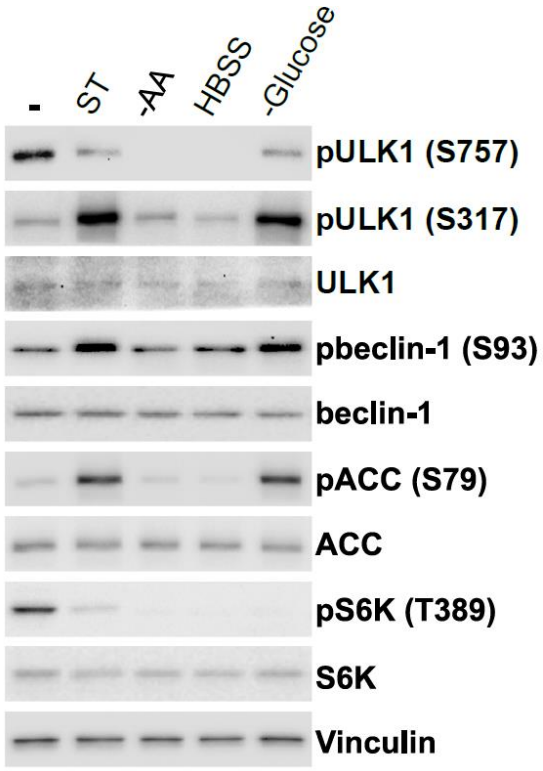

Fig 28. MEF cells were treated with either full medium, *Salmonella*, amino acid starvation medium, HBSS, or glucose deprivation medium for 1 hour. The regulation of ULK1 and the VPS34 subunit beclin-1 was determined by western blot.

We then sought to determine if the activity of proautophagic VPS34 complexes (those that contain beclin-1 and ATG14) is increased upon treatment with *Salmonella*. 293A cells transiently transfected with tagged ATG14 were treated with or without *Salmonella* and ATG14-containing VPS34 complexes were immunoprecipitated and analyzed by an *in vitro* lipid kinase assay at dot-blot assay as previously described[121]. We found that *Salmonella* treatment results in a significant upregulation of VPS34 activity as measured by the production of phosphatidylinositol(3)phosphate (PtdIns(3)P) from phosphatidylinositol (PtdIns) (Fig 29).

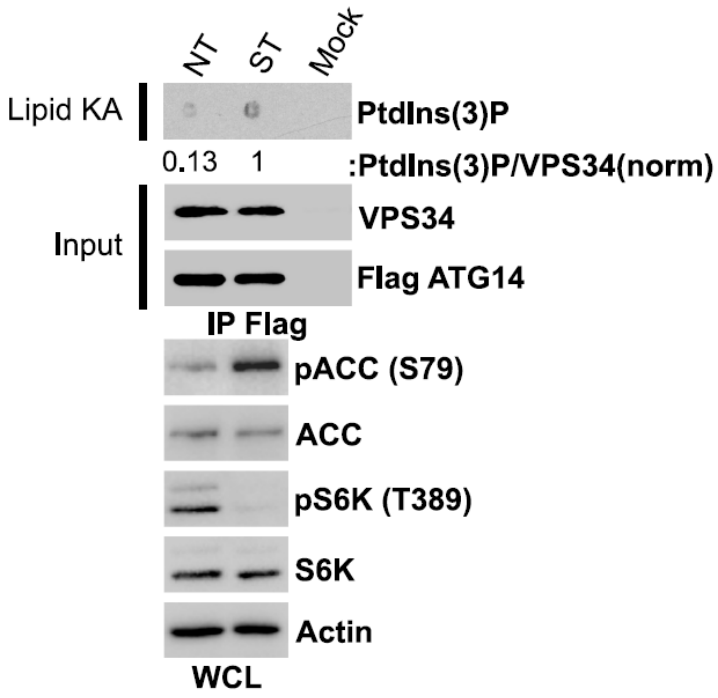

Fig 29. HEK293A cells transfected with flag-ATG14 were treated with or without *Salmonella* for 1 hour, followed by flag-ATG14 pulldown. The activity of ATG14-containing VPS34 complexes was analyzed by an *in vitro* lipid kinase assay and dot-blot assay blotting for PtdIns(3)P. Whole cell lysates were immunoblotted for analysis of AMPK and mTORC1-signalling.

Next we sought to show the regulation of VPS34 activity endogenously. MEF were treated with or without *Salmonella* and endogenous ATG14-containing VPS34 complexes were immunoprecipitated and subjected to an *in vitro* lipid kinase assay. Consistent with our observation that *Salmonella* infection promotes AMPK-mediated activation of beclin-1-containing VPS34 complexes we observed that the activity of VPS34 is enhanced upon exposure to *Salmonella* (Fig 30).

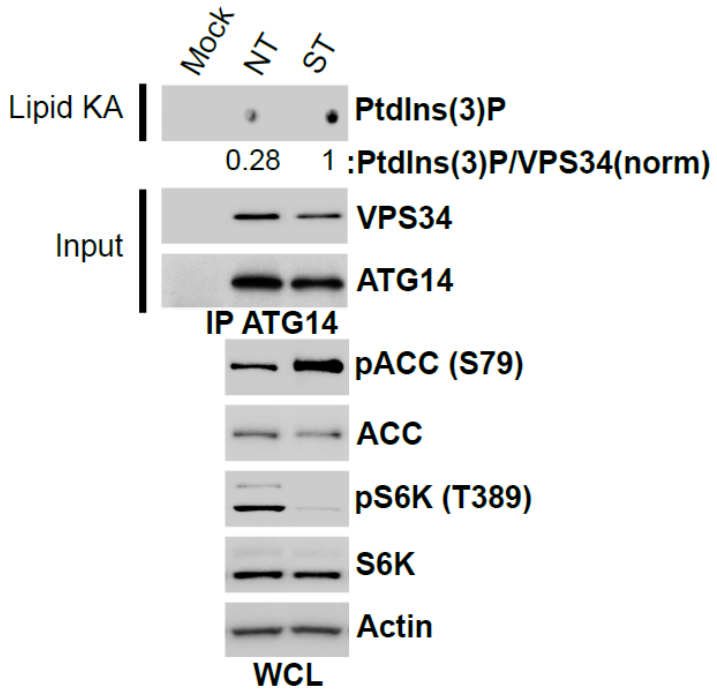

Fig 30. HEK293A wild-type cells were treated with or without *Salmonella* for 1 hour, followed by immunoprecipitation of endogenous ATG14. The activity of ATG14-containing VPS34 complexes was analyzed by an *in vitro* lipid kinase assay and dot-blot assay as described above. Whole cell lysates were immunoblotted for analysis of AMPK and mTORC1 signalling.

Together, our data indicate AMPK-mediated phosphorylation of the ULK1 and VPS34 kinase complexes results in their activation in response to *Salmonella* treatment, despite the absence of bulk autophagy induction (Fig 31). Moreover, we found that similar to *wild-type*, InvA-mutant *Salmonella* is also capable of activating ULK1 and VPS34 kinases in both epithelial cells and macrophages (Fig S12, S13, S14, S15). This raises the possibility that detection of pathogen results in an AMPK-dependent “priming” of key autophagy kinases responsible for induction of xenophagy, which may act to enhance the rate of bacterial capture by the autophagy pathway should invasion occur.

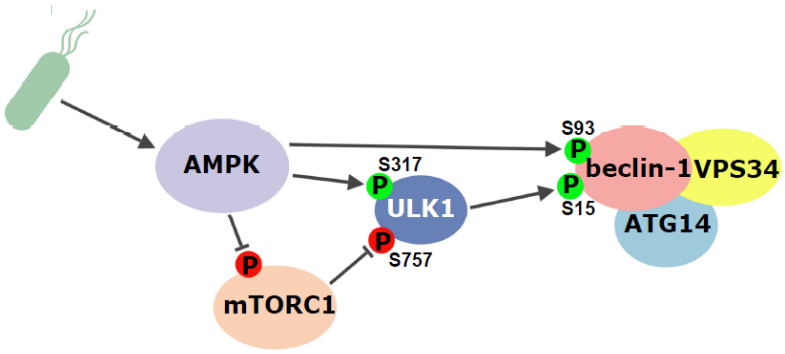

Fig 31. Model of AMPK-mediated activation of autophagy kinases upon detection of *Salmonella*.

Detection of pathogen-derived outer membrane vesicles (OMVs) promotes AMPK activation

We next sought to determine the mechanism by which the host cell detects *Salmonella* and activates AMPK. Mammalian cells have several pathogen recognition receptors (PRRs), which are capable of detecting a range of bacterial macromolecules and activate the host immune response[97]. The best characterized of these receptors are the Toll-like receptors (TLRs), which are capable of detecting LPS, bacterial DNA, or bacterial proteins including flagellin[96]. To determine if activation of TLRs was required for AMPK upregulation in response to extracellular bacteria we activated TLR receptors with lipopolysaccharide (LPS), R848 (resiquimod), and murine norovirus 1 (MNV1) that activate TLR4, TLR7/8, and TLR3/7/8, respectively[123]. Analysis of AMPK activation by western blot clearly showed that TLR ligands and MNV1 were not capable of activating AMPK signalling (Fig 32).

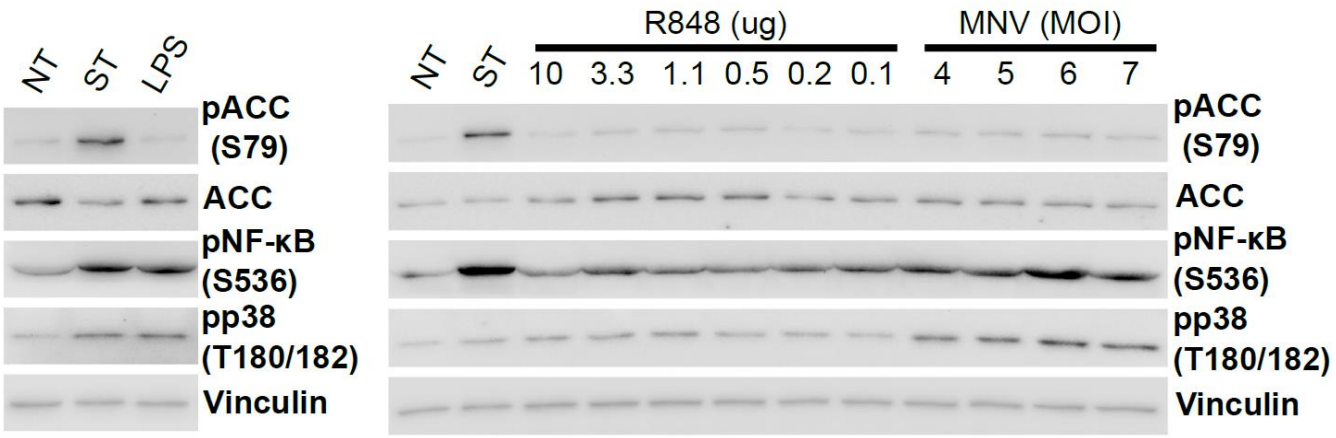

Fig 32. MEF cells were treated with *Salmonella*, lipopolysaccharide (LPS, 2 ug/mL), Resiquimod (R848, indicated concentrations) and murine noroviruses (MNV, indicated MOI) for 1 hour. Whole cell lysates were immunoblotted using the antibodies indicated.

Next, we attempted to activate the host response with an unbiased approach for bacterial antigens by treating cells with *Salmonella* that were killed by paraformaldehyde fixation to preserve bacterial PAMPs (pathogen-associated molecular patterns). We observed that fixed bacteria were unable to activate AMPK or inhibit mTORC1 (Fig 33), indicating that viable bacteria are required to stimulate AMPK-mediated signalling to the autophagy kinases.

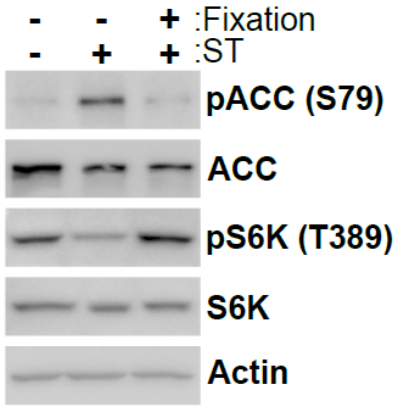

Fig 33. MEF cells were infected with either *Salmonella* (wild-type) or PFA-treated *Salmonella* for 1 hour. Whole cell lysates were immunoblotted for AMPK and mTORC1 activities using the antibodies indicated.

Upon re-analysis of our IF images we noted that cells that did not contain internalized bacteria contained small LPS-positive puncta, which were not present in the untreated samples (Fig S16). We hypothesized that these small puncta may be

Salmonella-derived outer membrane vesicles (OMVs). OMVs are produced by budding of the outer membrane of gram negative bacteria, which contain a diverse array of periplasmic cargo including proteins, nucleic acids, lipids and small molecules[85]. Pathogenic bacteria have also been described to deliver virulence factors to cells via OMVs and *Salmonella* have been shown to selectively load OMVs with different cargo depending on environmental stimuli[85]. Importantly, OMV production is independent of the T3SS and requires viable bacteria, which is consistent with the retention of AMPK activation in the T3SS-mutant *Salmonella* and failure of paraformaldehyde-inactivated *Salmonella* to activate signalling to the autophagy pathway. Therefore, we next sought to determine directly if *Salmonella* OMVs were responsible for AMPK activation by extracellular bacteria. OMVs from *Salmonella* were purified using a combination of established protocols, which included filtration, polyethylene glycol enrichment, and ultracentrifugation[85,124]. Purified OMVs were analyzed by laser scatter microscopy and were found to have an average diameter 140nm and were free of intact bacteria (Fig 34).

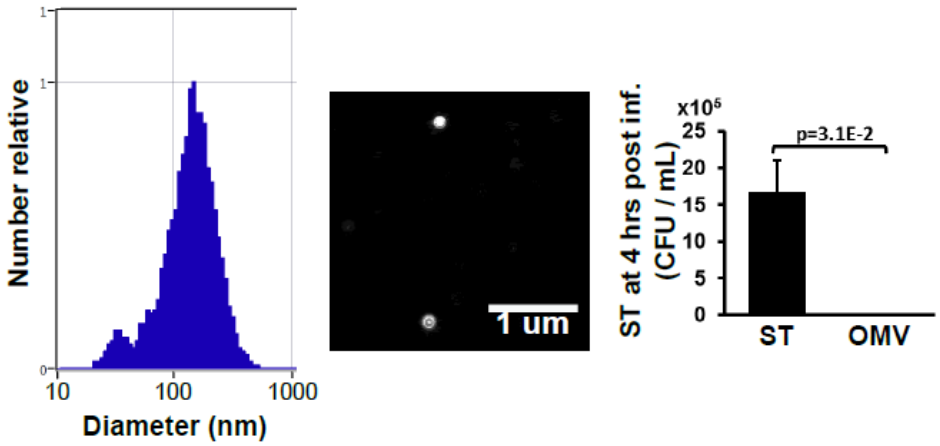

Fig 34. Purified OMVs were analyzed by ZetaView Nanoparticle Tracking Analysis showing distribution of OMV particle size (left panel) and showing a representative image of OMV particles (middle panel). OMVs were confirmed to be free of intact bacteria via CFU assays (right panel).

We next sought to determine if our purified OMVs were capable of entering mammalian cells and if OMVs produced during our standard *Salmonella* assay were entering the cell. Using sequential staining against *Salmonella* LPS (prior and post

permeabilization) we observed that OMVs were entering the cells during the infection or using our purified fraction (Fig 35, S17). Of note in *Salmonella*-treated cells both internal and external OMVs were observed in cells that did not harbour internalized bacteria (Fig 35, upper panels).

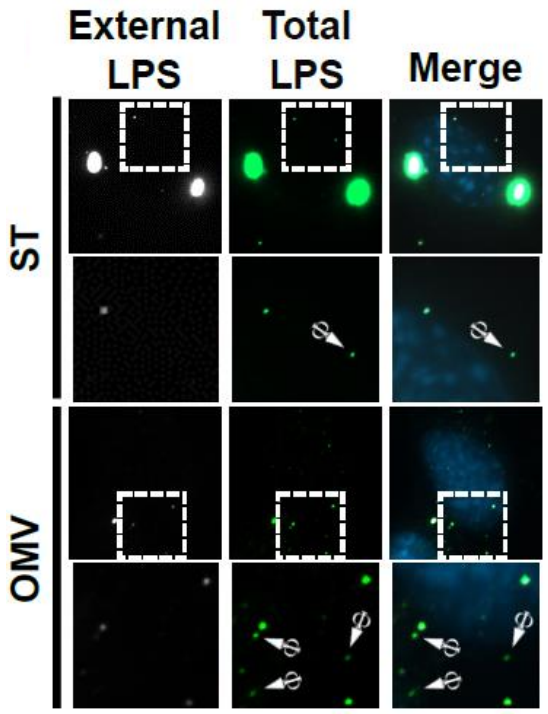

Fig 35. MEF cells were infected with *Salmonella* or purified OMVs (unless otherwise stated $3.6*10^{10}$ particles/mL were added) for 1 hour. External and total LPS were stained to highlight internalized OMVs and analyzed by immunofluorescence. Arrows with ϕ mark internalized OMVs.

We then treated cells with *Salmonella* or OMVs and analyzed AMPK activation and OMV entry by immunofluorescence and found that OMV treatment was sufficient to activate AMPK (Fig 36, S18).

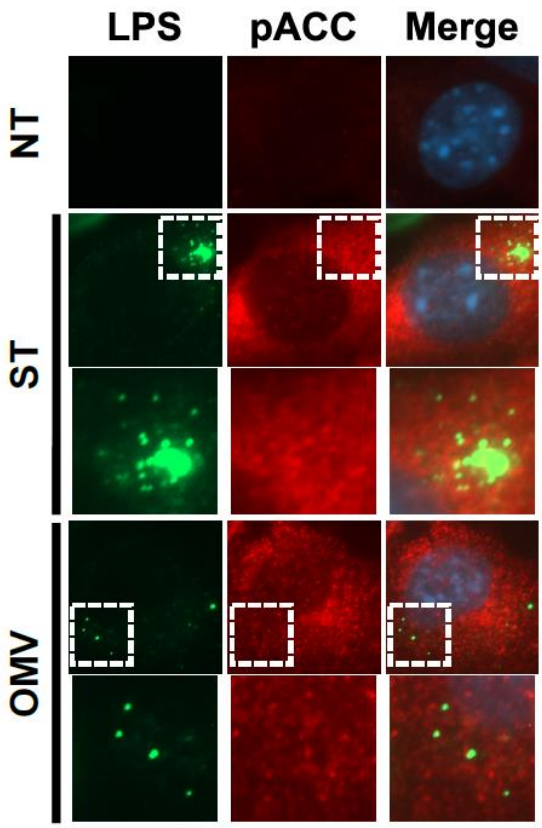

Fig 36. MEF cells were treated with *Salmonella* or purified OMVs for 1 hour. AMPK-mediated phosphorylation of ACC and LPS were stained and analyzed by immunofluorescence.

Next, AMPK activation and mTORC1 inhibition were analyzed by western blot after treatment with *Salmonella* or purified OMVs. We observed OMV-treatment triggered both AMPK activation and mTORC1 inhibition (Fig 37). Additionally, we found that OMVs purified from InvA-mutant *Salmonella* are also capable of inducing AMPK and mTORC1 signalling (Fig S19). Collectively, these data show that AMPK signalling is induced by *Salmonella*-derived OMVs, which can occur independently of bacterial invasion.

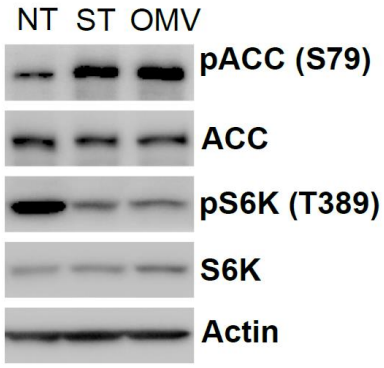

Fig 37. MEF cells were treated with either *Salmonella* or purified OMVs for 1 hour. Whole cell lysate was immunoblotted for the activities of AMPK and mTORC1.

OMV entry into host cells has been described to multiple entry points into mammalian cells[125]. In order to determine whether OMV uptake was required for AMPK signalling, we infected cells in the presence or absence of either Filipin III or dynasore, which are reported to inhibit OMV entry. We observed that Filipin-III activates AMPK independently of infection while dynasore fails to block OMV entry in cells treated with either OMVs or *Salmonella*, precluding their use for our study (Fig S20, S21). However, we found that fixation of OMVs by paraformaldehyde followed by stringent washing prevents entry without disrupting the integrity of the OMVs (Fig S22). We then treated cells with either control or fixed OMVs and analyzed downstream signalling. Fixation of OMVs resulted in a profound loss in AMPK activation despite retaining the ability to activate p38, indicating that OMV entry is required for detection and activation of the autophagy pathway (Fig S22). Membrane disruption caused by *Salmonella* infection has been described to result in amino acid loss and mTORC1 inhibition[111]. Therefore, we attempted to examine whether OMV-mediated membrane perturbation contributed to the regulation of AMPK and mTORC1. Using digitonin at previously reported levels for studying the effects of pathogen-induced membrane disruption we observed a decrease in membrane integrity, as measured by trypan blue uptake, and alterations in AMPK and mTORC1 signalling (Fig S23). However, OMV treatment did not increase membrane permeability indicating that OMVs may not induce stress signalling through disruption of the plasma membrane (Fig S23). We next reasoned that if stress signalling was due to membrane disruption then exosomes, mammalian-derived

secretory vesicles of similar size, should also activate AMPK. Therefore, we added an equal number of *Salmonella*-derived OMVs and neuron-derived exosomes to cells and analyzed AMPK and mTORC1 signalling. We observed that OMVs and not exosomes were capable of activating AMPK, which strongly indicates that AMPK and mTORC1 regulation is not a result of membrane perturbation (Fig 38).

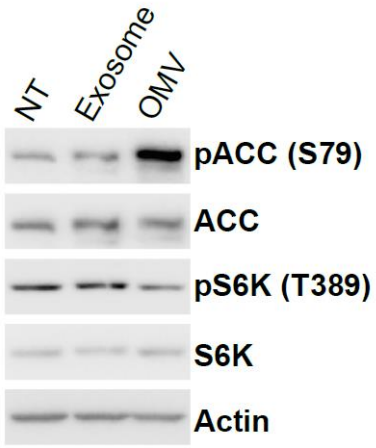

Fig 38. MEF cells were treated with either purified exosomes or OMVs for 1 hour. Whole cell lysate was immunoblotted for analysis of AMPK and mTORC1 signalling.

Next, in order to identify the PRR responsible for AMPK activation we used CRISPR/Cas9 to knock out genes involved in detecting pathogenic macromolecules and activating the host immune response, including IRAK, TRAF6, NOD1, NOD2, and STING. However, we observed no difference in AMPK regulation in the knock-out cell lines compared to the *wild-type*, which may suggest that signalling can be stimulated by more than one PAMP or sensed by more than one PRR (Fig S24, S25, S26). We next attempted to examine the biological properties of OMV-secreted PAMPs involved in AMPK signalling. We treated OMVs with a mild heat shock to denature proteins (55^{o}C) and observed that the heat-shocked OMVs are incapable of inducing AMPK signalling, even though they retained their structural integrity and the majority of their cargo (Fig 39, S27). The loss of AMPK activation by mild heat shock indicates that the PAMP(s) responsible may be protein, which has denatured under these conditions.

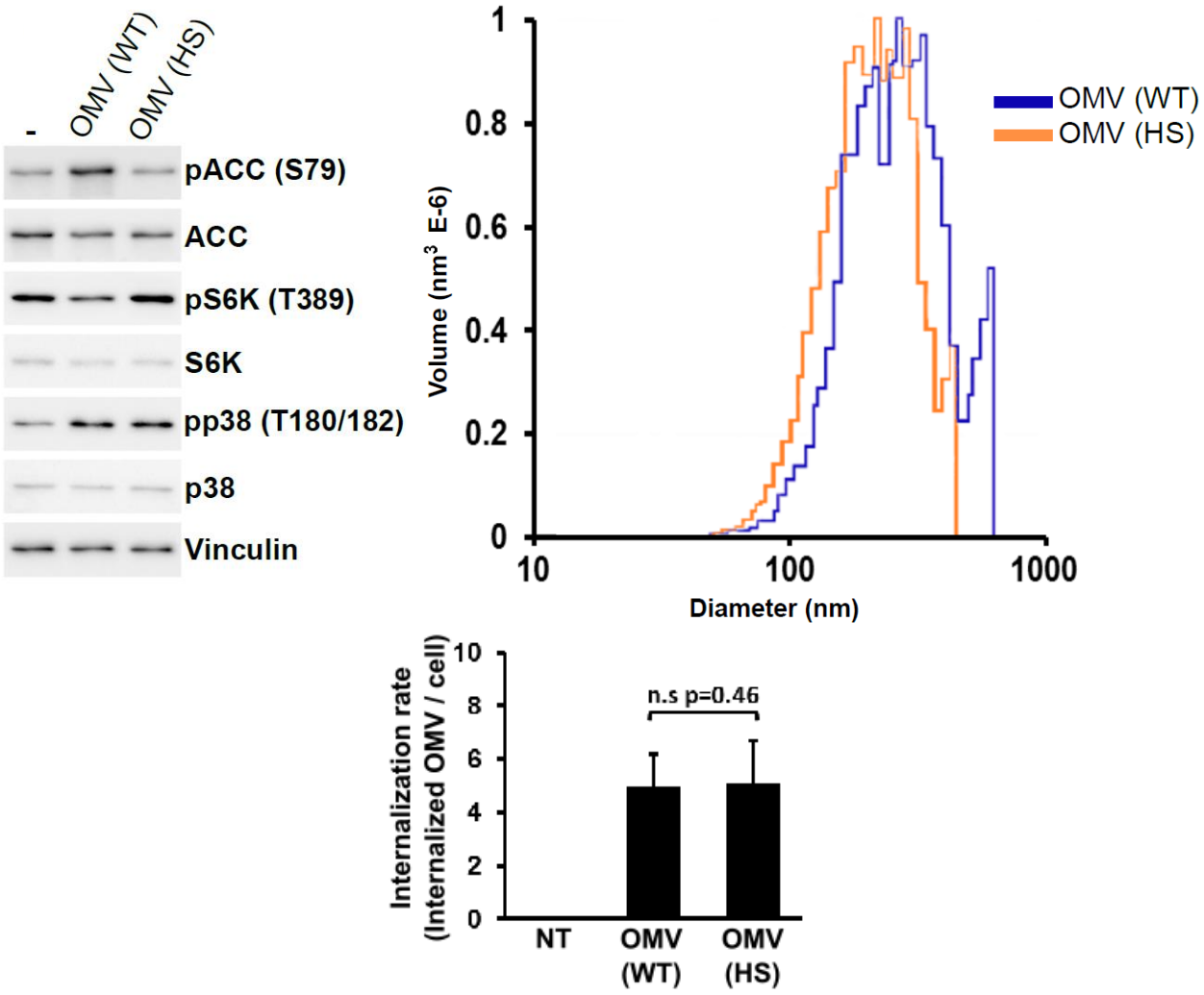

Fig 39. MEF cells were treated with either wild-type OMVs or 55ºC-treated OMVs for 1 hour. Whole cell lysates were immunoblotted using the antibodies indicated (top left panel). Heat-treated OMVs were analyzed by laser scattering microscopy and a graph generated by ZetaView Nanoparticle Tracking Analysis compares size distribution of wild-type and heat-treated OMV particles (top right panel). OMV internalization rates were quantified by immunofluorescence (bottom panel).

To directly test if the OMV-derived PAMP was a protein we introduced proteinase K into OMVs by electroporation and tested their ability to activate AMPK. We found OMVs electroporated with buffer alone maintained normal signalling indicating the electroporation itself did not affect OMV detection (Fig 40). However, we observed that proteinase K treatment resulted in a potent reduction in AMPK activation (Fig 40).

Taken together our data strongly indicate protein(s) from the OMVs are responsible for inducing AMPK signalling.

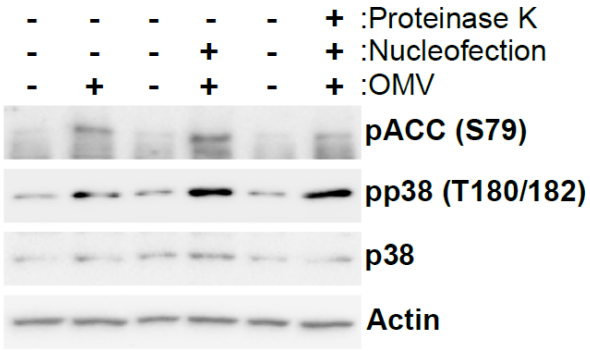

Fig 40. Proteinase K was inserted into OMVs via nucleofection. OMVs were repelleted and excess proteinase K removed by washing. MEF cells were then treated with wild-type OMVs, control nucleofected OMVs, or proteinase K-containing OMVs for 1 hour. Whole cell lysates were immunoblotted using the antibodies indicated.

AMPK signalling promotes xenophagy

A key prediction from our model linking *Salmonella*-induced AMPK signalling to activation of the xenophagic response is that cells lacking AMPK activity should have a reduction in autophagic capture of internalized *Salmonella.* To test this hypothesis and determine the biological contribution of AMPK signalling to the promotion of xenophagy we first quantified *Salmonella* incorporation into LC3B-positive vesicles in AMPK wild-type and deficient MEF. Unbiased quantification of LC3B-positive internalized bacteria was achieved using the blinded application of Volocity program object detection from IF images of triple stained for external bacteria (anti-LPS prior to permeabilization), total bacteria (anti-LPS after permeabilization) and LC3B-positive puncta (Fig S28). In agreement with our prediction we observed a reduction in the number of LC3B-positive internalized *Salmonella* in the AMPK double-knockout background (Fig 41).

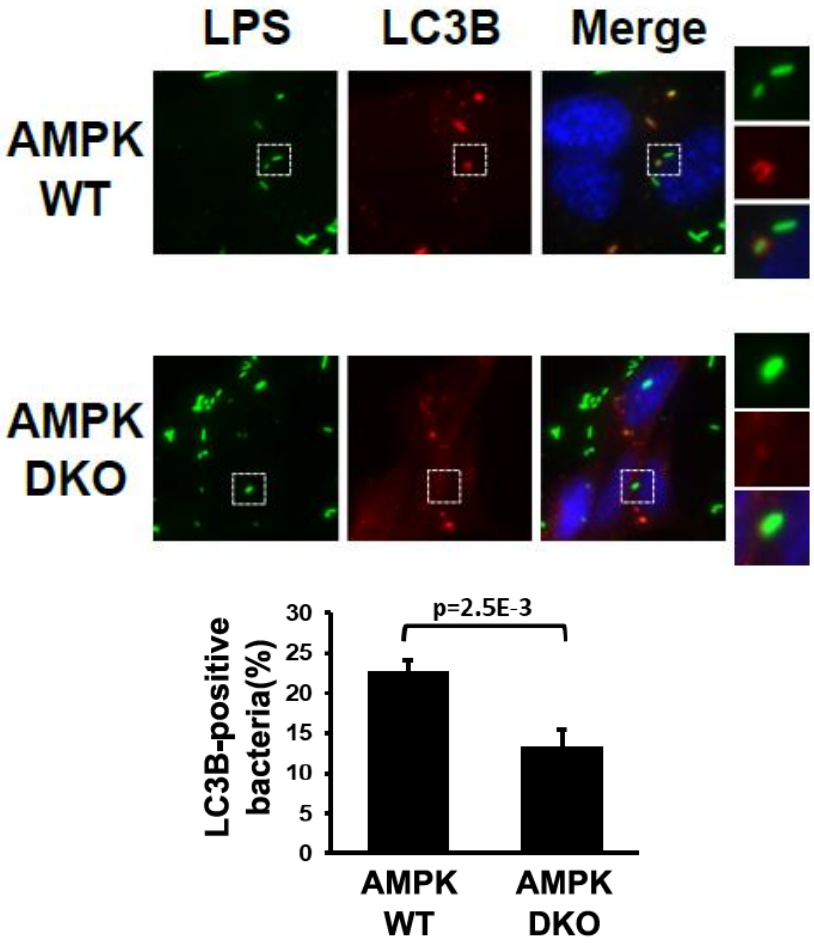

Fig 41. AMPK wild-type and alpha 1/2 knockout MEF cells were infected with *Salmonella* for 1 hour in the presence of 0.2 μM Bafilomycin A1. Bacteria were stained using anti-LPS antibodies to analyze localization in addition to the autophagy marker LC3B. Quantification of bacteria undergoing autophagic clearance is demonstrated in the bottom panel.

In order to determine whether the increase in LC3B-positive bacteria is a result of increased capture by autophagy or LAP we repeated the experiment using the same triple staining technique detailed above substituting LC3B for p62. p62 is reported not to localize to LAP vesicles[93] and is an established marker of bacteria that are targeted for autophagic degradation[126]. Quantification of p62-positive *Salmonella* showed a marked defect in the efficiency of AMPK-deficient cells in the targeting of *Salmonella* to p62 positive structures that was similar to the reduction observed from LC3B co-staining (Fig 42), indicating a defect in xenophagy in AMPK deficient cells.

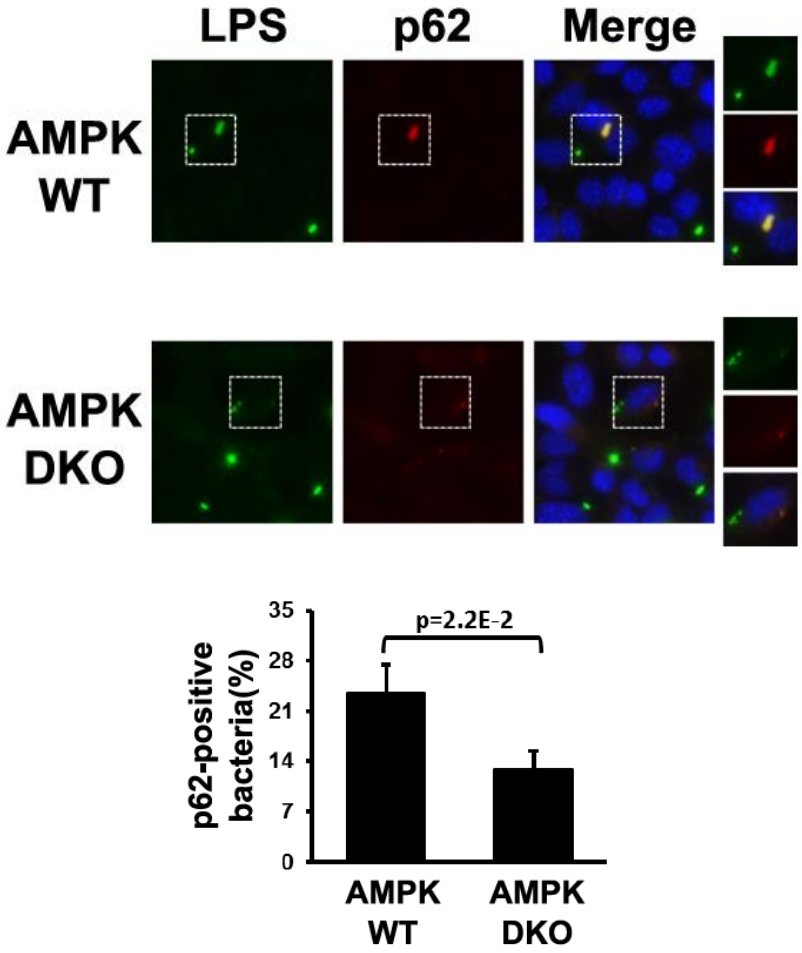

Fig 42. AMPK wild-type and alpha 1/2 knockout MEF cells were infected with *Salmonella* for 1 hour in the presence of 0.2 μM Bafilomycin A1. Bacteria were stained using anti-LPS antibodies to analyze localization in addition to the autophagy marker p62. Quantification of bacteria undergoing autophagic clearance is demonstrated in the bottom panel.

Next, in order to confirm if AMPK signalling promotes xenophagy we infected AMPK wild-type and deficient MEF with *Salmonella* and performed a colony forming unit (CFU) assay. Consistent with our previous data we found that AMPK deficient cells had significantly higher numbers of internalized bacteria at 4 hours post infection than AMPK wild-type cells, despite both lines starting out with an equal rate of infection (Fig 43).

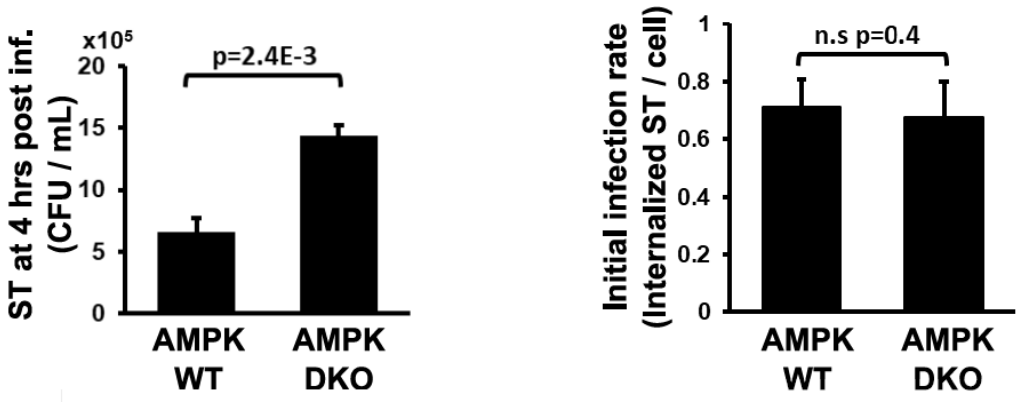

Fig 43. AMPK wild-type and alpha 1/2 knockout MEF cells were infected with *Salmonella* for 1 hour. Xenophagy rates were examined through CFU assays. Quantification of infection rates by immunofluorescence is demonstrated in the right panel.

Lastly, we wished to examine if OMVs from other gram negative bacteria, both infectious and non-infectious, could enhance the xenophagy rate of *Salmonella*. We found that 4 hours post infection priming with OMVs purified from *Shigella*, AIEC, or DH5α E. coli promotes bacterial clearance compared to samples without OMVs pre-incubation (Fig 44).

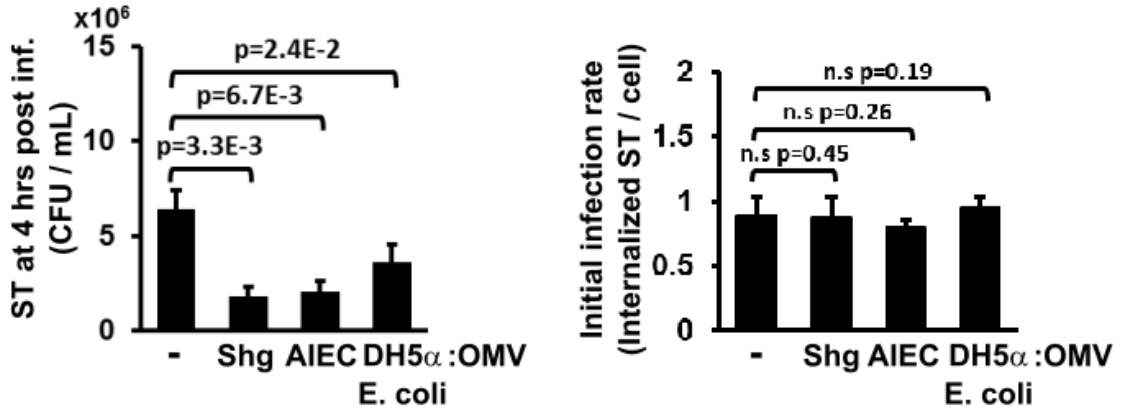

Fig 44. MEF cells were infected with *Salmonella* in the absence or presence of OMVs purified from *Shigella*, AIEC, or DH5α E.coli for 1 hour. Xenophagy rates were examined through CFU assays. Initial infection rates were quantified by immunofluorescence and is shown in the right panel.

Taken together, our data indicate that OMV-stimulated AMPK signalling plays an important role in the autophagic suppression of invading *Salmonella* (Fig 45).

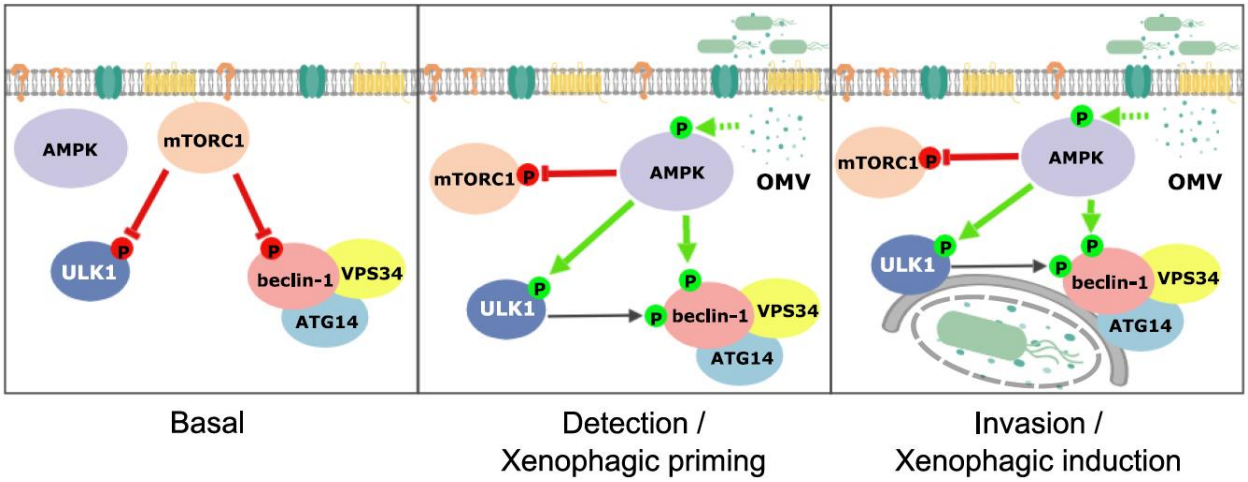

Fig 45. A working model of AMPK signalling through ULK1 / VPS34 complexes in response to *Salmonella* infection.

Discussion

As part of the innate immune system, xenophagy plays a key role in the restriction of intracellular bacterial growth. Here we describe a novel signalling pathway that promotes xenophagy through AMPK signalling. Previous studies showed that bacterial invasion contributes to amino acids leakage, which inactivates mTORC1 and subsequently induces autophagy[111]. We found that independently of amino acid loss AMPK is capable of inhibiting mTORC1 directly and robustly in response to infection. Additionally, we observed that detection of extracellular bacteria resulted in regulation of AMPK and mTORC1 activity as well as an activation of autophagy kinase complexes, but did not lead to an increase in bulk autophagy.

Several studies have shown that once *Salmonella* is internalized there are many events that contribute to bacterial capture by the autophagosome, including, but not limited to, targeting of damaged membranes, transient loss of nutrients, and ubiquitination of bacterial proteins[80,108,111]. Here we showed that AMPK signalling not only pre-activates the ULK1 and VPS34 kinase complexes, but is required for efficient xenophagy induction. Therefore, it will be of interest in future studies to determine if or how activation of the ULK1 and VPS34 kinase complexes is important for specific events associated with bacterial capture by autophagosomes.

Torin-1 has been shown to potently activate autophagy through inhibition of mTORC1[127]. Here we observed that co-treatment with *Salmonella* abolishes Torin-1-mediated autophagy induction. This led us to hypothesize that *Salmonella* may trigger a secondary signalling pathway to repress autophagy. It will be of great interest to the field to discover the identity of this autophagy inhibiting pathway as there are a lack of specific autophagy inhibitors available. Chloroquine, a lysosomal inhibitor, is usually used to repress autophagy, but results in several off-target effects. Therefore, characterizing T3SS effector(s) responsible for blocking autophagy induction is extremely beneficial for studies focusing on developing efficient and effective autophagy inhibitors.

While we do not yet have the full picture of how the cell selectively induces autophagy downstream of mTORC1 in response to *Salmonella,* the potential benefits to the cell are more obvious. Autophagy has a tremendous degradative capacity, capable of turning over up to 3% of total cellular proteins per hour when mTORC1 is inhibited by amino acid withdrawal[33]. If every cell that encountered pathogen, especially those never destined to be infected, began indiscriminate degradation of their cytoplasm this would be an enormously wasteful and inefficient way to target pathogens for clearance. Instead we have found the cell has developed a sophisticated method utilizing AMPK signalling to selectively 'prime' the autophagy pathway for clearance of pathogens even before the bacteria have a chance to enter the cell.

Moreover, we showed that OMVs shed by gram negative bacteria are responsible for AMPK and mTORC1 regulation, independently of bacterial invasion and internalization. Additionally, our data suggested that OMV-derived proteins are PAMPs that play a role in mediating host signalling. The demonstration that OMVs are capable of evoking signalling responses that have previously been attributed to cellular damage caused by bacterial invasion was unexpected. Therefore, it will be interesting to determine if other autophagy-related aspects of the innate immune response may be similarly affected by OMV-detection. For example, autophagy proteins have been described to influence the secretion of inflammatory cytokines[128]. It would be interesting to see if OMV-mediated activation of the autophagy pathway plays a role in the regulation of the inflammatory response.

Finally, we have established that activation of AMPK also occurs with other gram-negative pathogenic bacteria. It was interesting to observe that OMVs from different species, pathogenic or not, is capable of activating the autophagy pathway. OMVs from infectious bacteria have also been described to harbour virulence factors that can enhance pathogenicity[128]. Therefore, one might imagine that there is a trade-off for the bacteria where OMV production will lead to activation of xenophagy, but also act as a vehicle to deliver factors that will promote growth. In the course of this study we observed several instances where internalized bacteria were surrounded by OMVs and these bacteria were seldom targeted by autophagosomes. The Red Queen race

between host and pathogen makes it quite likely that *Salmonella* and other gram negative bacteria have already developed measures designed to circumvent or exploit the detection of OMVs and the characterization of this potential interplay warrants further investigation.

References

1. Ryter, S. W., Cloonan, S. M. & Choi, A. M. K. Autophagy: a critical regulator of cellular metabolism and homeostasis. *Mol. Cells* **36**, 7–16 (2013).
2. Reggiori, F., Komatsu, M., Finley, K. & Simonsen, A. Autophagy: More Than a Nonselective Pathway. *Int. J. Cell Biol.* **2012**, (2012).
3. Opperdoes, F. A Feeling for the Cell: Christian de Duve (1917–2013). *PLoS Biol.* **11**, (2013).
4. Sabatini, D. D. & Adesnik, M. Christian de Duve: Explorer of the cell who discovered new organelles by using a centrifuge. *Proc. Natl. Acad. Sci. U. S. A.* **110**, 13234–13235 (2013).
5. Bittar, E. *Cellular Organelles and the Extracellular Matrix*. (Elsevier, 1996).
6. The Case of Alex B. Novikoff. Available at: https://vermonthistory.org/research/research-resources-online/green-mountain-chronicles/the-case-of-alex-b-novikoff-1953. (Accessed: 2nd December 2018)
7. The Nobel Prize in Physiology or Medicine 1974. *NobelPrize.org* Available at: https://www.nobelprize.org/prizes/medicine/1974/duve/facts/. (Accessed: 1st December 2018)
8. Lysosomes, Autophagy | Learn Science at Scitable. Available at: https://www.nature.com/scitable/topicpage/the-discovery-of-lysosomes-and-autophagy-14199828. (Accessed: 2nd December 2018)
9. Straus, W. OCCURRENCE OF PHAGOSOMES AND PHAGO-LYSOSOMES IN DIFFERENT SEGMENTS OF THE NEPHRON IN RELATION TO THE REABSORPTION, TRANSPORT, DIGESTION, AND EXTRUSION OF INTRAVENOUSLY INJECTED HORSERADISH PEROXIDASE. *J. Cell Biol.* **21**, 295–308 (1964).
10. Zanvil Alexander Cohn 1926-1993. *J. Exp. Med.* **179**, 1–30 (1994).

11. Macroautophagy - an overview | ScienceDirect Topics. Available at: https://www.sciencedirect.com/topics/medicine-and-dentistry/macroautophagy. (Accessed: 2nd December 2018)
12. De Duve, C. The lysosome. *Sci. Am.* **208**, 64–72 (1963).
13. Sedwick, C. Yoshinori Ohsumi: Autophagy from beginning to end. *J. Cell Biol.* **197**, 164–165 (2012).
14. Kuma, A., Komatsu, M. & Mizushima, N. Autophagy-monitoring and autophagy-deficient mice. *Autophagy* **13**, 1619–1628 (2017).
15. Wong, P.-M., Puente, C., Ganley, I. G. & Jiang, X. The ULK1 complex. *Autophagy* **9**, 124–137 (2013).
16. Zachari, M. & Ganley, I. G. The mammalian ULK1 complex and autophagy initiation. *Essays Biochem.* **61**, 585–596 (2017).
17. Structure of the Human Autophagy Initiating Kinase ULK1 in Complex with Potent Inhibitors - ACS Chemical Biology (ACS Publications). Available at: https://pubs.acs.org/doi/10.1021/cb500835z. (Accessed: 2nd December 2018)
18. Bach, M., Larance, M., James, D. E. & Ramm, G. The serine/threonine kinase ULK1 is a target of multiple phosphorylation events. *Biochem. J.* **440**, 283–291 (2011).
19. Qi, S., Kim, D. J., Stjepanovic, G. & Hurley, J. H. Structure of the Human Atg13-Atg101 HORMA Heterodimer: An Interaction Hub within the ULK1 Complex. *Struct. Lond. Engl. 1993* **23**, 1848–1857 (2015).
20. Mercer, C. A., Kaliappan, A. & Dennis, P. B. A novel, human Atg13 binding protein, Atg101, interacts with ULK1 and is essential for macroautophagy. *Autophagy* **5**, 649–662 (2009).
21. Papinski, D. & Kraft, C. Regulation of Autophagy By Signaling Through the Atg1/ULK1 Complex. *J. Mol. Biol.* **428**, 1725–1741 (2016).

22. Alers, S., Löffler, A. S., Wesselborg, S. & Stork, B. Role of AMPK-mTOR-Ulk1/2 in the Regulation of Autophagy: Cross Talk, Shortcuts, and Feedbacks. *Mol. Cell. Biol.* **32**, 2–11 (2012).
23. Egan, D. F., Kim, J., Shaw, R. J. & Guan, K.-L. The autophagy initiating kinase ULK1 is regulated via opposing phosphorylation by AMPK and mTOR. *Autophagy* **7**, 645–646 (2011).
24. Saxton, R. A. & Sabatini, D. M. mTOR Signaling in Growth, Metabolism, and Disease. *Cell* **168**, 960–976 (2017).
25. Laplante, M. & Sabatini, D. M. mTOR signaling at a glance. *J. Cell Sci.* **122**, 3589–3594 (2009).
26. Foster, K. G. *et al.* Regulation of mTOR Complex 1 (mTORC1) by Raptor Ser863 and Multisite Phosphorylation. *J. Biol. Chem.* **285**, 80–94 (2010).
27. Kakumoto, K., Ikeda, J., Okada, M., Morii, E. & Oneyama, C. mLST8 Promotes mTOR-Mediated Tumor Progression. *PLoS ONE* **10**, (2015).
28. Yip, C. K., Murata, K., Walz, T., Sabatini, D. M. & Kang, S. A. Structure of the human mTOR Complex I and its implications for rapamycin inhibition. *Mol. Cell* **38**, 768–774 (2010).
29. Puertollano, R. mTOR and lysosome regulation. *F1000Prime Rep.* **6**, (2014).
30. Manifava, M. *et al.* Dynamics of mTORC1 activation in response to amino acids. *eLife* **5**,
31. Long, X., Lin, Y., Ortiz-Vega, S., Yonezawa, K. & Avruch, J. Rheb binds and regulates the mTOR kinase. *Curr. Biol. CB* **15**, 702–713 (2005).
32. Heard, J. J., Fong, V., Bathaie, S. Z. & Tamanoi, F. Recent Progress in the Study of the Rheb family GTPases. *Cell. Signal.* **26**, 1950–1957 (2014).
33. Nguyen, T. P., Frank, A. R. & Jewell, J. L. Amino acid and small GTPase regulation of mTORC1. *Cell. Logist.* **7**, (2017).
34. Manning, B. D. & Cantley, L. C. Rheb fills a GAP between TSC and TOR. *Trends Biochem. Sci.* **28**, 573–576 (2003).

35. Yu, J. S. L. & Cui, W. Proliferation, survival and metabolism: the role of PI3K/AKT/mTOR signalling in pluripotency and cell fate determination. *Development* **143**, 3050–3060 (2016).
36. Hardie, D. G. AMPK: A Target for Drugs and Natural Products With Effects on Both Diabetes and Cancer. *Diabetes* **62**, 2164–2172 (2013).
37. Garcia, D. & Shaw, R. J. AMPK: mechanisms of cellular energy sensing and restoration of metabolic balance. *Mol. Cell* **66**, 789–800 (2017).
38. Oligschlaeger, Y. *et al.* The recruitment of AMP-activated protein kinase to glycogen is regulated by autophosphorylation. *J. Biol. Chem.* **290**, 11715–11728 (2015).
39. Hardie, D. G. AMPK—Sensing Energy while Talking to Other Signaling Pathways. *Cell Metab.* **20**, 939–952 (2014).
40. Complexes between the LKB1 tumor suppressor, STRADα/β and MO25α/β are upstream kinases in the AMP-activated protein kinase cascade | Journal of Biology | Full Text. Available at: https://jbiol.biomedcentral.com/articles/10.1186/1475-4924-2-28. (Accessed: 2nd December 2018)
41. Mihaylova, M. M. & Shaw, R. J. The AMP-activated protein kinase (AMPK) signaling pathway coordinates cell growth, autophagy, & metabolism. *Nat. Cell Biol.* **13**, 1016–1023 (2011).
42. Gowans, G. J., Hawley, S. A., Ross, F. A. & Hardie, D. G. AMP Is a True Physiological Regulator of AMP-Activated Protein Kinase by Both Allosteric Activation and Enhancing Net Phosphorylation. *Cell Metab.* **18**, 556–566 (2013).
43. Hong-Brown, L. Q., Brown, C. R., Kazi, A. A., Navaratnarajah, M. & Lang, C. H. Rag GTPases and AMPK/TSC2/Rheb mediate the differential regulation of mTORC1 signaling in response to alcohol and leucine. *Am. J. Physiol. - Cell Physiol.* **302**, C1557–C1565 (2012).
44. Gwinn, D. M. *et al.* AMPK Phosphorylation of Raptor Mediates a Metabolic Checkpoint. *Mol. Cell* **30**, 214–226 (2008).

45. Parzych, K. R. & Klionsky, D. J. An Overview of Autophagy: Morphology, Mechanism, and Regulation. *Antioxid. Redox Signal.* **20**, 460–473 (2014).
46. Jin, M. & Klionsky, D. J. The Core Molecular Machinery of Autophagosome Formation. in (2015).
47. Raiborg, C., Schink, K. O. & Stenmark, H. Class III phosphatidylinositol 3-kinase and its catalytic product PtdIns3P in regulation of endocytic membrane traffic. *FEBS J.* **280**, 2730–2742 (2013).
48. Lőrincz, P. *et al.* Atg6/UVRAG/Vps34-Containing Lipid Kinase Complex Is Required for Receptor Downregulation through Endolysosomal Degradation and Epithelial Polarity during Drosophila Wing Development. *BioMed Research International* (2014). doi:10.1155/2014/851349
49. Yuan, H.-X., Russell, R. C. & Guan, K.-L. Regulation of PIK3C3/VPS34 complexes by MTOR in nutrient stress-induced autophagy. *Autophagy* **9**, 1983–1995 (2013).
50. Munson, M. J. *et al.* mTOR activates the VPS34–UVRAG complex to regulate autolysosomal tubulation and cell survival. *EMBO J.* **34**, 2272–2290 (2015).
51. Diao, J. *et al.* ATG14 promotes membrane tethering and fusion of autophagosomes to endolysosomes. *Nature* **520**, 563–566 (2015).
52. Russell, R. C. *et al.* ULK1 induces autophagy by phosphorylating Beclin-1 and activating VPS34 lipid kinase. *Nat. Cell Biol.* **15**, 741–750 (2013).
53. Obara, K. & Ohsumi, Y. PtdIns 3-Kinase Orchestrates Autophagosome Formation in Yeast. *J. Lipids* **2011**, (2011).
54. Kim, J. *et al.* Differential Regulation of Distinct Vps34 Complexes by AMPK in Nutrient Stress and Autophagy. *Cell* **152**, 290–303 (2013).
55. Kang, R., Zeh, H. J., Lotze, M. T. & Tang, D. The Beclin 1 network regulates autophagy and apoptosis. *Cell Death Differ.* **18**, 571–580 (2011).

56. Decuypere, J.-P., Parys, J. B. & Bultynck, G. Regulation of the Autophagic Bcl-2/Beclin 1 Interaction. *Cells* **1**, 284–312 (2012).
57. UVRAG - an overview | ScienceDirect Topics. Available at: https://www.sciencedirect.com/topics/biochemistry-genetics-and-molecular-biology/uvrag. (Accessed: 2nd December 2018)
58. Jiang, P. *et al.* The HOPS complex mediates autophagosome–lysosome fusion through interaction with syntaxin 17. *Mol. Biol. Cell* **25**, 1327–1337 (2014).
59. Geng, J. & Klionsky, D. J. The Atg8 and Atg12 ubiquitin-like conjugation systems in macroautophagy. 'Protein Modifications: Beyond the Usual Suspects'' Review Series'. *EMBO Rep.* **9**, 859–864 (2008).
60. Tanida, I. *et al.* Apg7p/Cvt2p: A novel protein-activating enzyme essential for autophagy. *Mol. Biol. Cell* **10**, 1367–1379 (1999).
61. Shintani, T. *et al.* Apg10p, a novel protein-conjugating enzyme essential for autophagy in yeast. *EMBO J.* **18**, 5234–5241 (1999).
62. Mizushima, N., Noda, T. & Ohsumi, Y. Apg16p is required for the function of the Apg12p-Apg5p conjugate in the yeast autophagy pathway. *EMBO J.* **18**, 3888–3896 (1999).
63. Kirisako, T. *et al.* The reversible modification regulates the membrane-binding state of Apg8/Aut7 essential for autophagy and the cytoplasm to vacuole targeting pathway. *J. Cell Biol.* **151**, 263–276 (2000).
64. Fujita, N. *et al.* The Atg16L complex specifies the site of LC3 lipidation for membrane biogenesis in autophagy. *Mol. Biol. Cell* **19**, 2092–2100 (2008).
65. WIPI proteins: essential PtdIns3P effectors at the nascent autophagosome | Journal of Cell Science. Available at: http://jcs.biologists.org/content/128/2/207. (Accessed: 2nd December 2018)
66. Dooley, H. C. *et al.* WIPI2 Links LC3 Conjugation with PI3P, Autophagosome Formation, and Pathogen Clearance by Recruiting Atg12–5-16L1. *Mol. Cell* **55**, 238–252 (2014).

67. Yoshii, S. R. & Mizushima, N. Autophagy machinery in the context of mammalian mitophagy. *Biochim. Biophys. Acta BBA - Mol. Cell Res.* **1853**, 2797–2801 (2015).
68. Takahashi, Y. *et al.* Bif-1 regulates Atg9 trafficking by mediating the fission of Golgi membranes during autophagy. *Autophagy* **7**, 61–73 (2011).
69. Young, A. R. J. *et al.* Starvation and ULK1-dependent cycling of mammalian Atg9 between the TGN and endosomes. *J. Cell Sci.* **119**, 3888–3900 (2006).
70. Burman, C. & Ktistakis, N. T. Regulation of autophagy by phosphatidylinositol 3-phosphate. *FEBS Lett.* **584**, 1302–1312 (2010).
71. Zhuang, X. *et al.* ATG9 regulates autophagosome progression from the endoplasmic reticulum in Arabidopsis. *Proc. Natl. Acad. Sci.* **114**, E426–E435 (2017).
72. The VMP1-Beclin 1 interaction regulates autophagy induction | Scientific Reports. Available at: https://www.nature.com/articles/srep01055. (Accessed: 2nd December 2018)
73. Nowak, J. *et al.* The TP53INP2 Protein Is Required for Autophagy in Mammalian Cells. *Mol. Biol. Cell* **20**, 870–881 (2009).
74. Yang, Z. & Klionsky, D. J. An Overview of the Molecular Mechanism of Autophagy. *Curr. Top. Microbiol. Immunol.* **335**, 1–32 (2009).
75. Johansen, T. & Lamark, T. Selective autophagy mediated by autophagic adapter proteins. *Autophagy* **7**, 279–296 (2011).
76. Svenning, S. & Johansen, T. Selective autophagy. *Essays Biochem.* **55**, 79–92 (2013).
77. Brenner, F. W., Villar, R. G., Angulo, F. J., Tauxe, R. & Swaminathan, B. Salmonella Nomenclature. *J. Clin. Microbiol.* **38**, 2465–2467 (2000).
78. Andino, A. & Hanning, I. Salmonella enterica: Survival, Colonization, and Virulence Differences among Serovars. *Sci. World J.* **2015**, (2015).
79. Garai, P., Gnanadhas, D. P. & Chakravortty, D. Salmonella enterica serovars Typhimurium and Typhi as model organisms. *Virulence* **3**, 377–388 (2012).

80. Rychlik, I. *et al.* Virulence potential of five major pathogenicity islands (SPI-1 to SPI-5) of Salmonella enterica serovar Enteritidis for chickens. *BMC Microbiol.* **9**, 268 (2009).
81. Ehrbar, K., Friebel, A., Miller, S. I. & Hardt, W.-D. Role of the Salmonella Pathogenicity Island 1 (SPI-1) Protein InvB in Type III Secretion of SopE and SopE2, Two Salmonella Effector Proteins Encoded Outside of SPI-1. *J. Bacteriol.* **185**, 6950–6967 (2003).
82. Coombes, B. K., Brown, N. F., Valdez, Y., Brumell, J. H. & Finlay, B. B. Expression and Secretion of Salmonella Pathogenicity Island-2 Virulence Genes in Response to Acidification Exhibit Differential Requirements of a Functional Type III Secretion Apparatus and SsaL. *J. Biol. Chem.* **279**, 49804–49815 (2004).
83. Kato, J. *et al.* A protein secreted by the Salmonella type III secretion system controls needle filament assembly. *eLife* **7**, e35886 (2018).
84. Steele-Mortimer, O. The Salmonella-containing Vacuole – Moving with the Times. *Curr. Opin. Microbiol.* **11**, 38–45 (2008).
85. Bai, J., Kim, S. I., Ryu, S. & Yoon, H. Identification and Characterization of Outer Membrane Vesicle-Associated Proteins in Salmonella enterica Serovar Typhimurium. *Infect. Immun.* **82**, 4001–4010 (2014).
86. MacDonald, I. A. & Kuehn, M. J. Offense and defense: microbial membrane vesicles play both ways. *Res. Microbiol.* **163**, 607–618 (2012).
87. Coburn, B., Sekirov, I. & Finlay, B. B. Type III Secretion Systems and Disease. *Clin. Microbiol. Rev.* **20**, 535–549 (2007).
88. Drecktrah, D. *et al.* Dynamic Behavior of Salmonella-Induced Membrane Tubules in Epithelial Cells. *Traffic Cph. Den.* **9**, 2117–2129 (2008).
89. Ramos-Morales, F. Impact of Salmonella enterica Type III Secretion System Effectors on the Eukaryotic Host Cell. *International Scholarly Research Notices* (2012). doi:10.5402/2012/787934

90. Castanheira, S. & García-del Portillo, F. Salmonella Populations inside Host Cells. *Front. Cell. Infect. Microbiol.* **7**, (2017).

91. Yu, H. B. *et al.* Autophagy facilitates Salmonella replication in HeLa cells. *mBio* **5**, e00865-00814 (2014).

92. Herhaus, L. & Dikic, I. Regulation of Salmonella-host cell interactions via the ubiquitin system. *Int. J. Med. Microbiol.* **308**, 176–184 (2018).

93. Lai, S. & Devenish, R. J. LC3-Associated Phagocytosis (LAP): Connections with Host Autophagy. *Cells* **1**, 396–408 (2012).

94. Broz, P., Ohlson, M. B. & Monack, D. M. Innate immune response to Salmonella typhimurium, a model enteric pathogen. *Gut Microbes* **3**, 62–70 (2012).

95. Mogensen, T. H. Pathogen Recognition and Inflammatory Signaling in Innate Immune Defenses. *Clin. Microbiol. Rev.* **22**, 240–273 (2009).

96. Yu, F.-S. X. & Hazlett, L. D. Toll-like Receptors and the Eye. *Invest. Ophthalmol. Vis. Sci.* **47**, 1255–1263 (2006).

97. Kawai, T. & Akira, S. The roles of TLRs, RLRs and NLRs in pathogen recognition. *Int. Immunol.* **21**, 317–337 (2009).

98. Troutman, T. D., Bazan, J. F. & Pasare, C. Toll-like receptors, signaling adapters and regulation of the pro-inflammatory response by PI3K. *Cell Cycle* **11**, 3559–3567 (2012).

99. Caruso, R., Warner, N., Inohara, N. & Núñez, G. NOD1 and NOD2: Signaling, Host Defense, and Inflammatory Disease. *Immunity* **41**, 898–908 (2014).

100. Masumoto, J. *et al.* Nod1 acts as an intracellular receptor to stimulate chemokine production and neutrophil recruitment in vivo. *J. Exp. Med.* **203**, 203–213 (2006).

101. Nod2 Is a General Sensor of Peptidoglycan through Muramyl Dipeptide (MDP) Detection. Available at: http://www.jbc.org/content/278/11/8869.full. (Accessed: 2nd December 2018)

102. Krieg, A. *et al.* XIAP mediates NOD signaling via interaction with RIP2. *Proc. Natl. Acad. Sci. U. S. A.* **106**, 14524–14529 (2009).

103. Myung, J., Kim, K. B. & Crews, C. M. The Ubiquitin-Proteasome Pathway and Proteasome Inhibitors. *Med. Res. Rev.* **21**, 245–273 (2001).

104. Suryadinata, R., Roesley, S. N. A., Yang, G. & Šarčević, B. Mechanisms of Generating Polyubiquitin Chains of Different Topology. *Cells* **3**, 674–689 (2014).

105. Zaffagnini, G. & Martens, S. Mechanisms of Selective Autophagy. *J. Mol. Biol.* **428**, 1714–1724 (2016).

106. Lippai, M. & Lőw, P. The Role of the Selective Adaptor p62 and Ubiquitin-Like Proteins in Autophagy. *BioMed Research International* (2014). doi:10.1155/2014/832704

107. Wang, L., Yan, J., Niu, H., Huang, R. & Wu, S. Autophagy and Ubiquitination in Salmonella Infection and the Related Inflammatory Responses. *Front. Cell. Infect. Microbiol.* **8**, (2018).

108. Liu, W. J. *et al.* p62 links the autophagy pathway and the ubiqutin–proteasome system upon ubiquitinated protein degradation. *Cell. Mol. Biol. Lett.* **21**, (2016).

109. Thurston, T. L. M., Wandel, M. P., von Muhlinen, N., Foeglein, Á. & Randow, F. Galectin-8 targets damaged vesicles for autophagy to defend cells against bacterial invasion. *Nature* **482**, 414–418 (2012).

110. Richter, B. *et al.* Phosphorylation of OPTN by TBK1 enhances its binding to Ub chains and promotes selective autophagy of damaged mitochondria. *Proc. Natl. Acad. Sci. U. S. A.* **113**, 4039–4044 (2016).

111. Tattoli, I. *et al.* Amino Acid Starvation Induced by Invasive Bacterial Pathogens Triggers an Innate Host Defense Program. *Cell Host Microbe* **11**, 563–575 (2012).

112. Chauhan, S., Mandell, M. A. & Deretic, V. IRGM governs the core autophagy machinery to conduct antimicrobial defense. *Mol. Cell* **58**, 507–521 (2015).

113. IRGM Is a Common Target of RNA Viruses that Subvert the Autophagy Network. Available at: https://journals.plos.org/plospathogens/article?id=10.1371/journal.ppat.1002422. (Accessed: 2nd December 2018)

114. Ganesan, R. *et al.* Salmonella Typhimurium disrupts Sirt1/AMPK checkpoint control of mTOR to impair autophagy. *PLOS Pathog.* **13**, e1006227 (2017).

115. Zhou, G. *et al.* Role of AMP-activated protein kinase in mechanism of metformin action. *J. Clin. Invest.* **108**, 1167–1174 (2001).

116. Hawley, S. A. *et al.* The ancient drug salicylate directly activates AMP-activated protein kinase. *Science* **336**, 918–922 (2012).

117. Owen, K. A., Meyer, C. B., Bouton, A. H. & Casanova, J. E. Activation of Focal Adhesion Kinase by Salmonella Suppresses Autophagy via an Akt/mTOR Signaling Pathway and Promotes Bacterial Survival in Macrophages. *PLoS Pathog.* **10**, e1004159 (2014).

118. Tattoli, I., Philpott, D. J. & Girardin, S. E. The bacterial and cellular determinants controlling the recruitment of mTOR to the Salmonella-containing vacuole. *Biol. Open* **1**, 1215–1225 (2012).

119. Galán, J. E. & Curtiss, R. Distribution of the invA, -B, -C, and -D genes of Salmonella typhimurium among other Salmonella serovars: invA mutants of Salmonella typhi are deficient for entry into mammalian cells. *Infect. Immun.* **59**, 2901–2908 (1991).

120. Cirillo, D. M., Valdivia, R. H., Monack, D. M. & Falkow, S. Macrophage-dependent induction of the Salmonella pathogenicity island 2 type III secretion system and its role in intracellular survival. *Mol. Microbiol.* **30**, 175–188 (1998).

121. Park, J.-M. *et al.* The ULK1 complex mediates MTORC1 signaling to the autophagy initiation machinery via binding and phosphorylating ATG14. *Autophagy* **12**, 547–564 (2016).

122. Kim, J., Kundu, M., Viollet, B. & Guan, K.-L. AMPK and mTOR regulate autophagy through direct phosphorylation of Ulk1. *Nat. Cell Biol.* **13**, 132–141 (2011).

123. Dammermann, W., Wollenberg, L., Bentzien, F., Lohse, A. & Lüth, S. Toll like receptor 2 agonists lipoteichoic acid and peptidoglycan are able to enhance antigen specific IFNγ release in whole blood during recall antigen responses. *J. Immunol. Methods* **396**, 107–115 (2013).

124. Rider, M. A., Hurwitz, S. N. & Meckes, D. G. ExtraPEG: A Polyethylene Glycol-Based Method for Enrichment of Extracellular Vesicles. *Sci. Rep.* **6**, (2016).

125. Mechanisms of outer membrane vesicle entry into host cells - O'Donoghue - 2016 - Cellular Microbiology - Wiley Online Library. Available at: https://onlinelibrary.wiley.com/doi/full/10.1111/cmi.12655. (Accessed: 2nd December 2018)

126. Wild, P. *et al.* Phosphorylation of the Autophagy Receptor Optineurin Restricts Salmonella Growth. *Science* **333**, 228–233 (2011).

127. Thoreen, C. C. *et al.* An ATP-competitive Mammalian Target of Rapamycin Inhibitor Reveals Rapamycin-resistant Functions of mTORC1. *J. Biol. Chem.* **284**, 8023–8032 (2009).

128. Lam, G. Y., Cemma, M., Muise, A. M., Higgins, D. E. & Brumell, J. H. Host and bacterial factors that regulate LC3 recruitment to Listeria monocytogenes during the early stages of macrophage infection. *Autophagy* **9**, 985–995 (2013).

129. Gaudet, R. G. *et al.* Innate Recognition of Intracellular Bacterial Growth Is Driven by the TIFA-Dependent Cytosolic Surveillance Pathway. *Cell Rep.* **19**, 1418–1430 (2017).

Appendices

Supplemental data

AMPK is activated by *Salmonella* and directly inhibits mTORC1

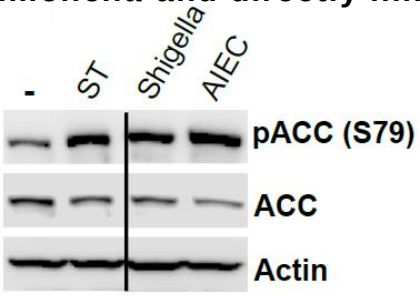

Fig S1. HCT116 were infected with *Salmonella*, Shigella, or AIEC for 1 hour. Whole cell lysates were immunoblotted for AMPK activity using the antibodies indicated. The vertical line demarcates discontinuous lanes from the same exposure of a single gel.

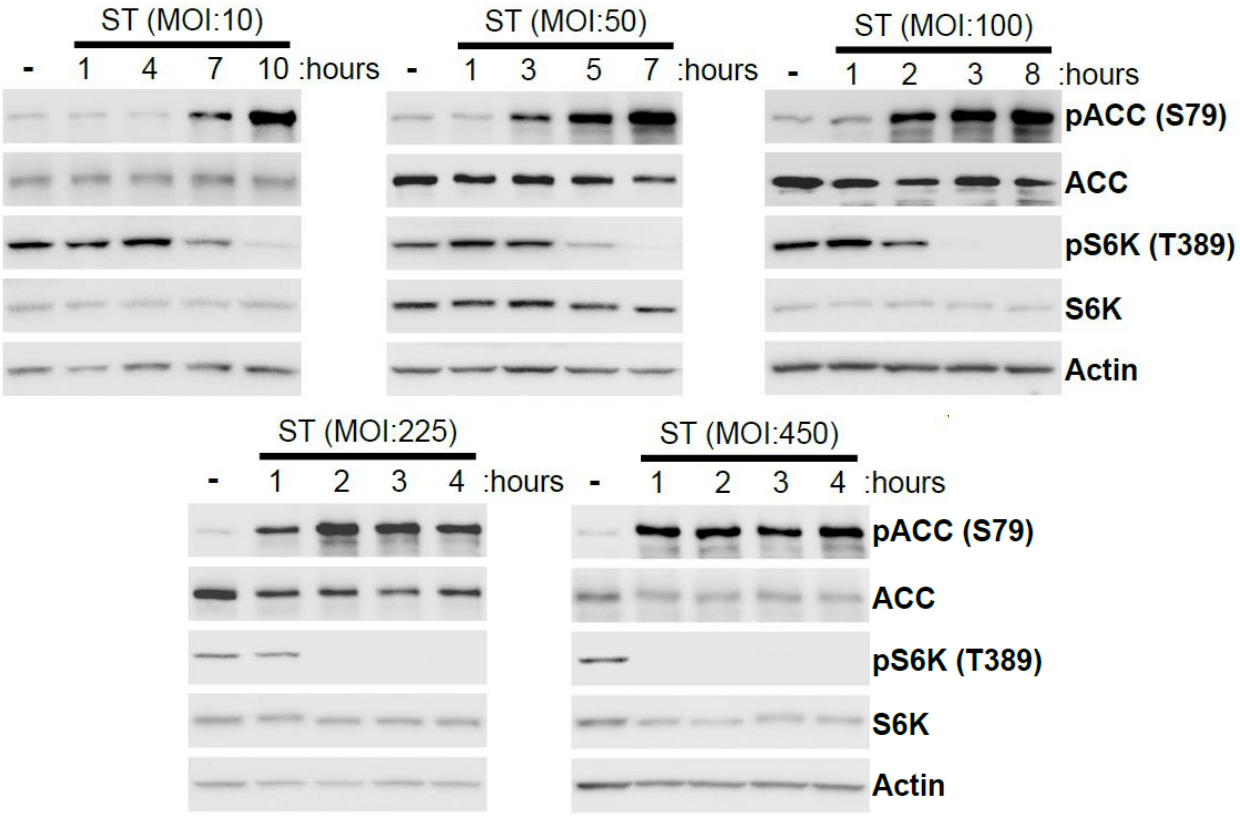

Fig S2. MEF cells were infected with increased amount of *Salmonella* for the indicated time points. Whole cell lysates were immunoblotted for AMPK and mTORC1 activity using the antibodies indicated.

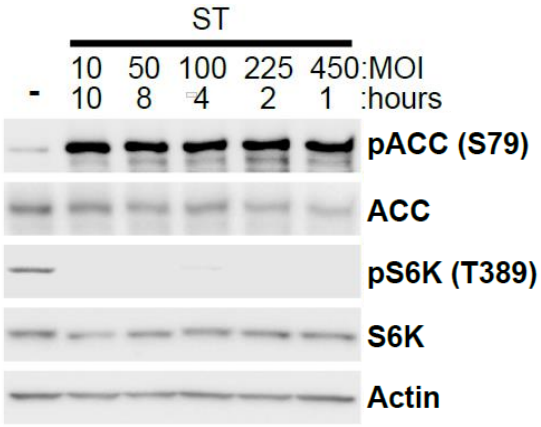

Fig S3. MEF cells were infected with increased amount of *Salmonella* for the indicated time points. Whole cell lysates were immunoblotted for AMPK and mTORC1 activity using the antibodies indicated.

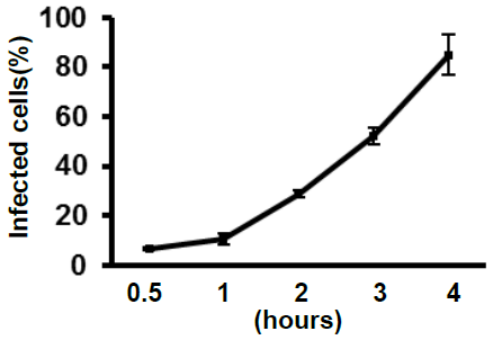

Fig S4. MEF cells were infected with *Salmonella* in a time course experiment. AMPK activity was analyzed by western blot.

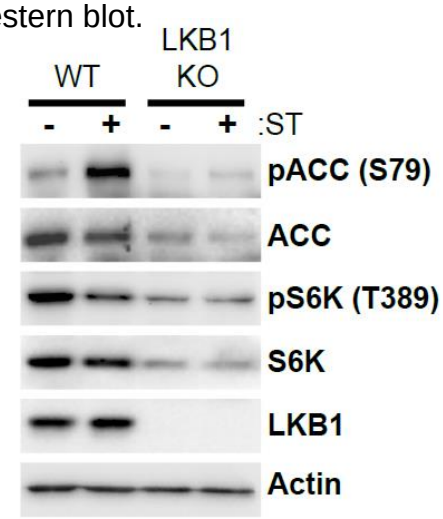

Fig S5. Wild-type and LKB1 knock-out MEF cells were infected with *Salmonella* for 1 hour. Whole cell lysates were immunoblotted for AMPK and mTORC1 activity using the antibodies indicated.

***Salmonella*-induced changes to AMPK-mTORC1 signalling do not require bacterial entry or SCV damage**

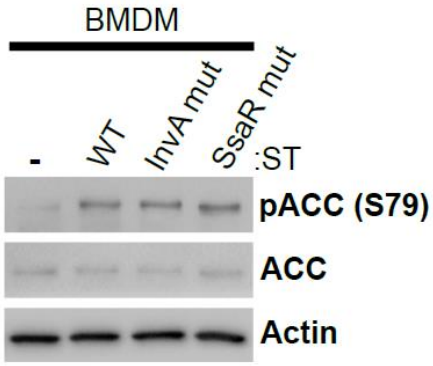

Fig S6. BMDM were infected with wild-type, invasion-deficient (InvA mutant), or replication-deficient (SsaR mutant) *Salmonella* for 1 hour. Whole cell lysates were immunoblotted for AMPK activity using the antibodies indicated.

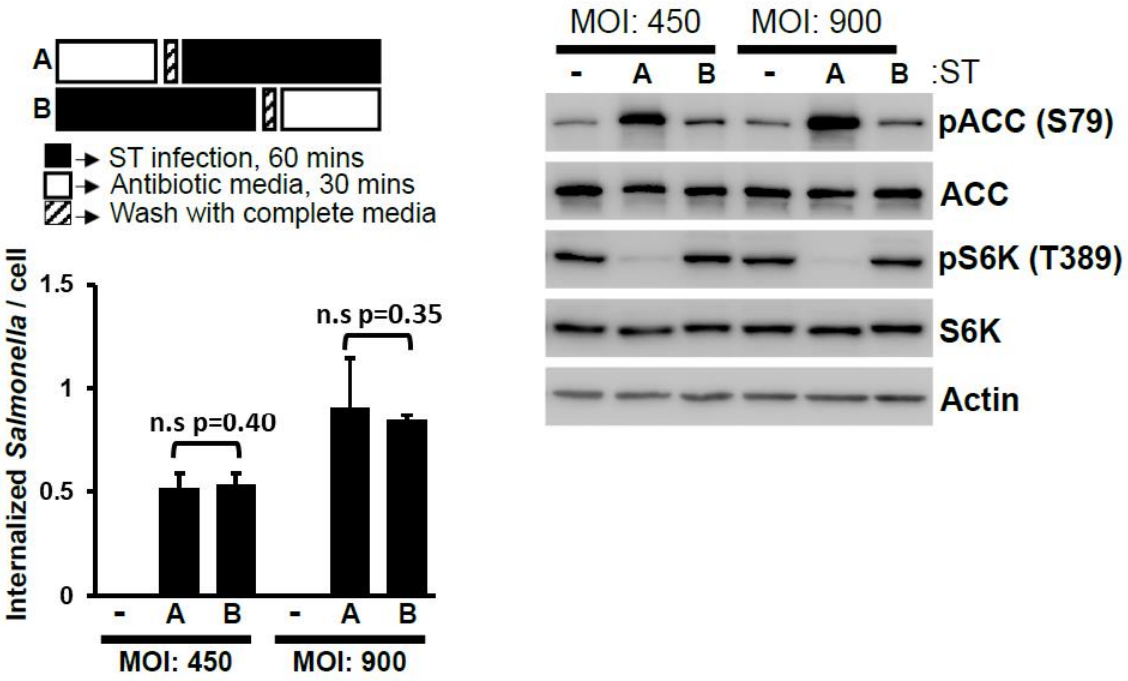

Fig S7. MEF cells were infected with *Salmonella* for 1 hour, which was preceded or followed by Gentamycin-containing media change for 0.5 hour. MOI of 450 and 900 were used. Infection rates were quantified by immunofluorescence and AMPK activation was determined by western blot.

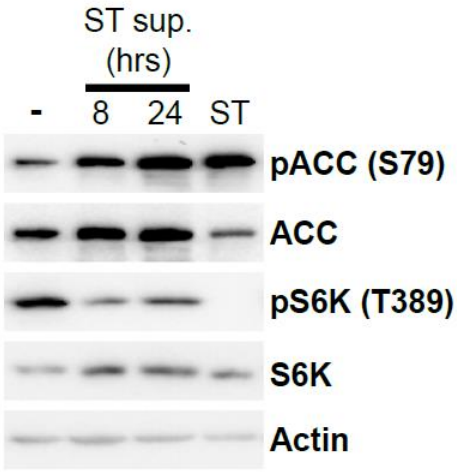

Fig S8. MEF cells were treated with either *Salmonella* or filtered bacterial supernatant harvested at the indicated time points for 1 hour. Whole cell lysates were immunoblotted for AMPK and mTORC1 activity using the antibodies indicated.

Salmonella-induced signalling to AMPK and mTORC1 does not result in an induction of bulk autophagy

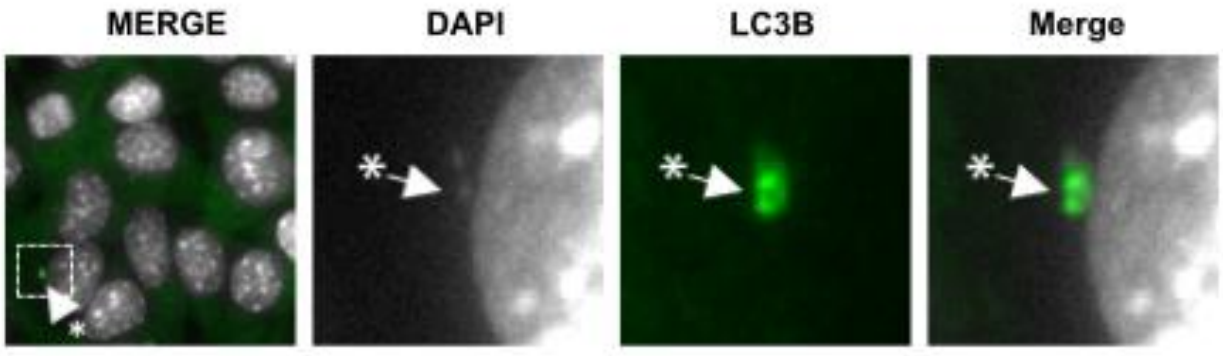

Fig S9. Full field of view for images shown in Fig 19.

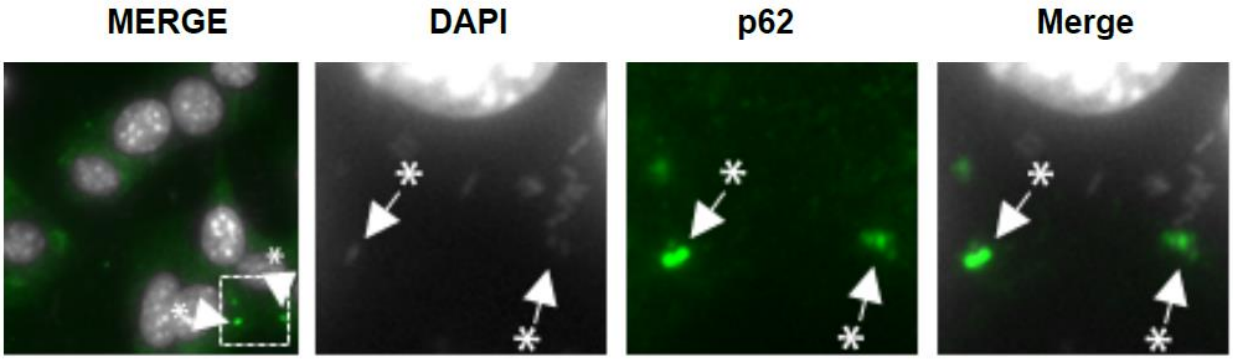

Fig S10. Full field of view for images shown in Fig 20.

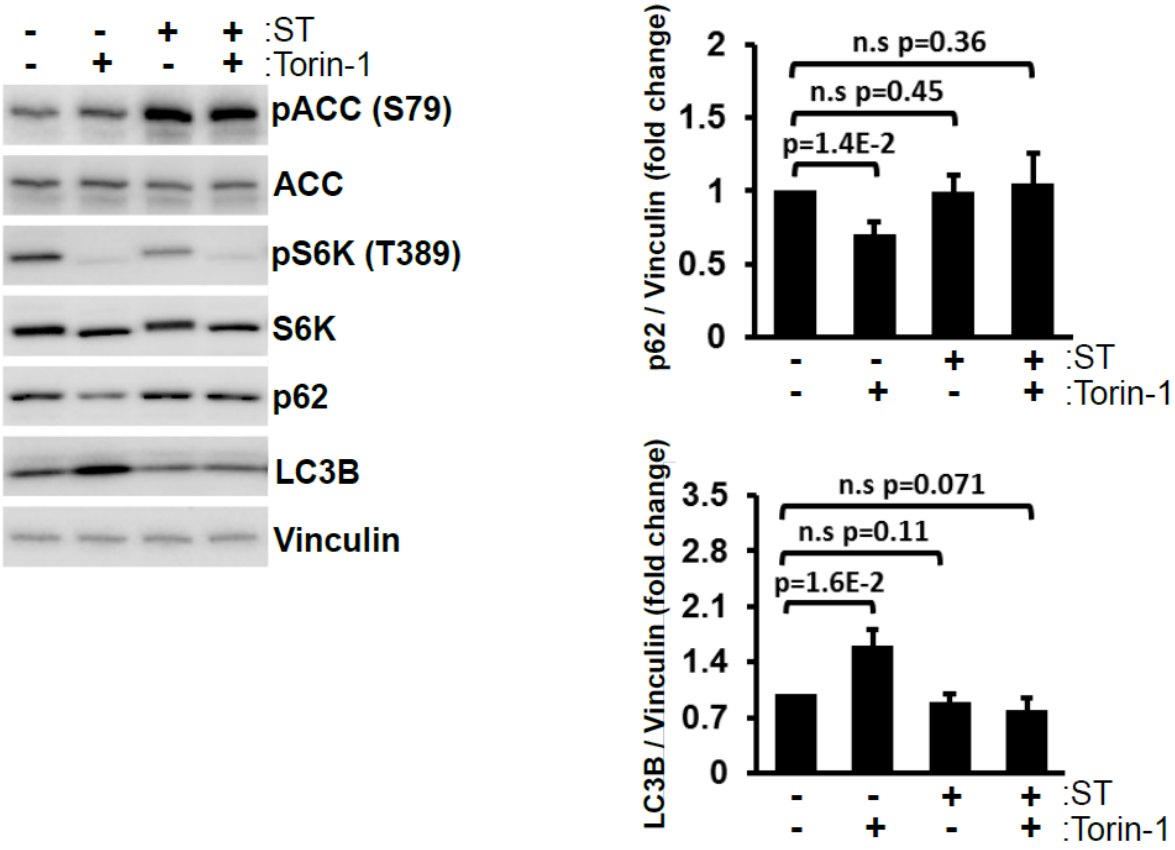

Fig S11. MEF cells were treated with *Salmonella* in the presence or absence of 0.2 μM Torin-1 for 1 hour. Whole cell lysates were immunoblotted using the antibodies indicated. Autophagy induction was analyzed by analysis of p62 clearance and LC3B-lipidation.

AMPK activates ULK1 and VPS34 kinases in response to *Salmonella*

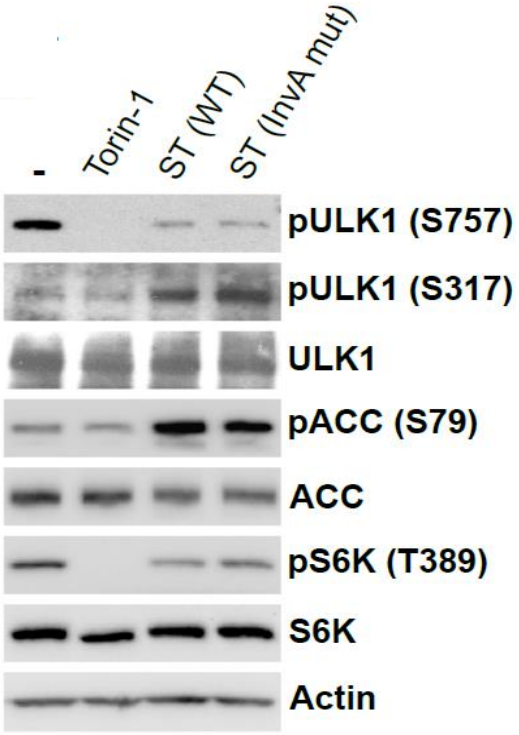

Fig S12. MEF cells were treated with either 0.2 μM Torin-1, *Salmonella* (wild-type), or *Salmonella* (InvA mutant) for 1 hour. Western blot was used to examine the regulation of ULK1.

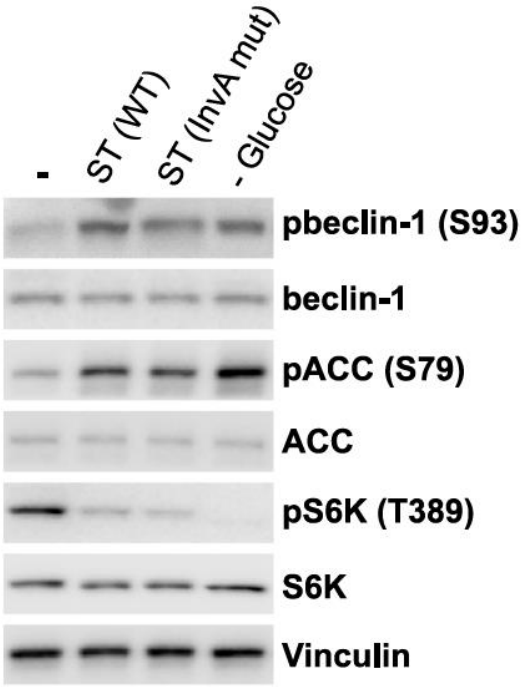

Fig S13. MEF cells were treated with either *Salmonella* (wild-type), *Salmonella* (InvA mutant), or glucose starvation medium for 1 hour. AMPK-mediated activation of the VPS34 complexes through beclin-1 phosphorylation was analyzed using western blot.

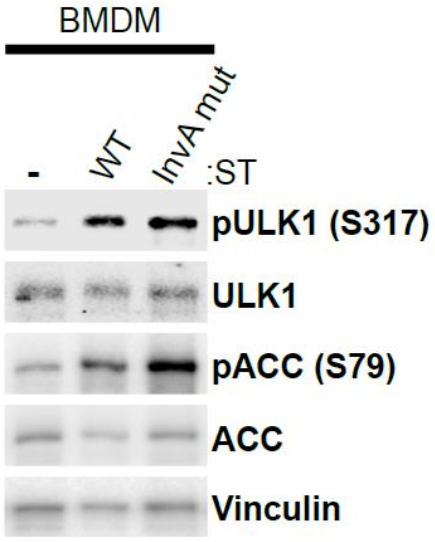

Fig S14. BMDM were treated with either *Salmonella* (wild-type) or *Salmonella* (InvA mutant) for 1 hour. Western blot was used to examine the regulation of ULK1.

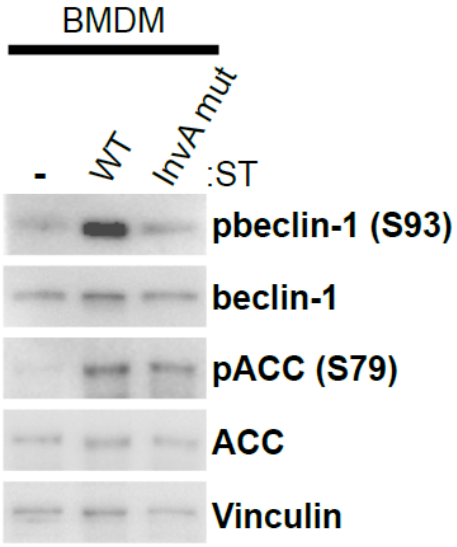

Fig S15. BMDM were treated with either *Salmonella* (wild-type) or *Salmonella* (InvA mutant) for 2 hours. AMPK-mediated activation of the VPS34 subunit beclin-1 was analyzed using western blot.

Detection of pathogen-derived outer membrane vesicles (OMVs) promotes AMPK activation

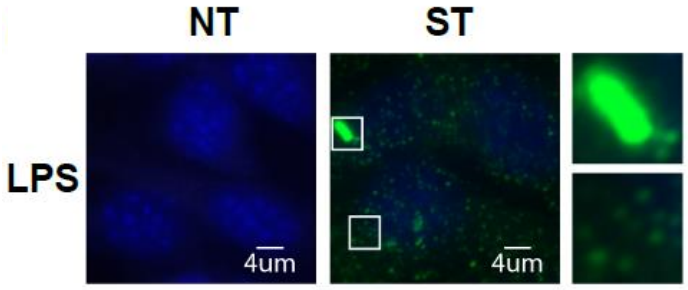

Fig S16. MEF cells were treated with *Salmonella* for 1 hour. Bacteria were stained using anti-LPS antibodies and visualized by immunofluorescence. The image was enlarged to demonstrate bacteria and LPS-positive OMVs.

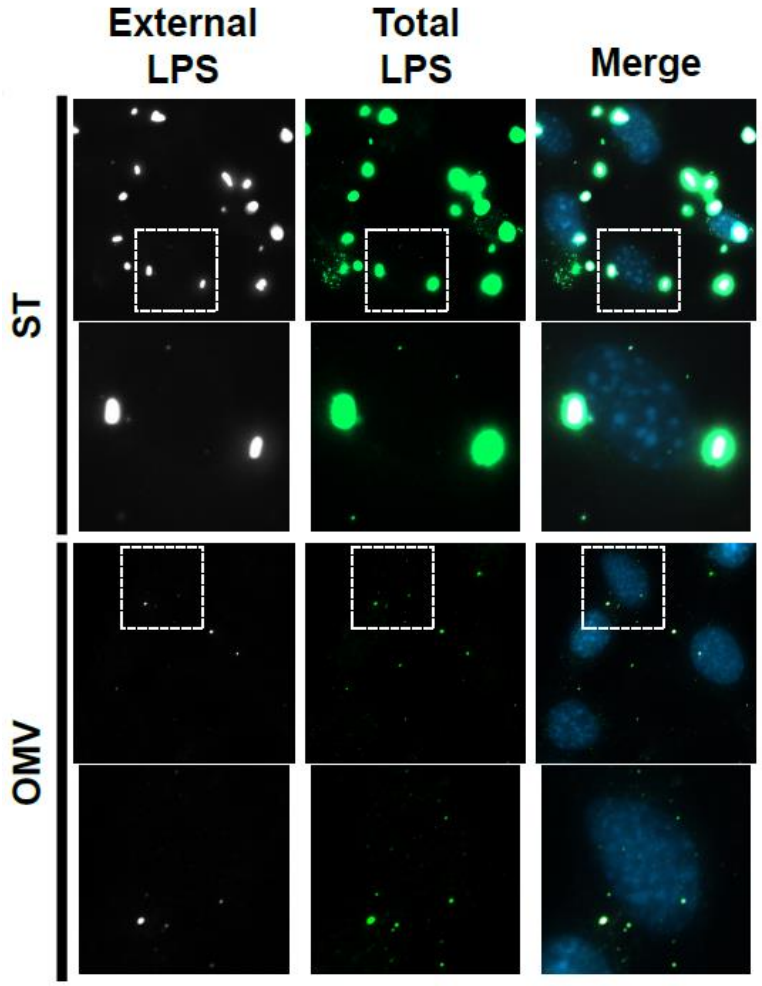

Fig S17. Full field of view from image shown in Fig 35 is shown. Dashed boxes represent selected regions for main figure.

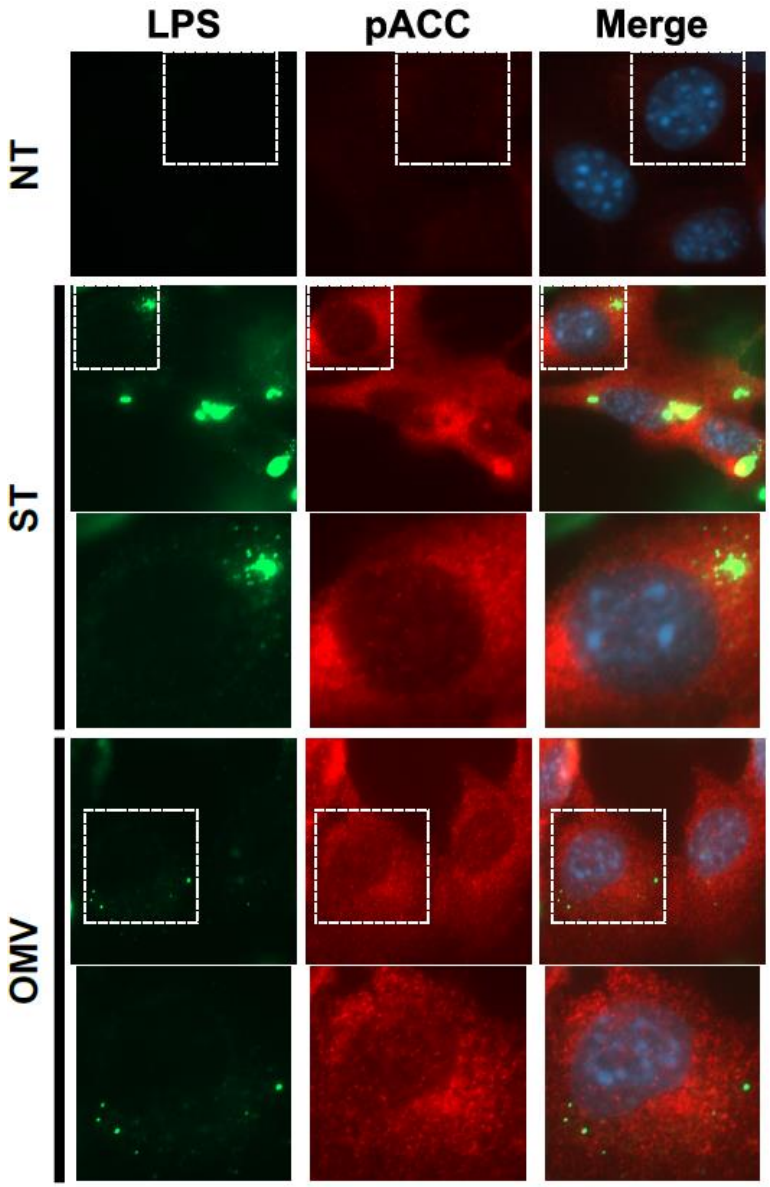

Fig S18. Full field of view from image shown in Fig 36 is shown. Dashed boxes represent selected regions for main figure.

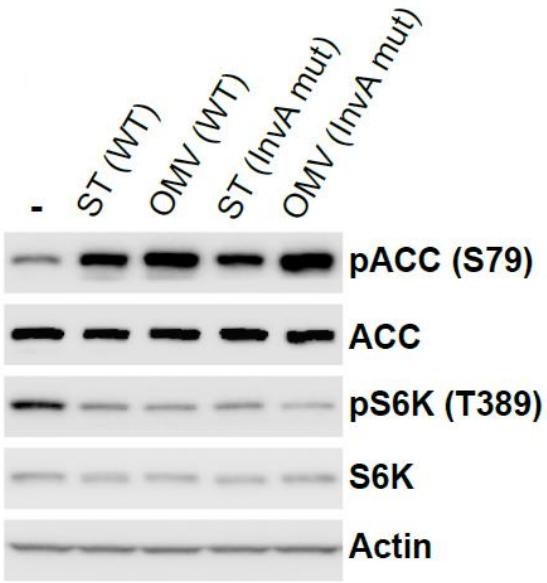

Fig S19. MEF cells were infected with either *Salmonella* (wild-type or InvA mutant), or their corresponding OMVs for 1 hour. Whole cell lysate was immunoblotted to analyze AMPK and mTORC1 signalling.

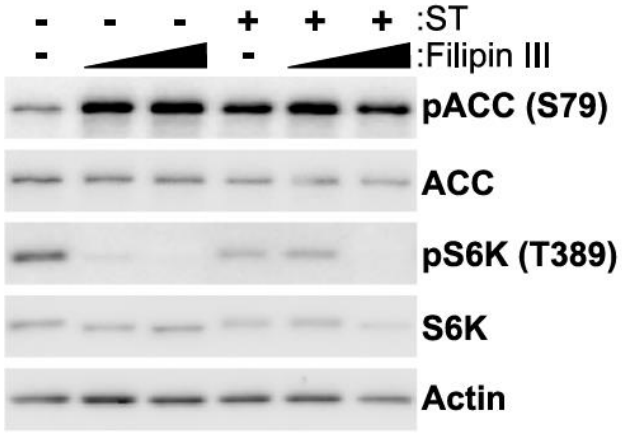

Fig S20. MEF cells were treated with *Salmonella* (wild-type) in the presence or absence of filipin III (7.5 or 10 µg/mL) for 1 hour. Whole cell lysates were immunoblotted for AMPK and mTORC1 activity using the antibodies indicated.

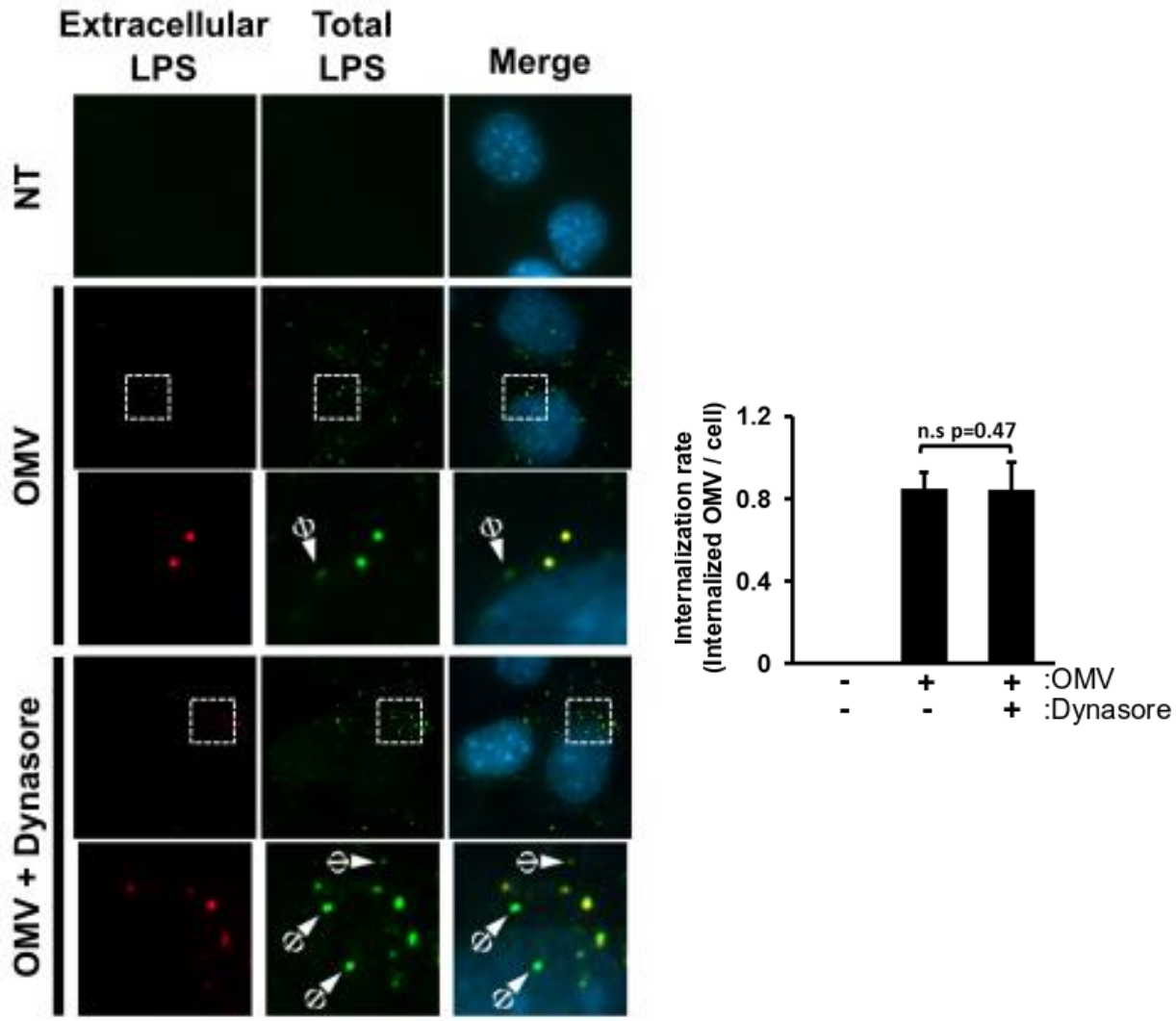

Fig S21. MEF cells were treated with purified OMVs in the presence or absence of 100 μM dynasore for 1 hour. Whole cell lysates were immunoblotted for the activities of AMPK and mTORC1. Internalization rates were determined by immunofluorescence. Arrows with ϕ mark internalized OMVs.

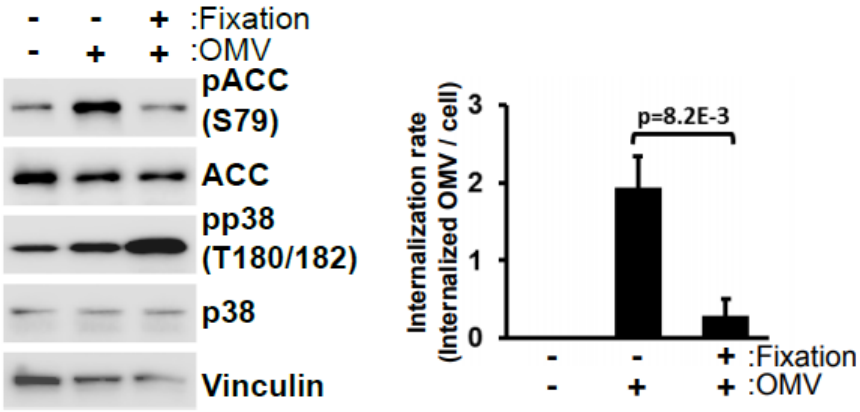

Fig S22. MEFs were treated with either wild-type or 4% PFA-treated OMVs for 1 hour. Whole cell lysates were immunoblotted using the antibodies indicated. Internalization rates were determined by immunofluorescence.

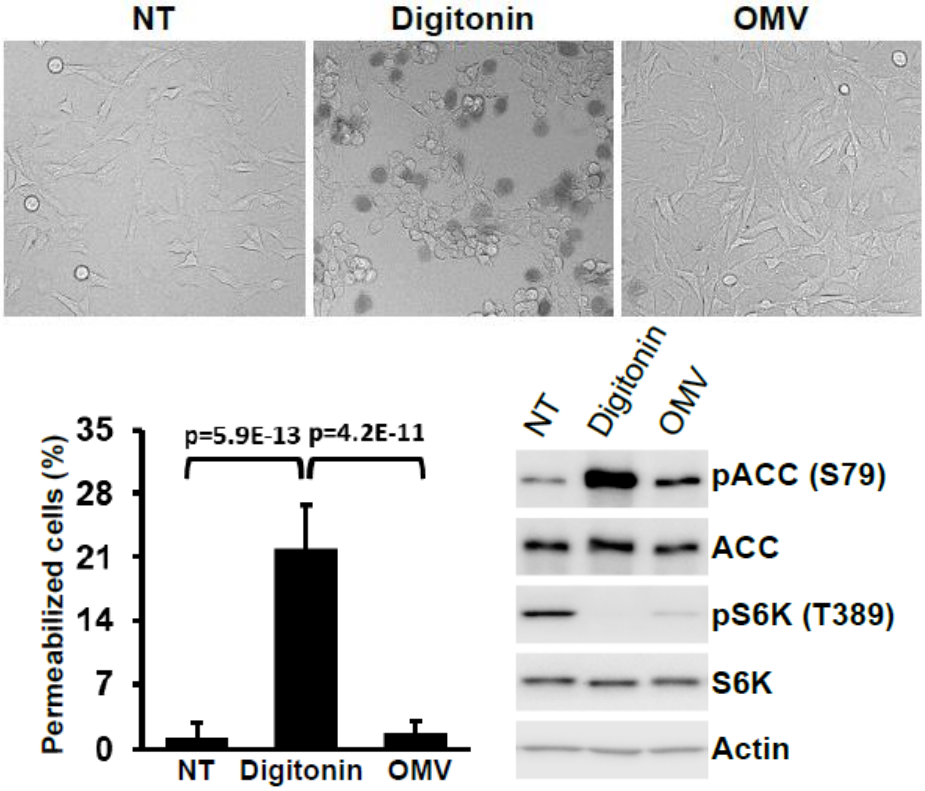

Fig S23. MEF cells were treated with either 10 µg/mL digitonin or purified OMVs for 20 min. Samples were analyzed by western blot or trypan blue staining using duplicate plates. Whole cell lysate was immunoblotted for analysis of AMPK and mTORC1 signalling. Trypan blue stain (0.04%) was added directly to samples and ZOE fluorescent cell imager was used to visualize and quantify permeabilized cells.

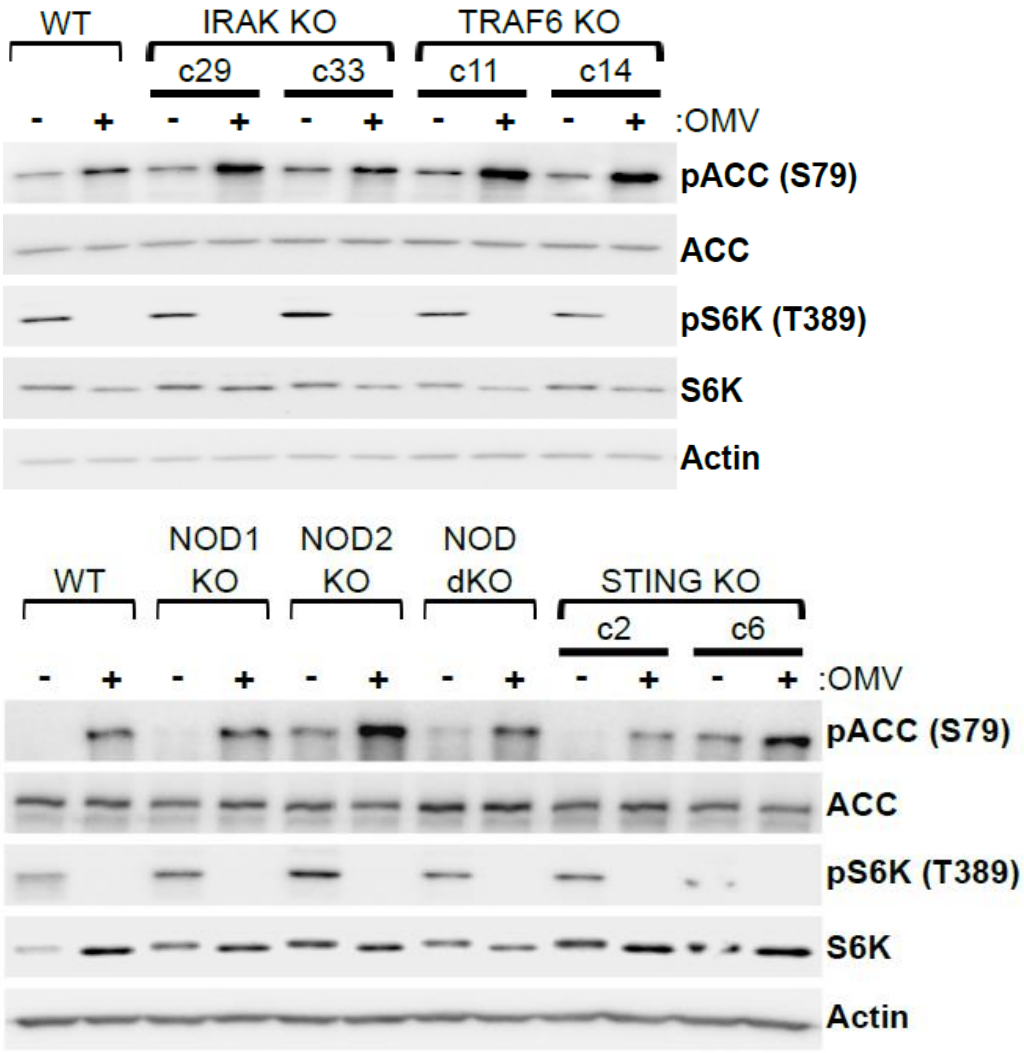

Fig S24. Wild-type, IRAK knock-out (KO), TRAF6 KO, NOD1 KO, NOD2 KO, NOD1/2 KO (dKO), and STING KO HCT116 cells were treated with purified OMVs for 1 hour. Whole cell lysates were immunoblotted using the antibodies indicated.

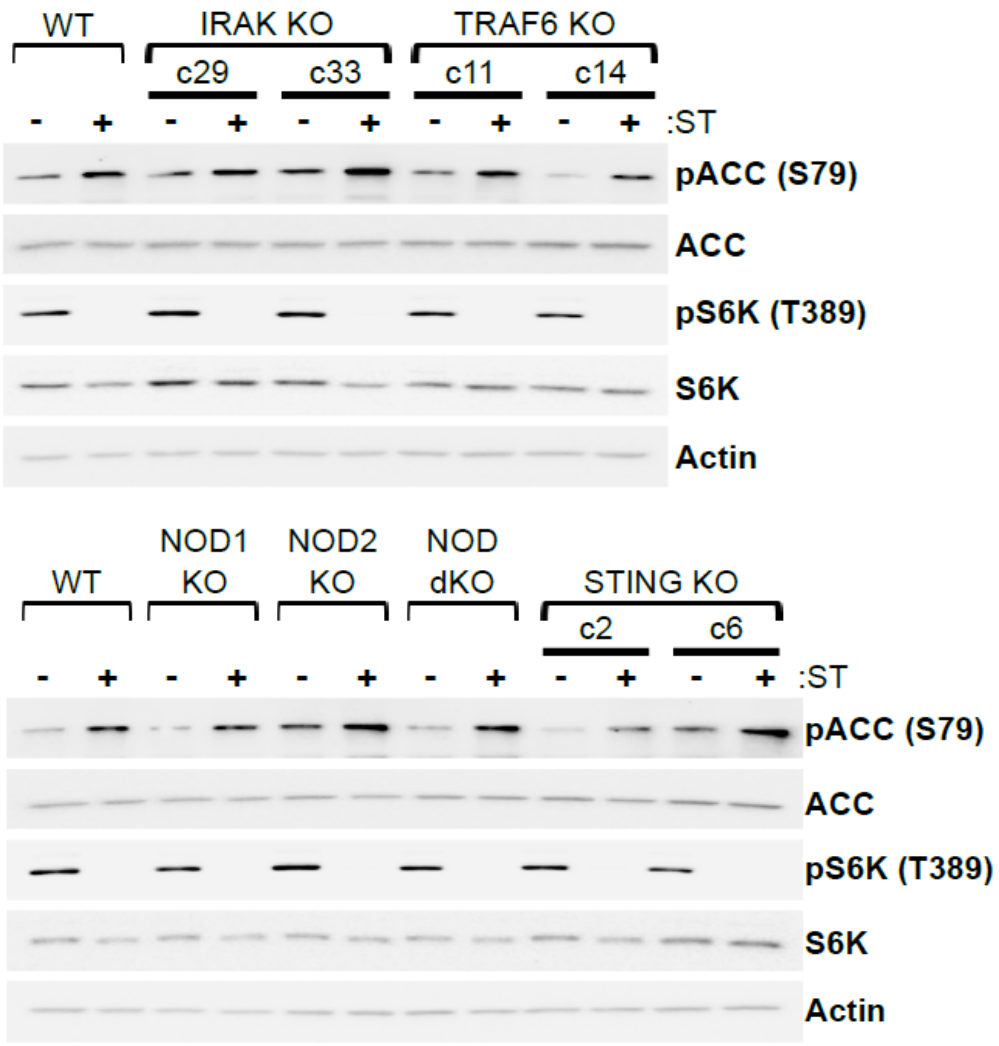

Fig S25. Wild-type, IRAK knock-out (KO), TRAF6 KO, NOD1 KO, NOD2 KO, NOD1/2 KO (dKO), and STING KO HCT116 cells were infected with *Salmonella* for 1 hour. Whole cell lysates were immunoblotted using the antibodies indicated.

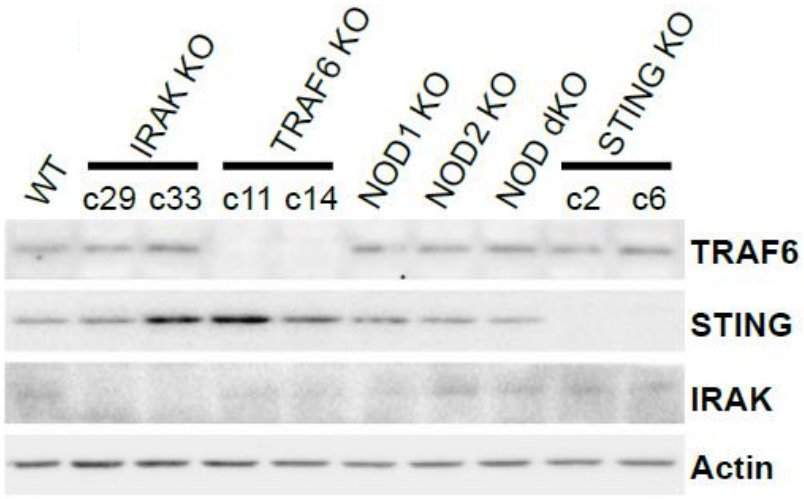

Gene	Clone	Mutations	
IRAK	c29 / c33	WT: acgaggtgccg.....ggtgggtggcggc A1/A2: acgaggtgccg---.....---ggtgggtggcggc	66 bp del.
TRAF6	c11	WT: actgctgtgtggccatggccagctcctgtagcgctgtaac A1: actgctgtgtggccatggccagct-ctgtagcgctgtaac A2: actgctgtgt----------gctgtaac	1 bp del. 22 bp del.
	c14	WT: actgctgtgtggccatggccagctcctgtagcgctgtaac A1: actgctgtgtggccatggccagctc--------ctgtaac A2: actgctgtgtggccatggccagctcctgtaCgcgctgtaac	8 bp del. 1 bp ins.
NOD2	-	WT: gtcctctcctgggaggacta cgagggcttc A1: gtcctctcctgggaggact-cgagggcttc A2: gtcctctcctggga------cgagggcttc	1 bp del. 6 bp del.
STING	c2	WT: acactctccggt.....aacggggtctgcag A1: acactctccgg---.....--aacggggtctgcag A2: acactctccggt--.....--aacggggtctgcag	45 bp del. 44 bp del.
	c6	WT: acactctccggta.....acggggtctgcag A1/A2: acactctccggta--.....--acggggtctgcag	44 bp del.

Fig S26. Knock-out cells were validated by either western blot or sequencing. NOD1 KO and NOD1/2 KO cells were previously characterized by Scott D. Gray-Owen[129].

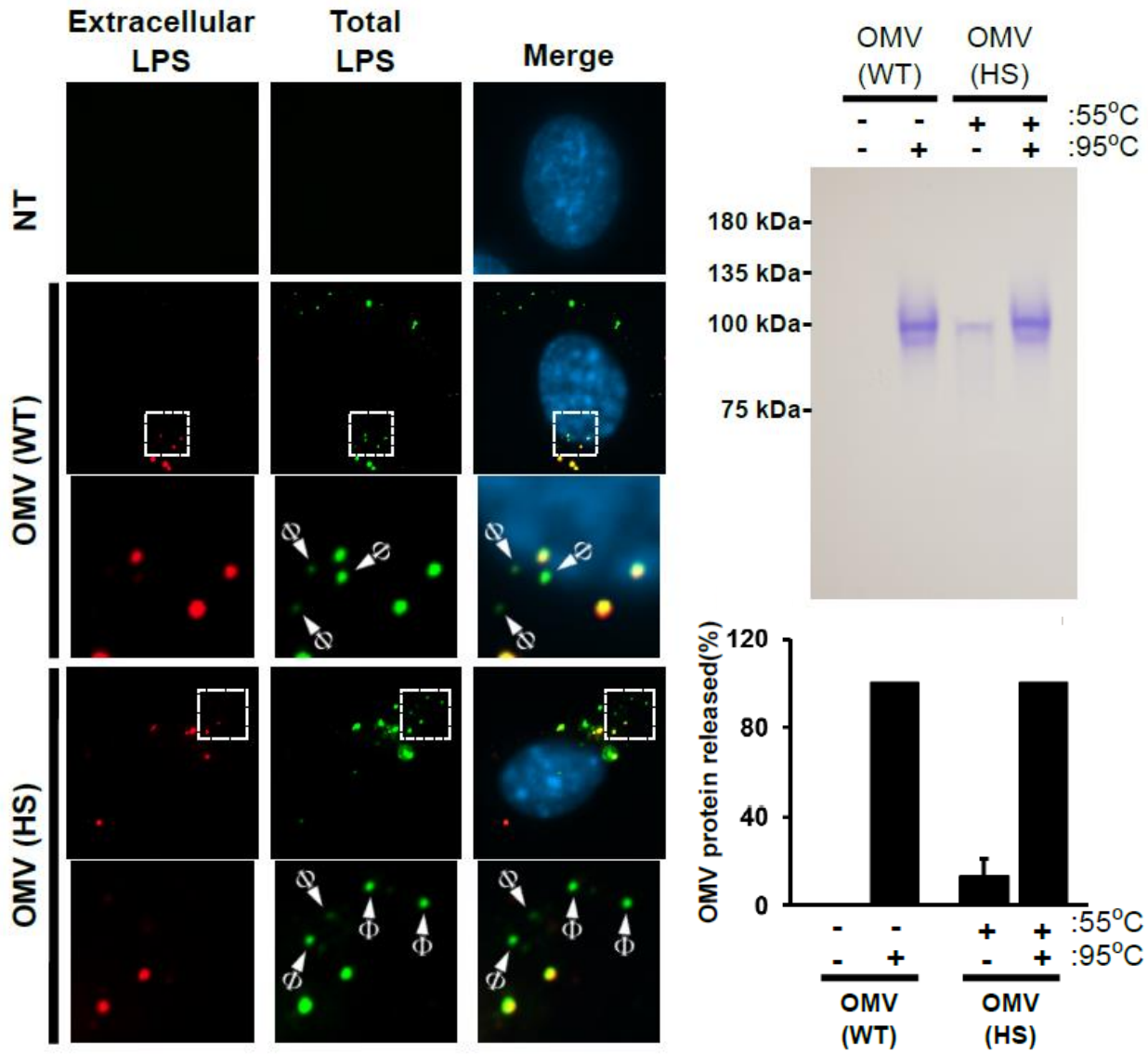

Fig S27. MEF cells were treated with either wild-type OMVs or 55ºC-treated OMVs for 1 hour. Internal and total LPS were stained and analyzed by immunofluorescence. Wild-type and heat-treated OMVs were run on native gels to examine the amount of released proteins. Arrows with ϕ mark internalized OMVs.

AMPK signalling promotes xenophagy

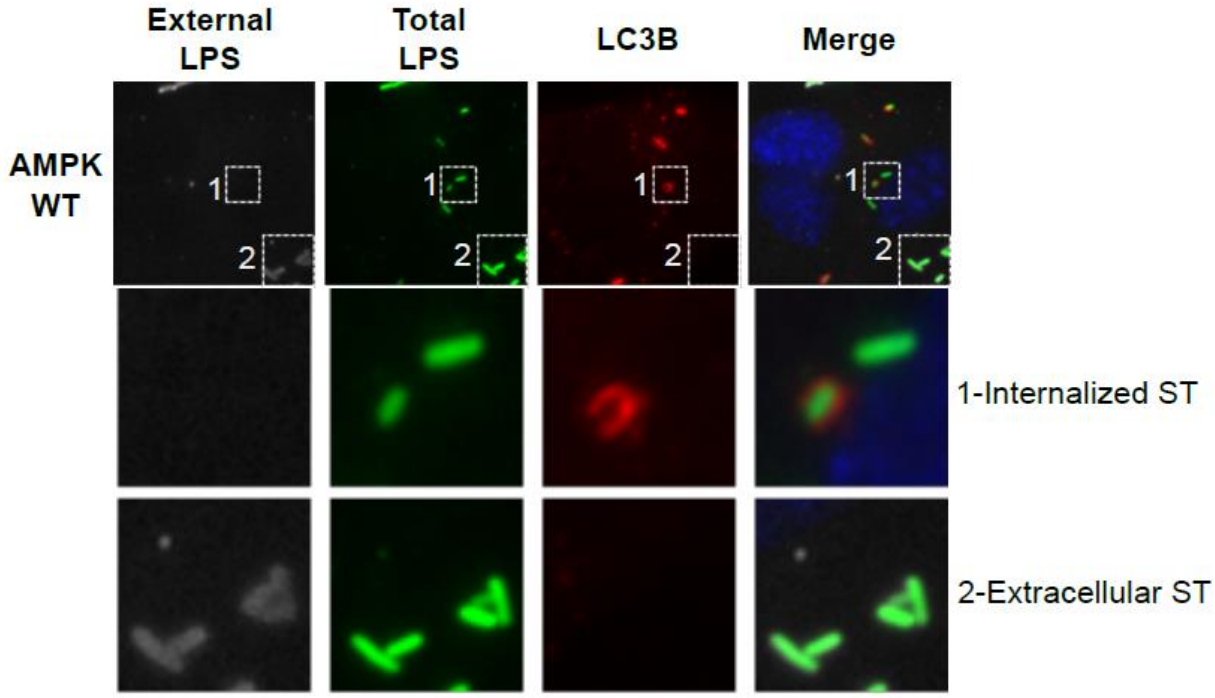

Fig S28. Example of triple stained for external bacteria (anti-LPS before permeabilization), total bacteria (anti-LPS after permeabilization) and LC3B-positive puncta.